

AN ASSESSMENT OF ROCKFALL ACTIVITY
USING DENDROGEOMORPHOLOGY: THE AMPHITHEATER, OURAY,
COLORADO, USA

A Thesis

by

JOHN CHRISTOPHER REED

Submitted to the Office of Graduate and Professional Studies of
Texas A&M University
in partial fulfillment of the requirements for the degree of

MASTER OF SCIENCE

Chair of Committee,	John R. Giardino
Committee Members,	Kevin R. Gamache
	Ryan C. Ewing

Head of Department,	Michael C. Pope
---------------------	-----------------

December 2016

Major Subject: Geology

Copyright 2016 John C. Reed

ABSTRACT

A U.S. Forest Service campground and adjacent hiking trails are subjected to rock-fall activity from a nearby bedrock escarpment. The campground is situated in a glacial-carved valley of the Ouray, Colorado, Amphitheater in the San Juan Mountains. A dendrogeomorphic assessment of the trees and steep slopes surrounding campground investigate the past and present stability conditions to answer the question: What are the spatial and temporal characteristics of rock fall? More specifically, for this area, where spatially is the slope subjected to rockfall activity and what are the magnitude and frequency of events? Also, will reconstructing a rockfall chronology using a dendrogeomorphic methodology of *Abies concolor* (White fir) help identify potential triggering mechanisms? To answer the research questions, the following two objectives were established for this study: (i) delineate the spatial patterns of rockfall activity, and (ii) establish a temporal chronology of rockfall activity. The spatial extent of rock-fall activity is assessed by mapping areas of talus accumulations and trees exhibiting visual evidence of rock-fall activity. Visible rock-fall induced tree disturbances observed in the study area include: impact scars, tree decapitation, curved or leaning trees, and elimination of neighboring trees or 'broken crown'. The area with the greatest hazard to rockfall activity is the area located below the gullies of the overlying cliffs and steep slopes, the scree slopes below the base of the cliff, and for ~70 m into the forest from the upper protective forest boundary and ~100 m from the base of the cliff. 'Centurion' trees are the most likely to record a growth defect as result of rockfall activity. The sampling

of selected trees with an increment borer allowed for microscopic analysis of the variations of tree-ring width measurements as a trees response to rock-fall induced growth defects (GD) (reaction wood, suppression and release, and cellular scarring/callus tissue). The initiation, duration, and termination of the growth defects (GD) allowed for the reconstruction of a rock-fall chronology. This reconstruction alluded to the observation of rockfall activity being dominated by low magnitude, high frequency events, and interpreted as being attributed to annual freeze and thaw activity. For the time period of investigation (1910-2015), no large mass movement event occurred within the study area. Although there were no observations of a large-scale mass movement event, several years recorded abnormally high rockfall rates, as determined from the reconstructed rockfall chronology. Years with abnormal rockfall rates are a result of some additional external factor ‘promoting’ and/or ‘triggering’ the rockfall event.

ACKNOWLEDGEMENTS

I would like to thank my committee chair, Dr. John ‘Rick’ Giardino, and my committee members, Dr. Ryan Ewing and Dr. Kevin Gamache, for their guidance and support throughout the course of this research.

Thanks also go to my friends and colleagues and the department faculty and staff for making my time at Texas A&M University a great experience. I also want to extend my gratitude to Dr. Charles Lafon, who provided the dendrochronology lab and to my field assistant, Akhil Amara.

Finally, thanks to my mother, father and siblings for their encouragement and to my fiancée, Chelsea for her assistance in the field and her patience and love.

TABLE OF CONTENTS

	Page
ABSTRACT	ii
ACKNOWLEDGEMENTS	iv
TABLE OF CONTENTS	v
LIST OF FIGURES	vii
LIST OF TABLES	x
CHAPTER I INTRODUCTION	1
1.1 Background and Problem Statement	2
1.2 Objectives	4
CHAPTER II LITERATURE REVIEW	5
2.1 Rockfall Fundamentals	5
2.1.1 Causes of Rockfall	5
2.1.2 Rockfall Movement	8
2.1.3 Rockfall Modeling	12
2.2 Hazard Assessment	14
CHAPTER III STUDY AREA	17
3.1 Study Area	17
3.2 Geology and Geomorphology	17
3.3 Climate	26
3.4 Vegetation	32
3.4.1 Lichen	32
3.5 Temporal Record of Activity	32
CHAPTER IV METHODS	34
4.1 Dendrogeomorphology	34
4.1.1 Identifying Tree Types	35
4.1.2 Dendrogeomorphic Evidence of Disturbed Trees	36
4.2 Field Methods	40
4.3 Lab Methods	44

CHAPTER V ANALYSIS	48
5.1 Tree Rings-Master Chronology.....	48
5.2 Rockfall History	48
5.3 Visible Defects and Growth Responses to Rockfall Activity	48
5.4 Spatial Distribution of Growth Disturbances	50
5.5 Rockfall Magnitude and Frequencies.....	60
5.6 Annual Variations in Rockfall Activity	60
CHAPTER VI DISCUSSION	64
6.1 Rockfall Chronology	64
6.1.1 Limitations.....	64
6.1.2 Evaluating Rockfall Activity.....	66
6.1.3 Notable Rockfall Activity	67
6.2 Spatial Extent of Rockfall Activity	69
6.2.1 Rockfall Distribution.....	69
6.2.2 Broader Impacts	72
CHAPTER VII CONCLUSION	73
7.1 Conclusions and Recommendations.....	73
REFERENCES	75
APPENDIX A	92
APPENDIX B	99
APPENDIX C	104
APPENDIX D	105
APPENDIX E.....	112

LIST OF FIGURES

	Page
Figure 1 Study area is located in the San Juan Mountains of southwestern Colorado, east of Ouray (Google).....	4
Figure 2 Rockfall modes of motion along a slope in relation to the mean slope gradients (modified from Dorren, 2003).....	9
Figure 3 Schematic diagram of the Ouray rockfall slope under investigation subdivided into departure, transit and deposition zone with graphical representation of the “Fahrböschung angle” and the “minimum shadow angle” (modified after Buwal et al., 1997; Dorren, 2003; Schneuwly, 2009).....	11
Figure 4 Study area is located in the San Juan Mountains of southwestern Colorado, east of Ouray, as denoted by bold black dashed line	18
Figure 5 Schematic diagram illustrating key slope components.....	19
Figure 6 (A) Fractured Sandstone and interbedded limestone and shale cliff is the source of the rockfalls; (B) Talus buildup into steep slopes; (C) Vegetated slopes acting as a protective forest to falling debris (Photos by Author)	19
Figure 7 Geologic map of Ouray, Colorado and the study area (modified after Luedke and Burbank, 1962).....	24
Figure 8 Stratigraphy of the Ouray, Colorado quadrangle (from Reed, 2013)	25
Figure 9 Daily temperature averages and extremes for weather station (056203) from 06/01/1893-05/31/2006 (WRCC, 2013).	29
Figure 10 Daily temperature averages and extremes for weather station (056205) from 01/02/2000-01/20/2015 (WRCC, 2013).	29
Figure 11 Daily precipitation averages and extremes for weather station (056203) from 06/01/1893-05/31/2006 (WRCC, 2013).	31
Figure 12 Daily precipitation averages and extremes for weather station (056205) from 01/02/2000-01/20/2015 (WRCC, 2013).	31
Figure 13 Diagram illustrating the methodology process	34
Figure 14 Dendrogeomorphic evidence to infer rockfalls. Variations of tree-ring width measurements (left) and the visual result of disturbed samples (Modified from Stoffel et al., 2005).....	37

Figure 15 Visualized locations of data samples.	41
Figure 16 Imagery displaying the location of sampled trees. Yellow circles represent sampling locations.	42
Figure 17 Core extracted from an injured tree using an ‘increment borer’ (Photo by Author)	43
Figure 18 Cross-section of scarred tree with ideal sampling positions A-D (Modified from Stoffel and Bollschweiler, 2008).....	44
Figure 19 Reconstructed rockfall return intervals.	51
Figure 20 Location of fresh or recent injuries of ‘category 1’ (filled circles). Open circles denote all visible rockfall induced injuries	54
Figure 21 Location of partially recovered tree scars of ‘category 2’ (filled circles). Open circles denote all visible rockfall induced injuries	55
Figure 22 Location of old scars and injuries of ‘category 3’ (filled circles). Open circles denote all visible rockfall induced injuries	56
Figure 23 Locations of rockfall deposits subdivided into clast sizes (see Table 7 for more detail)	58
Figure 24 (A) Large isolated disc shaped boulder surrounded by vegetation/soil, and (B) active scouring of the slope transporting varying clast sizes down slope (Photos by Author)	59
Figure 25 The spatial distribution of the lichen categories (see Table 8 for more details)	60
Figure 26 Reconstructed rockfalls based on analysis of GDs identified in tree cores (dashed line represents 7-year moving average)	61
Figure 27 The light gray represents the available sample depth per year and the dark gray represents the exposed diameter for each year under investigation.....	63
Figure 28 Rockfall ‘rate’ illustrated by the number of events $\text{m}^{-1}\text{yr}^{-1}$ (light-gray line represents 7-year moving average)	63
Figure 29 Event Timeline for rockfall occurrences and triggering mechanisms	69
Figure 30 Distribution of return periods for rockfalls with interpolated values. The red line indicates the mapped lower edge of talus and rockfall deposits.	70

Figure 31 Histogram of number of total injuries binned into distances from forest edge.

This illustrates that the farther into the forest, away from the source, the fewer impacts will be recorded as rocks are more likely to come to rest upslope (error bars and linear trend annotated)71

LIST OF TABLES

	Page
Table 1 The Colorado Department of Transportation (CDOT) “Rockfall Hazard Rating System” or “RHRS” (from Russell, 2005)	16
Table 2 Monthly climate summaries for the two weather stations in Ouray, Colorado from 06/01/1893 to 01/20/2015 (Source: Western Regional Climate Center, wrcc@dri.edu)	28
Table 3 Number of trees and injuries sampled.....	49
Table 4 Overview of visible defects used to determine rockfall events.....	49
Table 5 Overview of growth disturbances used to determine rockfall events	50
Table 6 Injured trees categorized by relative recovery state	52
Table 7 Classification of rockfall deposits based on sample diameters. Grain size adapted from International grain size scale (ISO 14688-1: 2002)	57
Table 8 Classification of lichen colonization into three age categories based on relative age and percent coverage	59

CHAPTER I

INTRODUCTION

Every summer, thousands of people visit the many national, state and city parks of Colorado to experience the beautiful outdoors and natural wonders that are present. For those who venture into the mountainous terrain of southwestern Colorado, they might experience some of the natural hazards that are present in the area, including steep topography and the potential for mass movement events. One of the common types of mass movement is rockfall. The steep slopes and cliffs of the San Juan Mountains are prime locations for rockfall activity. Glacial-carved valleys have created steep slopes and cliffs that have been exposed to significant weathering, creating potentially isolated areas of instability. Hiking trails and campgrounds are often located in these areas because of their scenic beauty and access to recreational spots. Unfortunately, this places them in areas vulnerable to mass movement hazards, specifically rockfall.

State, county and city officials have long recognized rockfall as a hazard and, thus, they require current research thinking to recognize and monitor new hazardous areas: rockfall can cause significant losses to life and property (CDEM, 2013). The 2013 Colorado natural hazards mitigation plan reported more than \$3 million in damages and five deaths resulting from landslide and rockfall activity (CDEM, 2013). Identifying areas of rockfall activity and understanding the driving forces allows state and city officials to not only plan for safety, but also promote public awareness of the hazard of rockfall activity and its associated risks. A study of rockfalls can also lead to preventative mitigation in necessary areas.

Many methodologies (Luckman and Fiske, 1995; Nesje et al., 1994; Bjerrum and Jorstad, 1968; Douglas, 1980; Andrew, 1994) exist to actively study the processes associated with rockfall; however, the most accurate method for dating rockfall activity when a log or record of activity is absent, is the analysis of impacted or disturbed trees and their associated growth response recorded in the tree-ring record (Schneuwly et al., 2009). This process is known as dendrogeomorphology (Alestalo, 1971). The goal of this thesis was to integrate dendrogeomorphic techniques with standard geomorphic practices to develop a record of the rockfall activity as well as an understanding of the processes responsible for activity on the steep slopes adjacent to the US Forest service campground in the Ouray area. The research from this thesis confirms the use of tree-ring analysis of *Abies concolor* (White fir) to be an effective tree species for rockfall analysis.

1.1 Background and Problem Statement

Ouray, is located in one of the many glacial-carved valleys of the Western San Juan Mountains of southwestern Colorado (figure 1). Adjacent to the southeastern side of Ouray is a U.S. Forest Service campground, which is situated within a large amphitheater.

The topography within the Amphitheater consists of multiple mass movement deposits, which have created 7.62 million m² (~82 million ft²) of 'landslide deposits (APPENDIX B1). Composed of San Juan tuff mixed with glacial deposits of Pleistocene age, the deposits are presently 'inactive' (Reed, 2013). Reed (2013) argues that Zaruba and Mencl (1982) are incorrect in classifying such deposits as relict. However, such

deposits, like the amphitheater deposits, cannot be relict, as they are either active or inactive. A landform can be relict, but not a process. Classification of this 'inactive state' for the deposits is supported by widespread vegetation cover on the deposits, as well as intermittent lines of drainage that extend across the landslide (Skempton and Weeks, 1976).

Reed (2013) provides a preliminary analysis of the extent and mechanism of the large amphitheater landslide; however, the occurrence of curved and leaning trees, impact scarring of trees, and steep slopes of alluvium/talus indicating unstable slope conditions surrounding the forest service campground and field observations suggest evidence for additional slope-instability conditions involving soil creep, avalanche debris, debris flows, rockfalls and rock slides all of which suggest further study is needed. This leads to the question: could these trees hold the key to understanding rockfall activity in this area?

The research of this thesis focused on the rock-fall activity occurring along the rock face around the upper circumference of the deposit. Injured and disturbed trees occur on the deposit as result of rockfall activity (APPENDIX B2). These scarred trees provide the opportunity to employ dendrogeomorphology in conjunction with standard geomorphic techniques to create a temporal and spatial assessment of rockfall activity and associated hazards.

The problem can be stated as: What are the spatial and temporal characteristics of rockfall? More specifically, for this area, where spatially is the slope subjected to rockfall activity and what are the magnitude and frequency of events? Also, will

reconstructing a rockfall chronology using a dendrogeomorphic methodology of *Abies concolor* (White fir) help identify potential triggering mechanisms?

1.2 Objectives

The following two objectives have been established for this study:

- (i) delineate the spatial patterns of rockfall activity and
- (ii) establish a temporal chronology of rockfall activity.

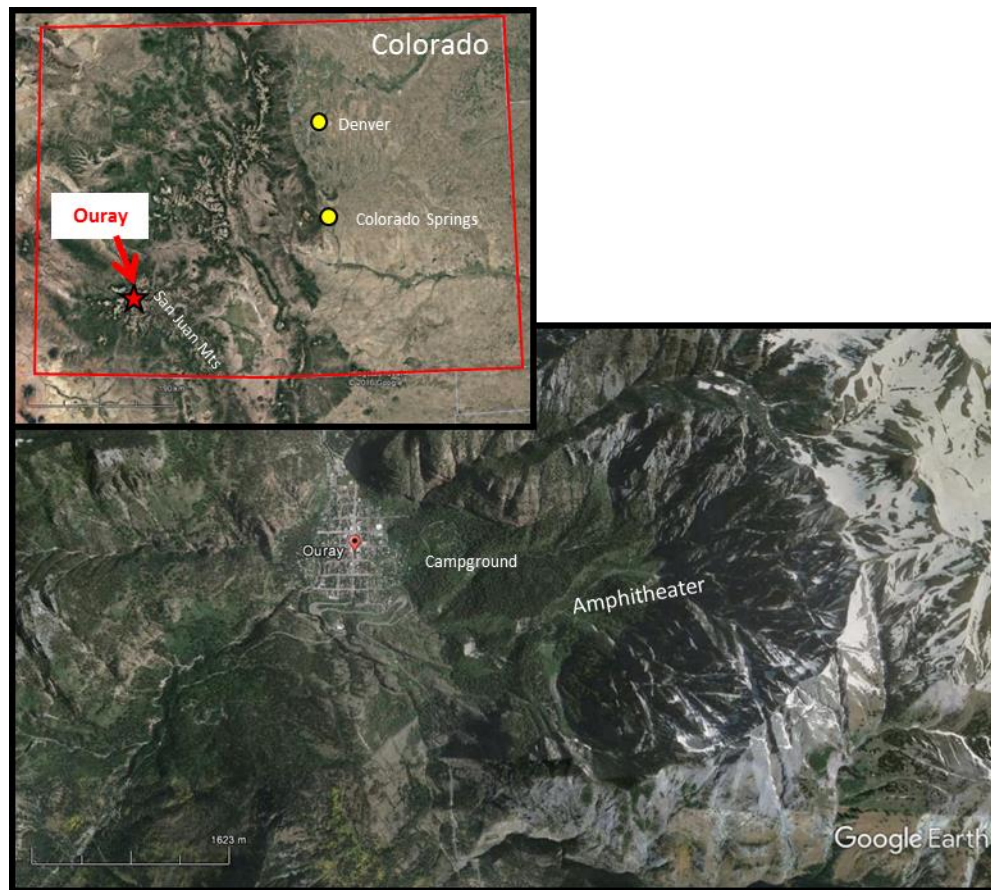


Figure 1 Study area is located in the San Juan Mountains of southwestern Colorado, east of Ouray (Google)

CHAPTER II

LITERATURE REVIEW

A literature review provides the necessary background information regarding the fundamentals of rockfall. Topics covered with this literature review include the causes of rockfall, rockfall movement, rockfall modeling, rockfall hazard assessment, and dendrogeomorphology.

2.1 Rockfall Fundamentals

2.1.1 Causes of Rockfall

Rockfall differs from other mass movement processes, in that rocks “free fall” as a result of gravity. Ritter et al.,(2002) defines rockfall as:

A single mass that travels as a freely falling body with little or no interaction with other solids. Movement is normally through the air, although occasional bouncing or rolling may be considered as part of the motion (Ritter et al. 2002 pg 105).

Rockfall begins with the detachment of a rock or rocks from a bedrock slope or cliff. All slopes have pre-existing morphological, geological, and geotechnical properties and are subjected to various degrees of physical and chemical weathering (Lee et al., 1997). For each slope, the pre-existing conditions, such as rock strength, degree of jointing, or crack presence can lead to the promotion of rockfall (Farran and Thenoz, 1965; Whalley, 1984; Dorren, 2003; Schneuwly, 2009). Therefore, the detachment of a rock from a slope is distinguished by the “promoter”, which may lead to favorable conditions for movement, and the “trigger”, or the mechanism that causes the actual start of movement.

There are many triggering mechanism that could lead to rockfall, however, in many cases, the rockfall promoter and trigger can be addressed together such as with the process of frost-thaw activity (Schumm and Chorley, 1966; Porter and Orombelli, 1981; Dorren, 2003; Matsuoka, 2008; Schneuwly, 2009). Alternating cycles of freezing and thawing, in conjunction with moisture can promote further weathering and cause the detachment of rockfall. When moisture or water, known as cleft water, within the intergranular void space (“primary porosity” associated “primary permeability”) begins to freeze; joints, cracks, and fissures will form as the volume increases (Terzaghi, 1962; Farran and Thenoz, 1965; Schumm and Chorley, 1966). “Secondary permeability” is the space between cracks and fissures. Repeat cycles of temperature increase and subsequent ice melting further widen of the cracks. The frequency and size of rockfall is controlled by the crack morphology and governed by the rock’s permeability, strength and proneness to failure (Farran and Thenoz, 1965; Ishikawa et al. 2004; Schneuwly, 2009). The scale at which freeze-thaw action propagates cracks in rocks will determine the size of the material that falls. Also, cracks in rocks and subsequent removal of finer material may cause vertical stacking which relies on the frictional component of the rock type (Hofmann, 1974). Further instability can be caused by the presence of expansive clays within the cracks and joints, that when wet, create a frictionless sliding plane (Barton and Choubey, 1977).

Rockfall caused by alternating freeze-thaw cycles are generally low magnitude, high frequency events (Matsuoka and Sakai, 1999) and are controlled by the geological, geotechnical, and morphological character of the cliff and surface temperature

fluctuations (Luckman, 1976; Douglas, 1980; Dorren, 2003). The effects of the micro-scale activity, such as water content or the rate and intensity of freezing will be greater on cliffs composed of rocks with higher porosity and permeability (Whalley, 1984).

Water in the form of rapid snowmelt can also trigger rockfall when increasing temperature begin to melt large amounts of ice and snow, outside of freeze-thaw cycles, filling the cracks and joints and increasing pore pressure (Schneuwly, 2009). In the absence of freeze-thaw cycles, rockfall can be triggered by extreme meteorological events, such as heavy rainfall, winter storms, and wind storms (Dorren, 2003). While there is potential for rockfall to have only one trigger, often rockfall is triggered by a combination of two or more factors of frost-thaw action, rapid melting, and heavy rainfall (Nyberg, 1991; Schneuwly, 2009).

Other processes known to trigger rockfall include earthquakes (Bull and Brandon, 1998; Bull, 2004), root penetration and wedging (Wieczorek et al., 1995, 2000), and chemical weathering (Carson and Kirkby 1972). Chemical weathering alters the rock strength, promoting rockfall release by exogenic processes: thermal effects of granular disintegration, salt crystallization, and chemical weathering of weaker minerals (Carson and Kirkby 1972; Whalley, 1984; Matsuoka, 2008).

When common triggers such as precipitation, seismic activity, and freezing conditions are absent, cyclic and cumulative deformation of exfoliation sheets can trigger rockfalls from the thermal heating and expansion of rock surfaces (Coutard and Francou, 1989; Gunzburger et al., 2005; Collins and Stock, 2016).

Finally, human activity can destabilize rock slopes through equipment vibrations, undercutting of slopes for roads, or loading from infrastructure (Giardino, in review). In addition, humans and animals can detach loose rocks when climbing steep cliffs or slopes (Dorren, 2003).

2.1.2 Rockfall Movement

Rockfall analysis investigates the objective ‘hazard’ of the rockfall itself, and the associated ‘risk’. Hazard and risk are often used interchangeably, even though they do not have the same meaning. The ‘hazard’ is the source of potential danger associated with rockfalls, and includes aspects of the slopes geology and geomorphology (Varnes, 1978; White and Wait, 2008). ‘Risk’ is the chance or probability of rockfalls interacting or causing damage to human life or property (Schuster R. L., 1978; Ritter, 2001; White and Wait, 2008).

The initial detachment of a rock fragment is called “primary removal”. Resting material that begins to move after its original weathering, when heavy rain or snowmelt creates a mechanism for material transport is called “secondary removal” (Luckman, 1976; Whalley, 1984). A detached rock descending a slope is distinguished by different modes of motion, which mainly depends on the mean slope gradient. The three main modes of motion are freefalling, bouncing and rolling on a slope (figure 2).

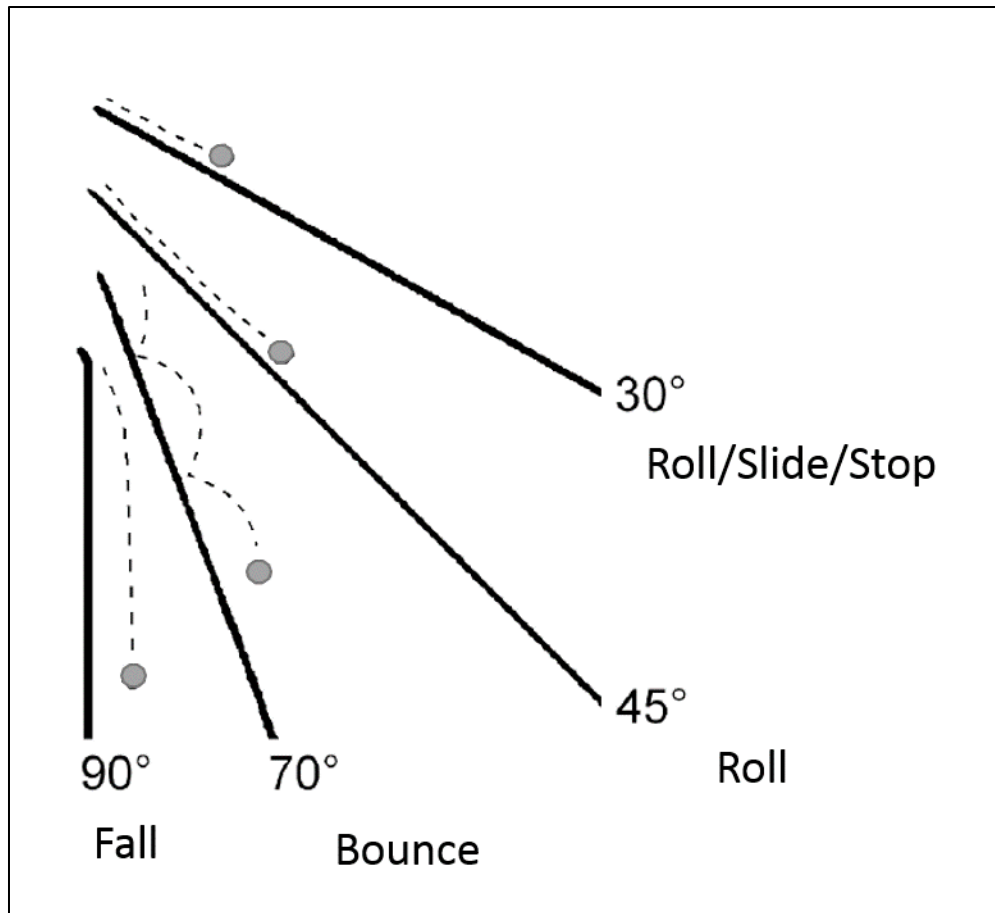


Figure 2 Rockfall modes of motion along a slope in relation to the mean slope gradients (modified from Dorren, 2003)

The location and type of movement of a rockfall on a slope is divided into three zones of the departure zone, transit zone, and deposition zone (Dorren, 2003; Schneuwly, 2009) (figure 3). The point where a rock fragment detaches from the slope is called the departure zone. A cliff slope of 70° is needed for a rock to fall (Dorren, 2003). A falling rock's initial impact with the surface of a slope is defined as a bounce and will generally break up into smaller pieces (Bozzolo and Pamini, 1986). The first impact will lose 75-86% of the initial energy gained from falling and is related to slope rock

hardness, slope saturation, and degree of loose material (Evans and Hungr, 1993). When the angle of a slope decreases to 45° , a bouncing rock will accumulate rotational energy and begin rolling. A rock will continue to lose energy as it descends a slope. The transit zone is the middle part of the slope where no primary removal occurs below the departure zone (Schneuwly, 2009). Rockfall material is 'passing through' the transit zone as the slope angle is too high for permanent storage. Resting material in the transit zone can be reactivated as secondary removal and continue down slope. When a rock comes to rest, it is deposited in the deposition zone, typically where the slope flattens to an angle of 30° (BUWAL et al., 1997). The exact critical angle however, is dependent on the rock shape (Azzoni et al., 1995).

The runout distance depends on the mean slope gradient, rock size, and slope cover (soil, talus/scree, and vegetation) (Azzoni et al., 1995). Larger rocks will tend to travel farther because they will have a higher kinetic energy than smaller rocks, which are more likely to be stopped by trees and large boulders (Dorren, 2003). Because of this, rockfall slopes will show evidence of clast sorting with smaller material depositing at the base of the cliff as a talus slope and larger boulders further down slope. On alpine slopes, large boulders may also be transported further down slope by avalanches so the boulder size and talus slope/ forested interaction should be carefully considered (Schneuwly, 2009).

The stopping of a rock is a process through which energy is lost through collisions and by friction. Friction is the result of rock shape and slope surface characteristics (BUWAL et al., 1997; Azzoni et al., 1995; Dorren, 2003). The friction

component is realized using the dynamic angle of friction (Kirkby and Statham, 1975) and the surface roughness (Chang, 1998; Andrew et al., 2012).

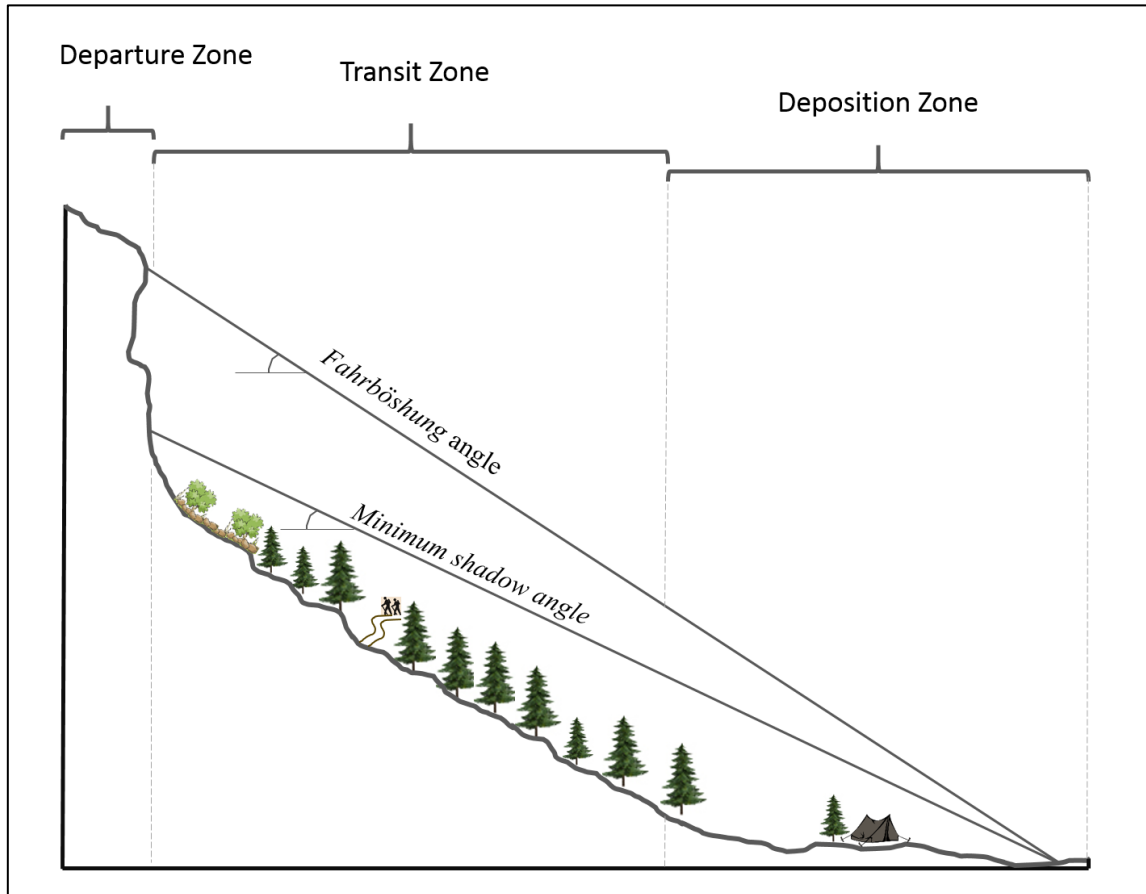


Figure 3 Schematic diagram of the Ouray rockfall slope under investigation subdivided into departure, transit and deposition zone with graphical representation of the “Fahrböschung angle” and the “minimum shadow angle” (modified after Buwal et al., 1997; Dorren, 2003; Schneuwly, 2009)

Experimental studies (BUWAL, 1997; Azzoni and Rossi, 1991) and reconstructions (Rickli et al., 2004; Dorren et al., 2006) suggest rockfall material could have average velocities $\sim 11 \text{ ms}^{-1}$ ($\sim 36 \text{ fts}^{-1}$), maximum velocities $\sim 30 \text{ ms}^{-1}$ (98 fts^{-1}), and

large boulders reaching rebound jump distances of ~30 m (~98 ft) and average heights of 1.5 m (5 ft), max. 8 m (26 ft).

Rockfall movement tends to be most frequent along the gullies of steep slopes (Whalley, 1974). Gullies and large cracks originate from 'residual' stresses in the mountain as a result from orogenic activity (Hast, 1969). Gullies collect rain and snowmelt as a channelized flow and isolating the erosive force of the water to a limited area. The collected water also saturates into the surrounding rocks inducing increased weathering, specifically suitable for freeze-thaw conditions. Because of this, primary removal/rockfall is more likely in gullies. In addition, gullies provide and collect small talus material which can be activated or reactivated as secondary removal from the rockfall impact of previously weathered rocks (Caine, 1974; Whalley, 1984). Thus, rockfall activity in gullies are frequent and provide an abundance of small talus material down the steep slope. In contrast, buttresses are much larger and rarer falls due to the complex nature of the forces and stresses applied to the rock slope (Hast, 1969; Whalley, 1984).

2.1.3 Rockfall Modeling

Rockfall modeling of calculating runout zones began as a way to satisfy the general principle of hazard mapping procedure: a) determine the location of the hazard potential and departure/release zones, and b) estimate maximum run-out distances (Berger and Dorren, 2006; Berger et al., 2013). The differing models aim to understand how falling rocks move along a slope and estimate run-out distances. The three most

common methodologies for rockfall modeling include empirical models, process-based models and GIS-based models (Dorren, 2003; Berger et al., 2013)

Empirical methods are commonly used for identifying potential release and propagation zones based on the relationships between topographical factors and maximum rockfall run-out distances (Dorren, 2003; Berger et al., 2013). Probabilistic empirical models use analysis of past databases (Berger and Dorren, 2006). Heim (1932) introduced the *Fahrböschung* angle, or the Energy Line Angle (ELA) which states: for any rockfall, there is a specific slope angle between a horizontal plane and a straight line that connects the top of the rockfall source to the stopping point (figure 3). Evans and Hungr (1993) proposed the *minimum shadow angle* as an alternative method. The *minimum shadow angle* is the angle between a horizontal plane and a straight line connecting the point where the base of a cliff intercepts a talus slope and the longest run-out boulder (figure 3). Evans and Hungr (1993) suggests a *minimum shadow angle* of 27.5° for maximum rockfall run-out distances.

In addition to empirical methods, process-based methods model the modes of motion along a slope surface (Dorren, 2003). With the advent of modern technologies, these empirical and process-based methods can be simulated rockfall motion and its interaction with the slope surface in three-dimensional space (GIS-based models). GIS-based models identify the source area, determines the falltrack, and calculates the run-out zone (Hegg and Kienholz, 1995).

2.2 Hazard Assessment

The hazard analysis and risk assessment of rockfall has received increased interest over the last couple decades. A successful hazard assessment will investigate: the special extent of where rockfall occurs, rock-fall frequency and magnitude, and potential triggering mechanisms (Schneuwly, 2009).

Many techniques have been applied to gather data assessing rock fall activity. Lichenometry is used to compare lichen size to annual growth rates (Luckman and Fiske, 1995). Lichenometry assumes the largest lichen growing on a surface is the oldest. Thus, if growth rates are known, the minimum age of when a rock was deposited can be estimated from the maximum lichen size (Bull and Brandon, 1998, Bull, 2004, Porter and Orombelli, 1981). Mapping and dating of rockfalls by studying lichen growing on the surface of boulders and talus has been successfully carried out by (Hale, 1967; Carrara and Andrews, 1973; Porter and Orombelli, 1981; Luckman and Fiske, 1995; Bull and Brandon, 1998; Bull, 2004).

Nesje et al. (1994) used another method in dating rockfall deposits by identifying unique weathering indicators as a response to hammer impact. Others such as Bjerrum and Jorstad (1968) and Douglas (1980) measured qualitative and quantitative results of rockfalls by collecting fallen material on large tarps or blankets and recording rock type, size, and distribution of size over a set period of time and statistically applying a variable mean in monthly increments over the course of a year.

In recent years, dendrogeomorphic techniques have been applied in rockfall reconstructions to establish specific rockfall rates (Stoffel et al., 2005b; Stoffel & Bollschweiler, 2008; Stoffel, 2006; Schneuwly et al., 2009).

As a result of roads being constructed in areas of steep terrain where rockfall is common, many local and state governments have developed hazard rating systems to assess the local hazardous conditions of roadways and populous areas. The Colorado Department of Transportation (CDOT) developed the Colorado “Rockfall Hazard Rating System” or “RHRS” (Andrew, 1994; modified by Russell, 2005; Russell et al., 2008). This approach ranks the dominating factors (geology, slope morphology, rockfall volume or triggering factors) that contribute to rockfall (table 1) and categorizes rock slopes to produce an overall hazard rating (Patrick and Manitou-Alvarez). The Colorado RHRS was originally designed to assess the rockfall hazards to roads and state highways. Authors such as (Guzzetti et al., 2003; Jaboyedoff and Labiouse, 2003; Patrick and Manitou-Alvarez) have modified these rating systems to emphasize the hazards associated with the slope, climate, and geological characteristics.

Table 1 The Colorado Department of Transportation (CDOT) “Rockfall Hazard Rating System” or “RHRS” (from Russell, 2005)

Colorado Rockfall Hazard Rating Field Worksheet						
Sight Information						
ROUTE NO.	SEGMENT ID NUMBER	ENGINEERING REGION	MAINTENANCE SECTION	DATE		
COUNTY	BEGIN MILE POST	END MILE POST	R. / L. OF CENTERLINE	RATER		
Actual Values		Remarks				
Slope Height	Ditch Depth	Major rockslide potential:				
Slope Angle	Sight Distance	Dominating rockfall mode: Block-in-matrix / Sedimentary rock / Crystalline rock				
Ditch Slope	Speed Limit	Dominating sight distance: Horizontal / Vertical				
Ditch Width	ADT	Mitigation effectiveness: A B C D F				
Rating Cut Slope / Total Slope (Circle one)						
		3 Points	9 Points	27 Points	81 Points	
Slope	Slope Height	25 to 50 ft	50 to 75 ft	75 to 100 ft	>100 ft	
	Rockfall Frequency	> 2 years	1 to 2 years	Yearly, seasonal	Year round / severe events	
	Average Slope Angle Score	0 to 2	2 to 4	4 to 8	> 8	
	Launching Features	None (smooth slope)	Minor (< 2 ft. surface variation)	Many (2 to 6 ft. surface variation)	Major (> 6 ft. surface variation)	
	Ditch Catchment	95% to 100% / Class 1	65% to 94% / Class 2	30% to 64% / Class 3	< 30% / Class 4 / ≥ Major launching features	
Climate	Annual Precipitation	< 10 inches	10 to 20 inches	20 to 35 inches	> 35 inches	
	Annual Freeze Thaw Cycles	1 to 5	6 to 10	11 to 15	16 or more	
	Seepage / Water	Dry	Damp / wet	Dripping	Running water	
	Slope Aspect	N	E, W, NE, NW	SE, SW	S	
Geology	Sed. Rock	Degree of Under-Cutting	0 to 1 ft	1 to 2 ft	2 to 4 ft	> 4 ft
		Jar Slake	6	5	3 to 4	1 to 2
		Degree of Interbedding	1 to 2 weak interbeds, < 6 in.	1 to 2 weak interbeds, > 6 in.	> 2 weak interbeds, < 6 in.	> 2 weak interbeds, > 6 in.
	Crys. Rock	Rock Character	Homogeneous / massive	Small faults / strong veins	Schist / shear zones < 6 in.	Weak pegmatite / micas / shear zones > 6 in.
		Degree of Overhang	0 to 1 ft	1 to 2 ft	2 to 4 ft	> 4 ft
		Weathering Grade	Fresh	Surface staining	Slightly altered / softened	Core stones
	Discontinuities	Block Size / Volume	<1 ft / <1 cy	1 to 2 ft / 1 to 3 cy	2 to 5 ft / 3 to 10 cy	>5 ft / >10 cy
		Number of Sets	1	1 plus random	2	> 2
		Persistence, Orientation	< 10 ft and dips into slope	> 10 ft and dips into slope	< 10 ft and daylight out of slope	> 10 ft and daylight out of slope
		Aperture	Closed	0.1 to 1 mm	1 to 5 mm	> 5 mm
		Weathering Condition	Fresh	Surface staining	Granular infilling	Clay infilling
		Friction	Rough	Undulating	Planar	Stickensided
	Block in Mat.	Block Size (x3)	< 1 ft	1 to 2 ft	2 to 5 ft	> 5 ft
		Block Shape (x3)	Tabular	Blocky	Blocky to angular	Rounded and smooth
		Vegetation (x3)	Fully vegetated	Patchy vegetation	Isolated plants	None
Total Hazard Score:						
Traffic	Sight Distance	> 80 %	60 % to 80 %	40 % to 60 %	< 40 %	
	Avg. Vehicle Risk	0 to 24%	25 to 49%	50 to 74%	75% or more	
	No. of Accidents	0 to 2	3 to 5	6 to 8	9 and over	
Total Risk Score:						
Additional Rater's Comments:						

CHAPTER III

STUDY AREA

This chapter provides an overview of the investigated study area; the location of the study site; how to access the site; and an overview of its geology, geomorphology, climate, and vegetation.

3.1 Study Area

The study area is located ~2.4 km (~1.5 miles) northeast of the town of Ouray, (38°1'24"N, 107°40'20"W) Colorado, United States (figure 1). The study area encompasses the National Forest Service campground at an elevation of 2,580 m (8,470 ft).

Access to the study area from Ouray, CO, is provided by county road 16 off of State Highway 550. The investigated forest, as outlined by the thin dashed line in figure 4 is located between 2,560 and 2,660 m (8,400 and 8,730 ft) elevation northeast of the campground and has an area of 43,500 m² (468,230 ft²).

3.2 Geology and Geomorphology

The steep slopes surrounding the campground is covered by Quaternary talus overlying Pleistocene landslide material composed of San Juan tuff mixed with glacial deposits. Talus material is derived from the nearby bedrock escarpment composed of Pennsylvanian – Tertiary sediments (figure 5, figure 6). The entire study area noted by the bolded dashed line of figure #, which includes all departure and deposition zones, covers ~ 325,500 km² (3,501,527 ft²).

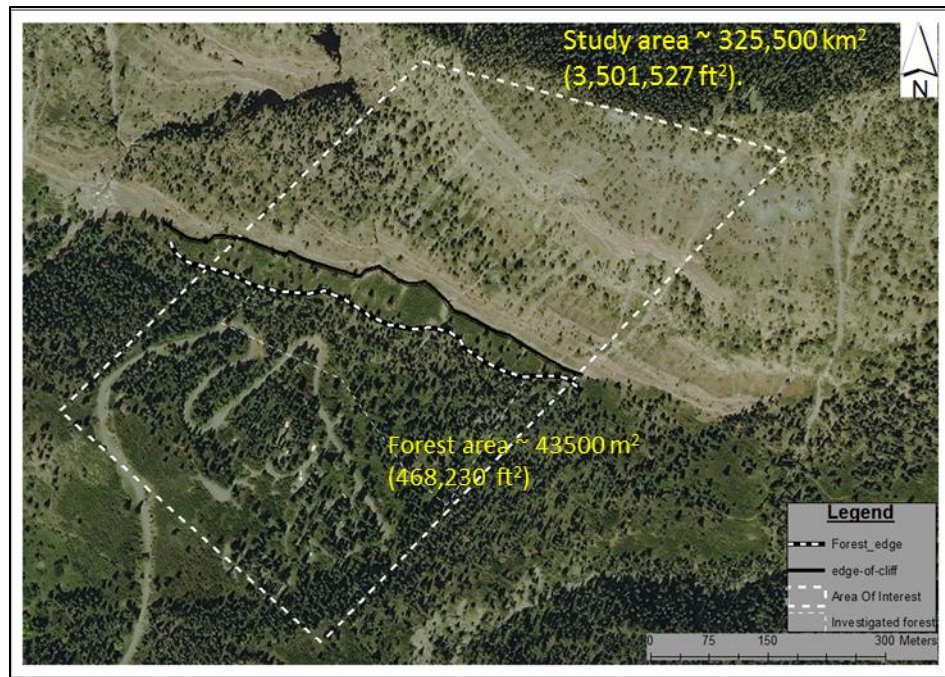


Figure 4 Study area is located in the San Juan Mountains of southwestern Colorado, east of Ouray, as denoted by bold black dashed line

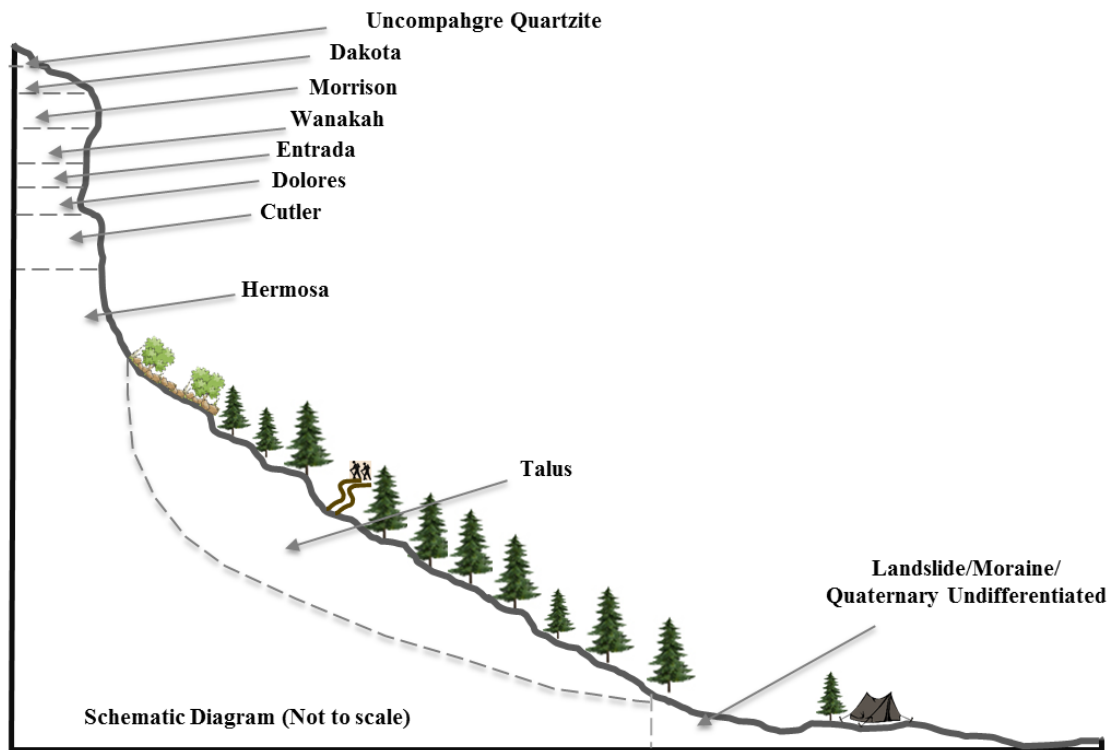


Figure 5 Schematic diagram illustrating key slope components

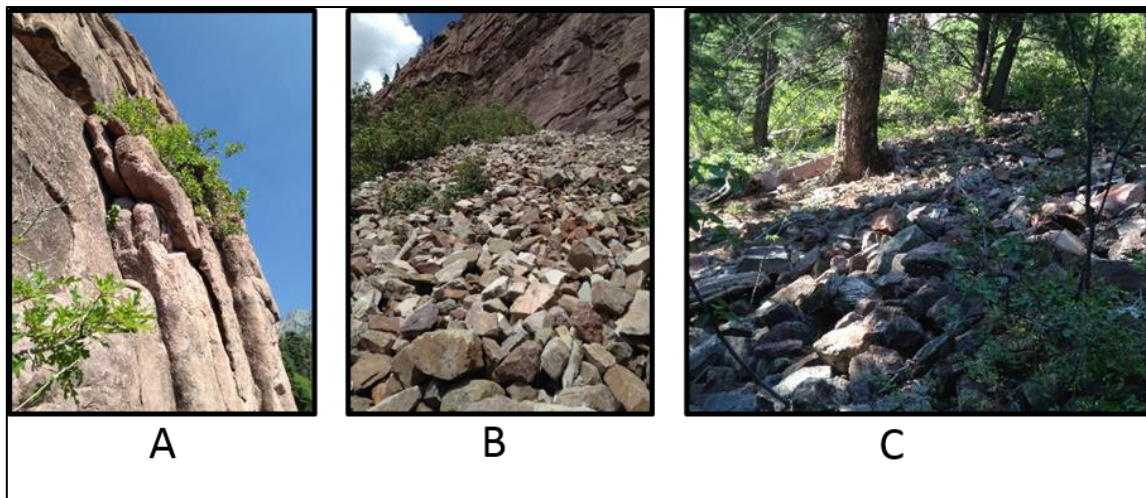


Figure 6 (A) Fractured Sandstone and interbedded limestone and shale cliff is the source of the rockfalls; (B) Talus buildup into steep slopes; (C) Vegetated slopes acting as a protective forest to falling debris (Photos by Author)

Rocks are being detached from a ~430 m (~1,400 ft) thick section of intervening cliffs, slopes and ledges of various sedimentary lithologies (figure 5; figure 6; figure 7, figure 8) (Cross et al., 1907; Luedke and Burbank, 1962; Franczyk, 1993; Luedke and Burbank, 1994). The base of the cliff/talus slope is ~80 m (~260 ft) of cliff forming massive red-pink gritty channelized-sandstone, siltstone and shale of the middle member Pennsylvanian Hermosa formation ($\mathcal{P}h$). Also present are occasional interbedded thin red and gray fossiliferous shales and limestone. This unit has higher concentrations of feldspathic and conglomeritic sandstones and micaceous shales. The middle Hermosa is highly fractured providing evidence for differential weathering and possible frost-wedging (figure 6 A).

The upper Hermosa is ~90 m (~ 300 ft) thick and grades from greenish-gray ledges and cliffs of thin- to thick-bedded, red arkosic, coarse-grained sandstone and conglomerate to partially vegetated, scree slope conformable with the overlying Permian Cutler formation (Pc).

Within the study area, the Cutler is mostly identified as partially vegetated talus/scree slopes of the northeast and benches and cliffs to the southwest. The upper contact with the overlying Triassic Dolores formation (T_{RD}) is an angular unconformity. The nearly 60 m (200 ft) thick section pinches out to zero to the east. Where exposed, the Cutler crops out as benches and cliffs of thin to massive bedded pink to reddish-brown shales, siltstones and sandstones. The Cutler also has conglomerate beds of pebbles and cobbles with very little interstitial material. Conglomerate material is

predominantly Precambrian metamorphic and igneous rocks as well as, limestone derived from the older underlying rocks.

The overlying Triassic Dolores formation crops out as 12-24 m (40-80 ft) of steep rubble covered slopes or cliffs and benches due to its variable lithology. The Dolores is composed of sandstone and siltstone with minor mudstones, limestones and conglomerates. The thin beds of sandstone are reddish-brown and the thick beds of massive sandstone are mottled red and white. The mudstone is reddish-brown, green and yellow and the limestones and reddish-brown conglomerates are on average .3 m (1 ft) thick.

The steep to rounded white cliffs above the Dolores is the Jurassic Entrada Sandstone formation (Je). The Entrada is a friable, calcareous, fine-grained quartz sandstone with thick to massive crossbedding. The sandstone is observed to be 12-24 m (40-80 ft) thick within the study area.

The entrada is overlaid by the Jurassic Wanakah formation (Jw) which crops out as a cliff in lower part and gentle to steep slopes in upper part. Luedke and Burbank (1962, 1994) broke this unit into three members: the lower limestone and breccia (Pony Express limestone member), a middle sandstone (Bilk Creek sandstone member), and an upper marl-mudstone (Marl member). The lower member is composed of thinly bedded dark gray/black limestone and interbedded black bituminous shale. The upper part of the Bilk Creek member contains nodular gypsum surrounded by dark black shale and porous breccia. The middle member contains greenish-gray, silty or fine grained, calcareous sandstone and greenish shales. The sandstone is very friable except where mineralized

and contains a thin resistive bed of greenish-gray medium grained sandstone with jasper grains that is common among the fallen talus and alluvium debris in the forest stand. The upper marl member is composed of thin-bedded, reddish-brown, calcareous mudstone-siltstone, interbedded with fine sandstones and nodular crystalline limestones. Much like the middle member, the upper Wanakah also contains a greenish bed of silty limestone with jasper grains and green chert. The Wanakah is 12-24 m (40-80 ft) within the study area.

The contact between the Wanakah and overlying Jurassic Morrison formation (Jm) is marked by a line of trees where the steep cliff grades into ledges, cliffs, and steep slopes partially covered by a soft layer of weathered rock and soil. The Morrison at this location is ~210 m (700 ft) thick and can be broken into two lithologic units, the lower Salt Wash sandstone member, and the upper Brushy Basin shale member. The lower Salt Wash is a fine to medium-grained sandstone with interbedded mudstones and the occasional limestone bed. Lenticular- and cross-bedding is common within the lower Salt Wash. Joint surfaces are sometimes covered by carbonates. The sandstones are yellowish white, yellowish brown and pink and in situ weathered surfaces are often covered in “bluish-black desert varnish”. The number of mudstone layers and their thickness increase in the upper part of the Salt Wash member and grades into the upper Brushy Basin shale member. The Brushy Basin member is a calcareous mudstone with interbedded fine sandstones and limestones.

The Pack trail crosses the top of the ridge at ~3,078 m (~10,100 ft) through the slightly weathered cliffs of the Cretaceous Dakota Sandstone formation (Kd). The cliffs

have thin to massive lenticular, cross-stratification and graded sandstone beds. The sandstones are yellowish gray, and yellowish white and locally ~30 m (~100 ft) thick. The Dakota at this location is heavily vegetated.

The Dakota is uncomfortably overlaid by a Porphyritic Granodiorite (gp) associated with the Laramide orogeny during late Cretaceous-early Tertiary. It is uniform in composition and texture and is 12-30 m (40-100 ft) thick and thickens outside of the study area.

Much of stratigraphy is covered to the east of the study area by Pleistocene landslide deposits mixed with alluvium and glacial till. Several large gullies have formed along the steep slopes and cliffs cutting through the multiple lithologies. These gullies act to channelize runoff from storms and meltwater and are prime examples of the variability of the different rock type's resistivity.

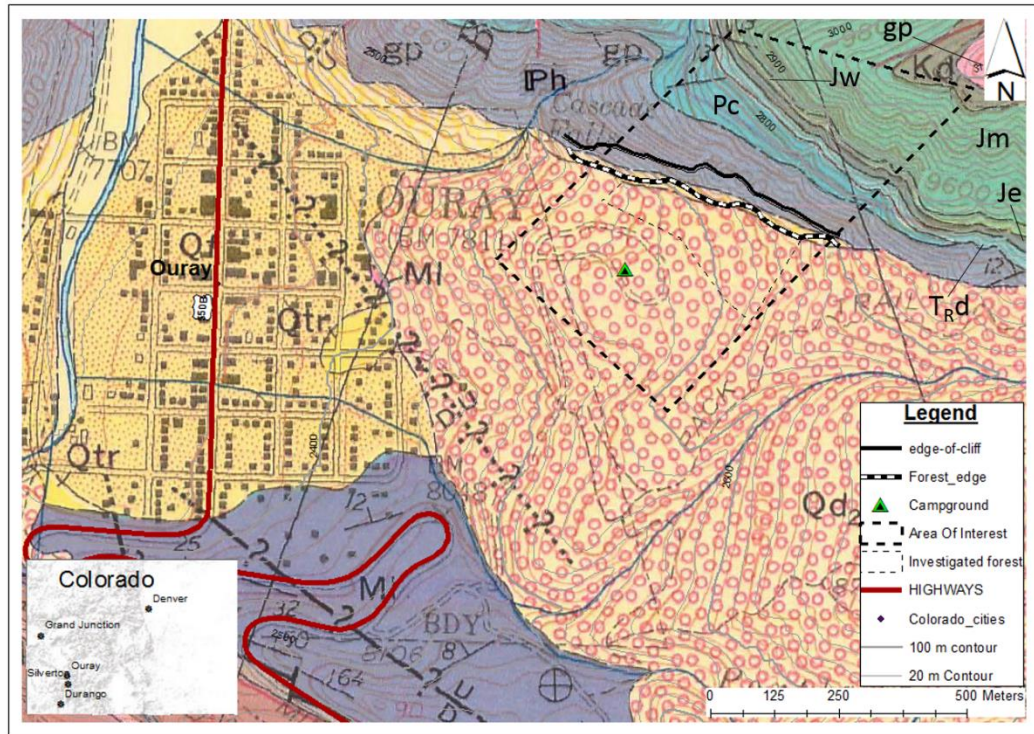


Figure 7 Geologic map of Ouray, Colorado and the study area (modified after Luedke and Burbank, 1962)

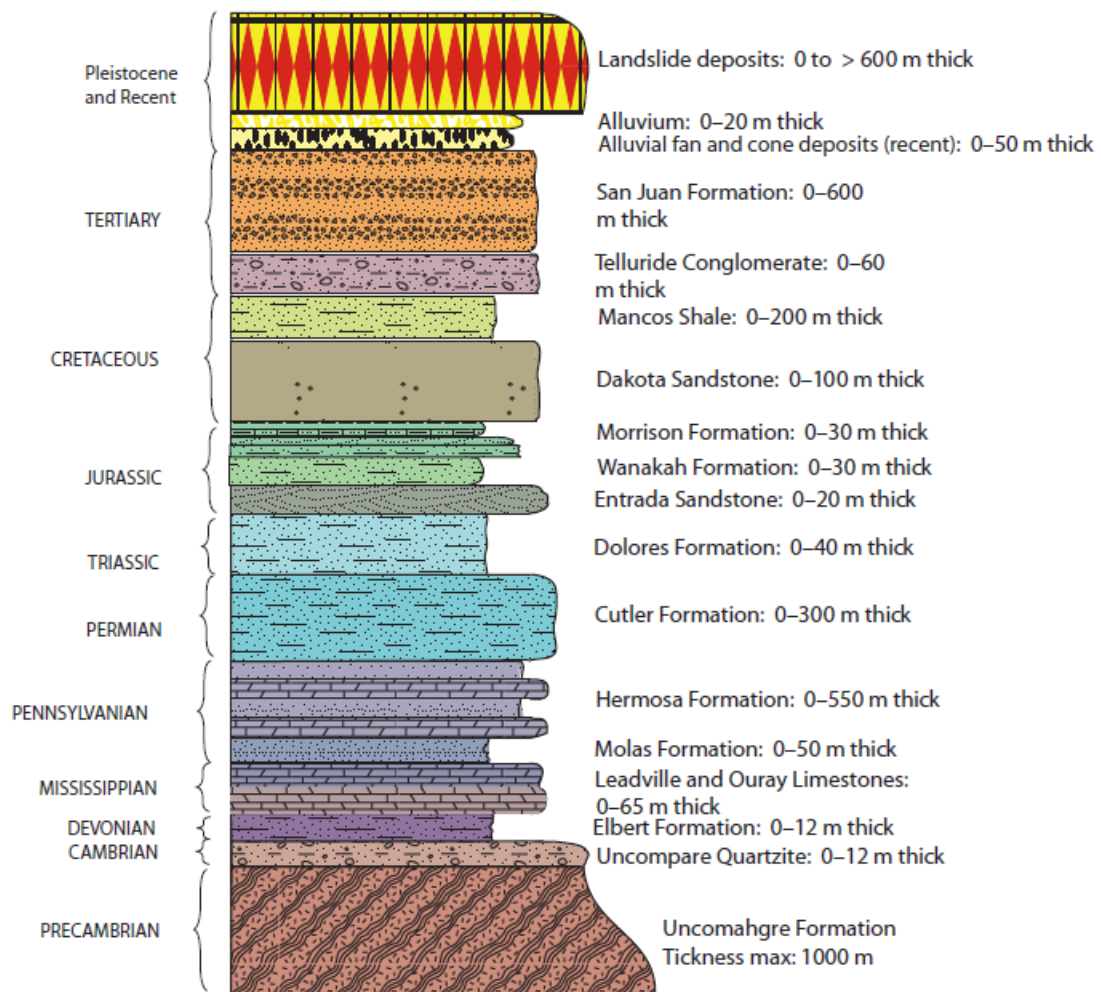


Figure 8 Stratigraphy of the Ouray, Colorado quadrangle (from Reed, 2013)

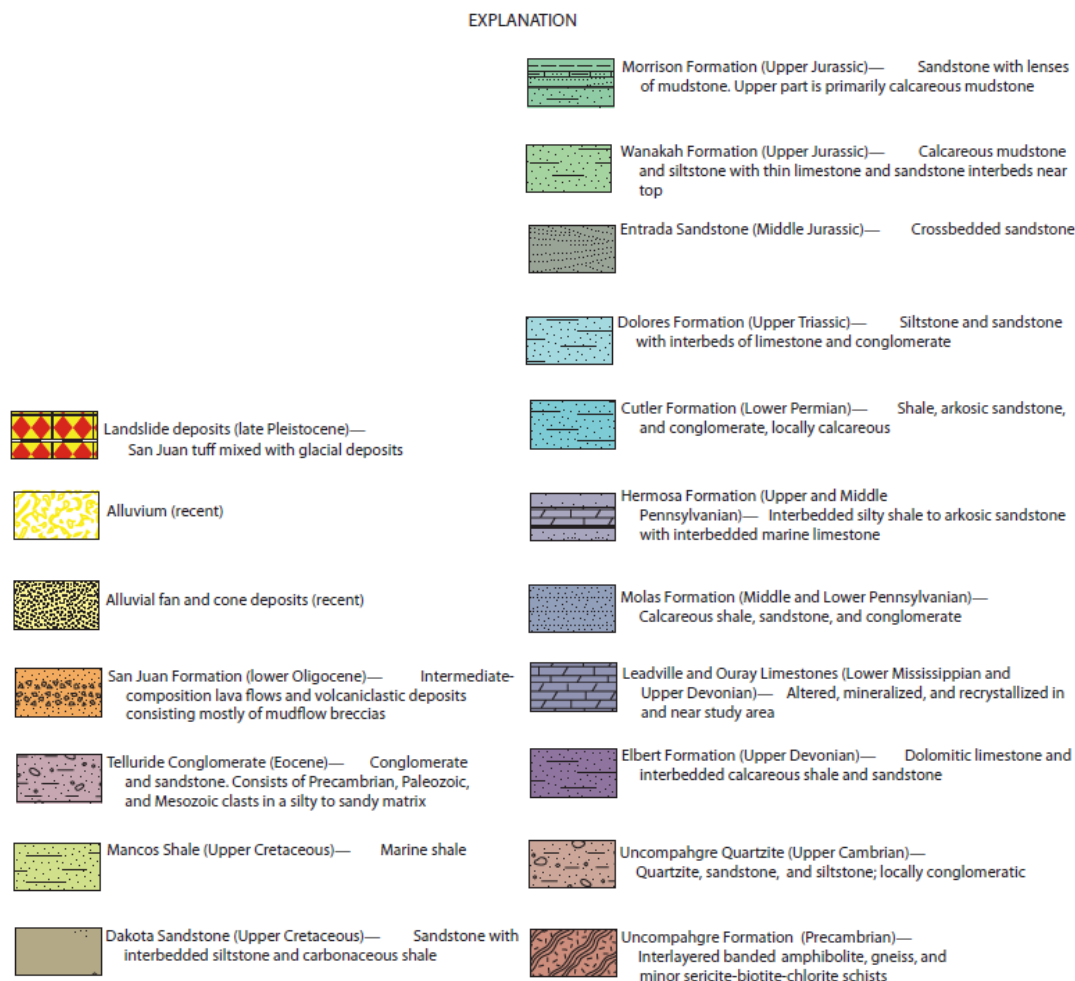


Figure 8 Continued

3.3 Climate

The climate of Ouray is humid continental and has four distinct seasons. Temperature and precipitation are slightly increased at higher elevations (Ouray, 2008). The annual average length of the day is 12.7 hours (NOAA, 2013). Table 2 provides monthly climate summaries for Ouray. Average annual max. temperature C° (F°) for Ouray is 13.7° (56.6°) and average annual min. temperature is 0° (32°). Total annual precipitation based on monthly averages is 23.1 m (75.8 ft) and total annual snowfall

based on monthly averages is 140.2 m (460 ft) (NOAA, 2013). Figures (9 and 10) show Ouray's daily temperature averages and extremes. The coldest months in Ouray are December, January, and February. The last freeze usually occurs late May to early June. The warmest months in Ouray are June, July, and August. Overall, daily temperature fluctuates ~25 ° F.

Annual precipitation is ~ 100 cm (40 in) in the high mountainous regions near Ouray, however, is ~ 30-40% of precipitation is snowfall (WRCC, 2015; Ouray, 2008). Much of the rainfall occurs during the spring, summer, and early fall. The rainfall's duration and intensity is highly dependent on the "southwest monsoon" from mid-July to late August. Ouray, on average experiences more rainfall from the seasonal monsoon during La Nina years (WRCC, 2015; Ouray, 2013). More information regarding notable historic and recent floods can be found at the Storm Events Database -National Climatic Data Center (<http://www.ncdc.noaa.gov/stormevents/>).

Table 2 Monthly climate summaries for the two weather stations in Ouray, Colorado from 06/01/1893 to 01/20/2015 (Source: Western Regional Climate Center, wrcc@dri.edu)

OURAY, COLORADO (056203) & (056205)													
Period of Record Monthly Climate Summary													
Period of Record : 06/01/1893 to 01/20/2015													
	Jan	Feb	Mar	Apr	May	Jun	Jul	Aug	Sep	Oct	Nov	Dec	Annual
Average Max. Temperature (F)	35.95	38.2	45.85	53.55	63.1	75.15	79.15	76.85	70.6	59	46.45	36.4	56.65
Average Min. Temperature (F)	14.35	16.65	22.9	29.5	37.25	45.8	51.85	50.8	44.1	33.75	24.1	16.25	32.3
Average Total Precipitation (in.)	1.64	1.84	2.22	2.44	1.865	1	2.625	2.25	1.865	2.035	1.58	2.16	23.52
Average Total SnowFall (in.)	25.65	27.7	32.65	22.8	6.8	0.15	0	0	0.15	6.1	18.45	31.45	171.8
Average Snow Depth (in.)	9	11	7.5	2	0	0	0	0	0	0	2	6	3
Source: Western Regional Climate Center, wrcc@dri.edu													

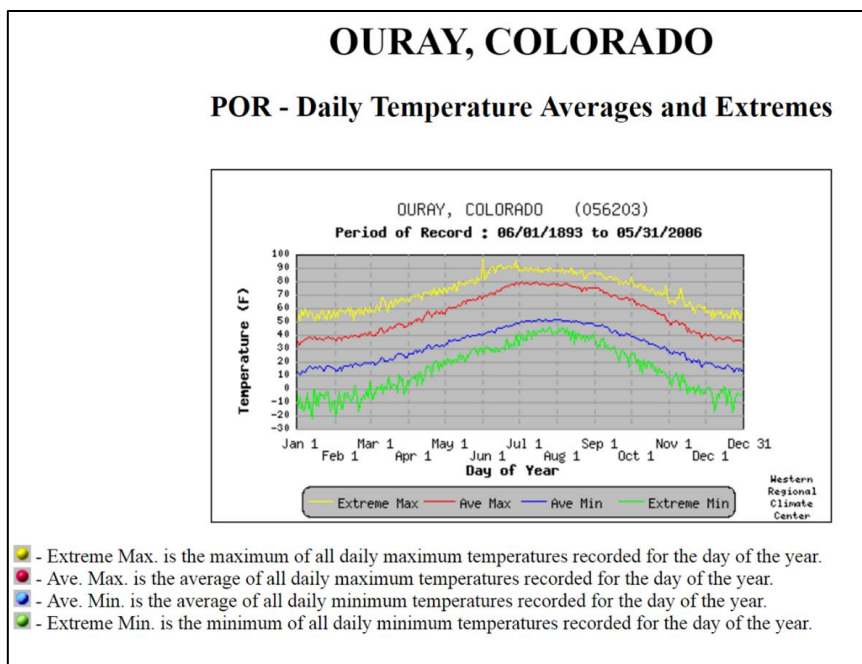


Figure 9 Daily temperature averages and extremes for weather station (056203) from 06/01/1893-05/31/2006 (WRCC, 2013).

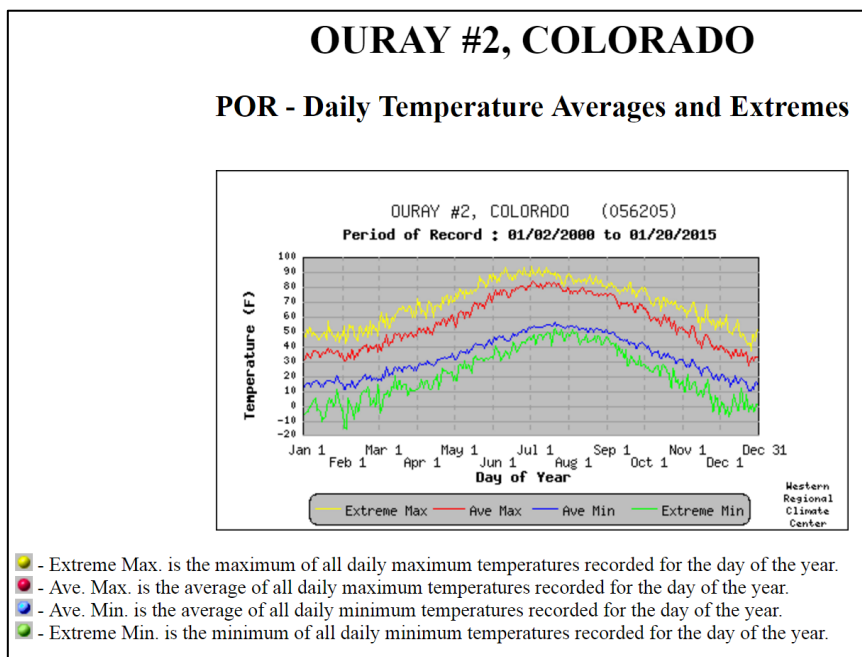


Figure 10 Daily temperature averages and extremes for weather station (056205) from 01/02/2000-01/20/2015 (WRCC, 2013).

Figures 11 and 12 show snowfall and snowdepth averages and extremes for Ouray from 1893 to 2016. Winter storms can produce high winds, extreme temperatures, and deposit large volumes of snow in a short period of time. Large winter storm events can detach boulders from cliffs or initiate movement of unconsolidated rock fragments on steep slopes. Notable winter weather events can be found at (SHELDUS, 2013; Ouray, 2008). Notable wind storms, excluding winter storm events, usually occur between the months of April and September (SHELDUS, 2013; Ouray, 2008).

Colorado has experienced periods of significant drought in 1890-1894, 1898-2004, 1930-1940, 1950-1956, 1974-1978, 1980-1981, 1989-1990, 1994-1997, 2000-2006, and 2010-2013 (State of Colorado Drought Mitigation and Response Plan, 2013; Drought and Water Supply Assessment, 2004). Droughts can inhibit tree growth and destabilize root structures (Shroder, 1978). Colorado experienced notably dry winters during 1976-1977 and 1980-1981 (Drought and Water Supply Assessment, 2004). Ouray County experienced multi-year droughts from 2000-2006 and 2010-2013 (Fuchs and Bathke, 2016). Notable recent droughts occurred during the summer of 2002, and from 2010-2013 (State of Colorado Drought Mitigation and Response Plan, 2013; Fuchs and Bathke, 2016).

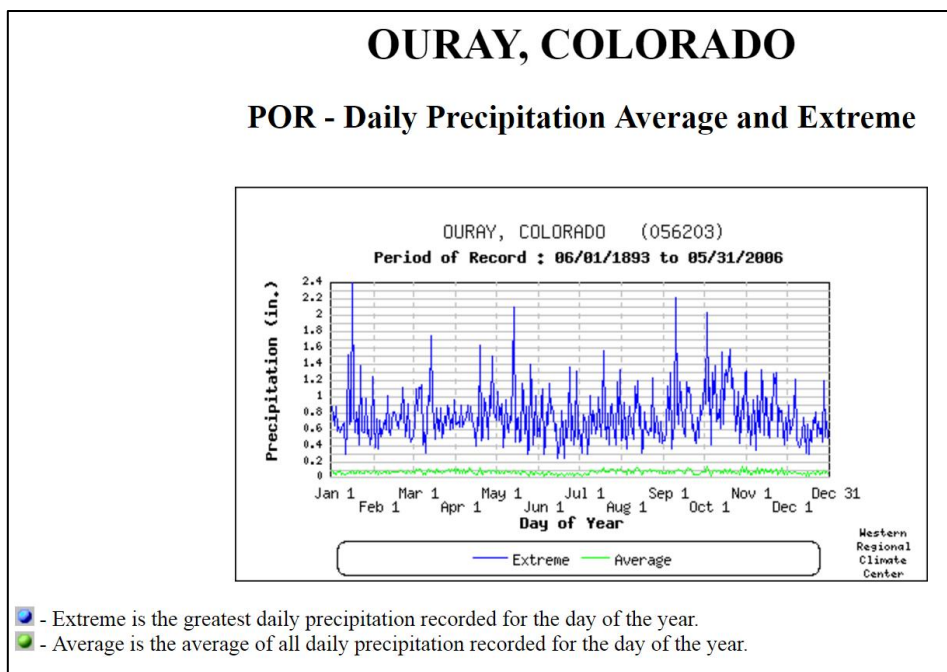


Figure 11 Daily precipitation averages and extremes for weather station (056203) from 06/01/1893-05/31/2006 (WRCC, 2013).

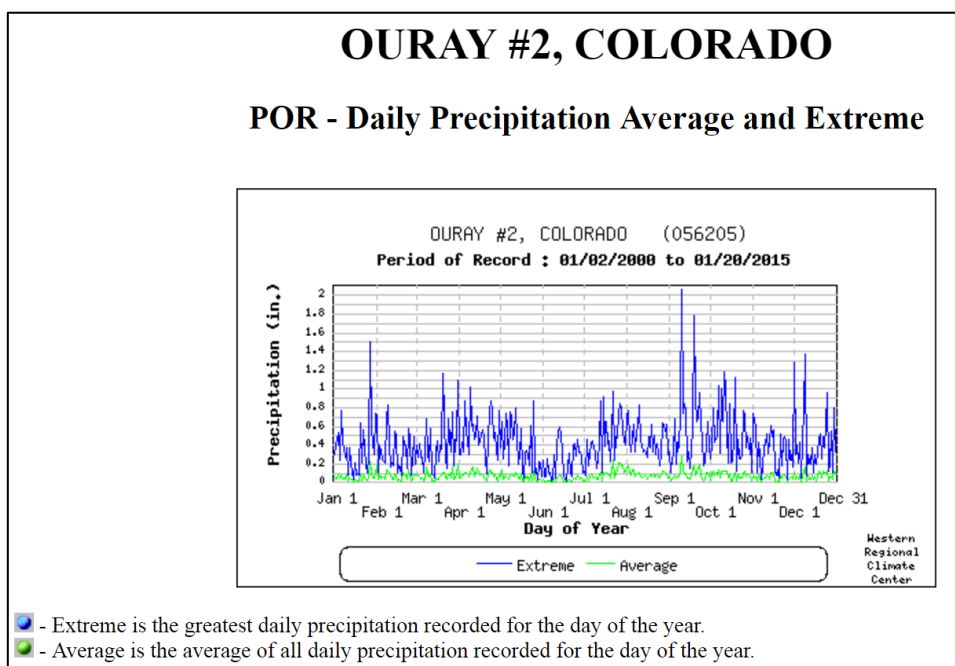


Figure 12 Daily precipitation averages and extremes for weather station (056205) from 01/02/2000-01/20/2015 (WRCC, 2013).

3.4 Vegetation

The investigated forest stand is approximately 43,500 m² (468,230 ft²) and has moderate to high vegetation cover. The forest is predominately *Abies concolor* (White fir), *Pseudotsuga menziesii* (Douglas fir), *Picea pungens* (Blue spruce), a few *Pinus ponderosa* (Ponderosa pine), *Picea engelmannii* (Engelmann spruce), *Abies lasiocarpa* (Subalpine fir), and dwarf stands of *Quercus gambelii* (Gambel oak or Oak brush).

The forest floor is relatively clear and easy to navigate through, consisting primarily of fallen fir and downed logs and snags of White fir (*Abies concolor*). Navigation became extremely difficult through areas with dense stands of Gambel oak or Oak brush (*Quercus gambelii*), typical of the proximal talas slope and areas with limited canopy coverage. This advantageous growth likely a result of the removal of larger vegetation from mass-movement events or beetle infestations.

3.4.1 Lichen

The five dominant species of lichen in Ouray are *Lecidea atrobrunnea* (brown crustose), *Lecanora thomsonii* (pale green foliose), *Parmelia spp.* (plae green fruticose), *Xanthoria elegans* (orange foliose), and *Rhizocarpon geographicum* (green crustose) (Hale, 1967; Carrara and Andrews, 1973).

3.5 Temporal Record of Activity

Two reports compiled for the city of Ouray (2008, 2013) and Jochim (1986) document notable debris flow events in the vicinity of Ouray, Colorado, that occurred in 1878, 1909, 1927, 1929, 1951, 1965, 1971, 1973, 1981, 1982, 1988, 2002, 2003, 2005, 2008, 2010, and 2013. The events of 1929, 1981 and 1982 were particularly wide spread

and devastating. The Colorado Geological Survey's (CGS) 2002 Landslide Mitigation Plan Update p. 3-190 listed the City of Ouray as a "Tier one debris flow area" and "needing immediate or ongoing action or attention because of the severity of potential impacts".

Active faulting in the region creates the potential for earthquake induced rockfalls. Notable earthquakes with epicenters in Ouray County or the neighboring San Miguel and Hinsdale Counties include 1894, 1897, 1913, 1955, 1960, 1962, 1967, 1970, 1989, 1994, 2006, and 2013. (Colorado Earthquake Evaluation Report, 2007; Colorado Geological Survey, 2015; Ouray, 2008, 2013) The strongest earthquakes occurred during 1913 and 1960 with reports of rocks rolling down the steep slopes and cliffs surrounding Ouray (Ouray, 2013).

The Ouray County Multi-Hazard Mitigation Plan (Ouray, 2013) lists areas at risk for landslides and rockfalls. Records of rockfall activity usually occur along roadways, specifically highway 550, as the increase traffic will record more events. Other areas, such as the study site considered for this assessment will require an alternative approach to create a record of rockfall activity.

CHAPTER IV

METHODS

Chapter IV presents the methodology used in this thesis and recaps specific techniques used in the field and in the lab. The reader is provided criteria for site selection, procedures for core extraction and associated tree-ring analysis, and descriptions of the dendrogeomorphic approaches considered for this assessment (figure 13).

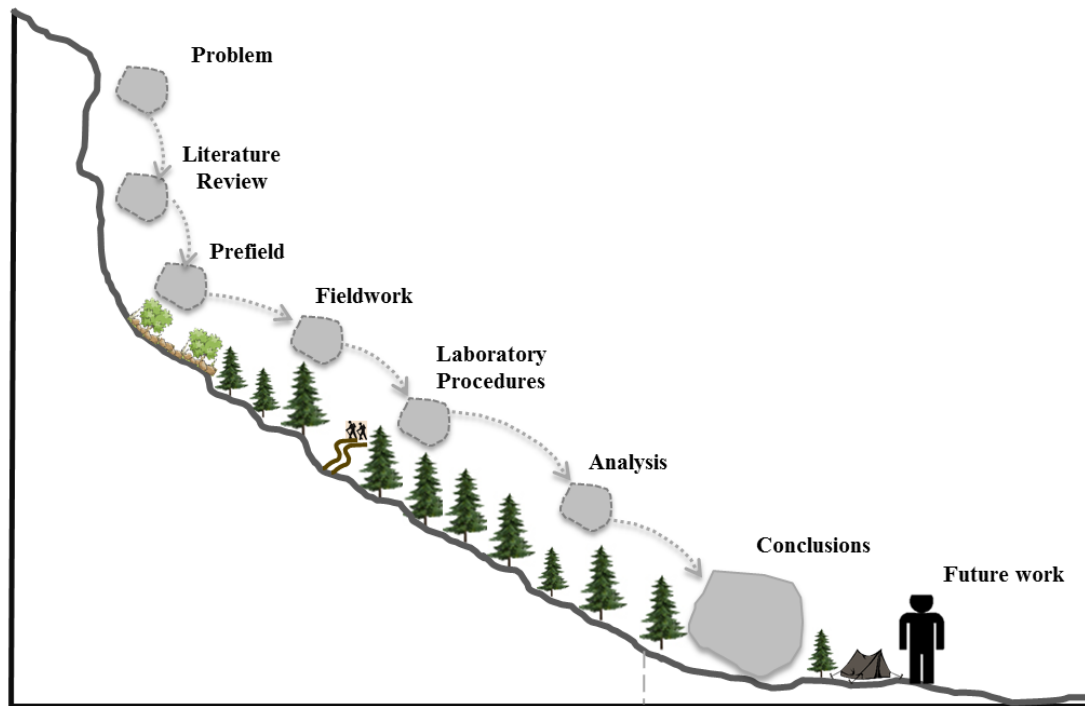


Figure 13 Diagram illustrating the methodology process

4.1 Dendrogeomorphology

The term 'dendrogeomorphology' was coined by Alestalo (1971) and stands for the analysis of growth reactions of trees affected by geomorphological processes by

dendrochronological methods (Alestalo, 1971). Annual tree-ring growth is initiated in the cambium as phloem and xylem cells differentiate. The internal heterogeneity of the tree rings are a result of the variations in the cell sizes and cell-wall thickness. The initial spring-time growth termed ‘earlywood’, is characteristic of large thin-skinned cells.

Earlywood growth is followed by ‘latewood’ growth nearing the end of the growing season with cells tending to flatter and thick-skinned cell walls (Shroder, 1978). Annual ring growth can be altered where the sequence is missing a ring or contains a false ring if normal growing conditions are interrupted (Schweingrober, 1996).

4.1.1 Identifying Tree Types

Trees are either coniferous or deciduous, and exhibit unique growth rituals.

Deciduous trees produce new leaves every spring after dropping them in fall, and remain leafless in winter. Deciduous trees grow in nutritious soil in temperate climates and have broadleaves, where the thin large surface can collect large amounts of sunlight for photosynthesis. Deciduous trees are commonly referred to as “hardwood”. Coniferous trees produce seed-bearing cones and are typically needle leaved evergreens (Strunk, 1997). Conifers grow in areas with nutrient poor soils and extreme environments. The needles are small and durable as they retain their needles for photosynthesis year round. The steep slopes and shallow soils of landslide materials on the Ouray, Colorado Amphitheater are typical for coniferous trees. The conifer species observed in this study are pine, fir and spruce trees. Tree species are differentiated using standard botanical techniques (Petrides and Petrides, 1992).

Abies concolor (White fir) wood is light, soft, weak, deteriorates shortly after death and is usually not sought out for its lumber. It has wide annual tree rings and lighter colored sapwood. *Abies concolor* typically has a slow growth rate and medium tolerance to drought and restricted water conditions. The annual radial growth of *Abies concolor* is highly responsive to annual climate fluctuations (Hurteau et al., 2007). The strong influence of climate on annual tree-ring growth can create difficulties isolating changes of increment rates as a result of changes to microsite conditions (i.e. geomorphic processes) or from climate effects (Tardif et al., 2003; Hurteau et al., 2007).

4.1.2 Dendrogeomorphic Evidence of Disturbed Trees

Shroder (1978, 1980) presented the “process-event-response” model to expand upon the interrelationship of key characters of dendrogeomorphology. The “process” is the rockfall or other geomorphic agent. An individual geomorphic “event” that affects the tree may result in a unique growth “response”. Figure 14 illustrates the visual evidence of disturbed trees as a response to rock-fall activity including: (a) Decapitation, (b) visible injury or scarring from impact, (c) tilting, or (d) elimination of neighboring trees or ‘broken crown’ (Schweingruber, 1988; Stoffel et al, 2005a; Stoffel et al, 2005b; Stoffel, 2006; Stoffel and Bollschweiler, 2008; Stoffel and Corona, 2014).

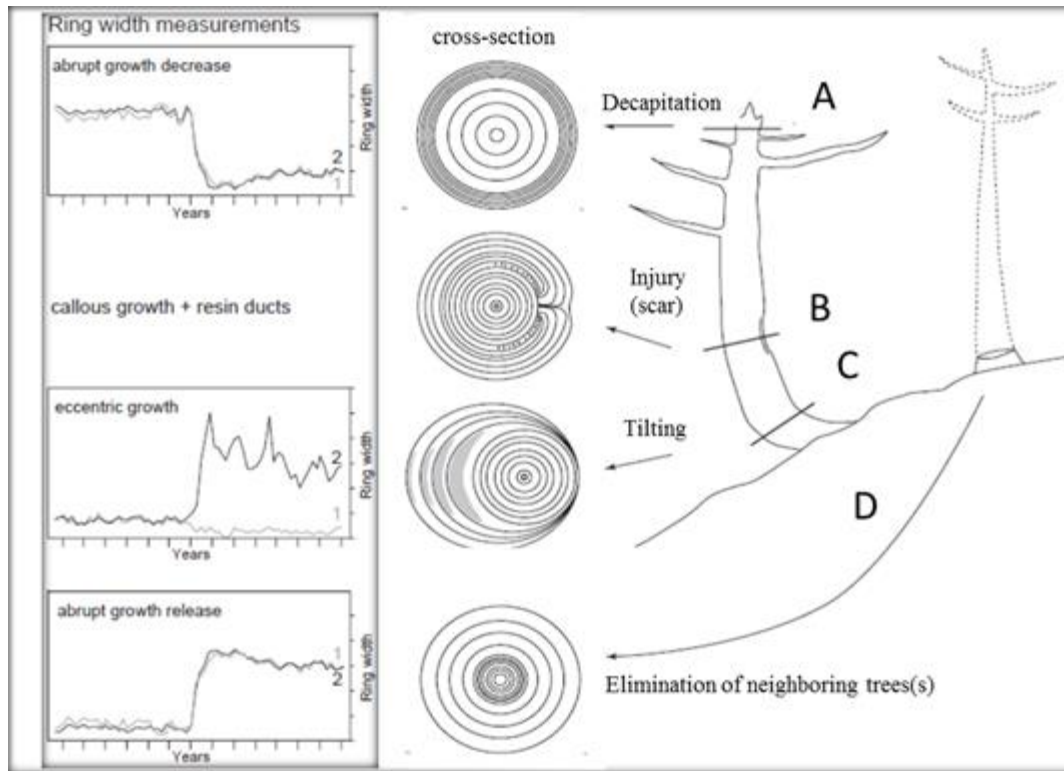


Figure 14 Dendrogeomorphic evidence to infer rockfalls. Variations of tree-ring width measurements (left) and the visual result of disturbed samples (Modified from Stoffel et al., 2005)

4.1.2.1 Decapitation

The decapitation of a tree or the removal of its branches as a result of falling or bouncing rocks and boulders will result in an abrupt decrease of annual ring growth or suppression. Suppression is growth retardation in which stressed trees produce less wood and the annual increment is smaller whereas tension is the opposite. When new sprouting branches form apical dominance that replaces the broken stem or crown, it is referred to as “candelabra” growth (Stoffel et al., 2005c).

4.1.2.2 *Injuries or Wounds (Scars)*

When falling rocks or debris impact a tree with enough force, a mechanical wound (injury or scar) will respond with the growth of callus tissue or tangential rows of traumatic resin ducts (TRDs) (Stoffel et al., 2010; Schneuwly et al., 2009). Injuries or wounds can occur on a tree's trunk, branches or roots (Stoffel et al., 2010). Impacts can cause local destruction of the cambium, to which the tree will respond by halting new cell formation in the injured area, and will start producing chaotic callus tissue on the edges in an attempt to overgrow the wound with cambium cells from the edges (Larson, 1994; Schweingruber, 2001, Stoffel et al., 2010). The nature of the wounds healing is dependent on several factors and will be discussed in greater detail in a later section.

Impacts to select conifer species will produce tangential rows of traumatic resin ducts (TRD) in the developing xylem. *Abies concolor* (White fir) does not produce TRD's. Erosion or other geomorphic processes can partially expose roots. Root damage or injury can cause periods of suppression of tree-ring growth (Rizzo and Harrington, 1988; Stoffel et al, 2010).

4.1.2.3 *Tilting (Inclination) of Stems*

The sudden or gradual introduction of stress or pressure applied to a tree by a geomorphic agent or by the destabilization of a trees foundation will result in the inclination, or tilting or bending of trees (Schweingruber, 1996; Bollschweiler, 2007). Growth responses attributed to inclination include eccentric ring growth and; for deciduous trees, the pith is displaced on the downslope side and reaction wood (tension) balancing it on the opposite side; for coniferous trees, the displaced pith is upslope

coupled with (suppression) and balanced on the downslope side by reaction wood (Braam *et al.*, 1978a). Normal (complacent) ring growth consists of concentric ring development at equal rates, whereas (sensitive) ring development occur within stressed trees (Winchester *et al.*, 2007). Normal ring growth must be evaluated considering all influencing factors as suggested by (Schweingruber, 1990): “exposure, temperature, precipitation, wind, light, growing period length; competition and soil (type, texture, water, nutrient and oxygen availability).” Additional growth responses can be related to geomorphic processes.

Another growth response is the disruption of original apical dominance and formation of new sprouts which commonly grow vertically upward from the tilted trunk (Schroder, 1980). Note reaction-wood growth is the gravity controlled response of a tilted tree to strengthen its lower trunk when supporting the returned vertical alignment of the upper trunk (Schroder, 1980). The adverse tree ring growth response of tree tilt and position with respect to the slope is fundamental in differentiating annual ring width variations.

In the event of a sudden geomorphic event, such as a debris flow, landslide, rockslide, or other movement deposited material may bury the base of a trunk of a tree. The disruption of the water and nutrient supply will cause temporary annual increment growth suppression (Strunk, 1997).

4.1.2.4 Elimination of Neighboring Trees and Colonization

Geomorphic processes, such as rockfalls, debris flows or avalanches can eliminate trees in its pathway while leaving surrounding trees standing. The lack of

competition creates favorable growing conditions which are observed in core as growth release or larger increment rings (Schweingruber, 1996; Stoffel et al., 2005a.c). In the case of elimination of large portions of the forest stand, germination ages of new trees colonizing the bare landform can be used to establish a minimum date of disturbance (Schneuwly, 2009; Stoffel et al., 2010).

4.2 Field Methods

To delineate areas of rock-fall activity, a detailed geomorphic investigation will include remote sensing and on site field analysis. Satellite and aerial photography along with topographic, geologic and vegetation surveys were used to determine the geographical extents of the study area of interest.

A global positioning system (GPS) and aforementioned maps were used in the field to map areas of talus accumulation. The block shape, lithology, and diameter of selected cobbles and boulders were recorded and a note was made of their general relationship to surrounding clasts. In addition, this study followed standard lichenometry procedures (Hale, 1967; Carrara and Andrews, 1973; Luckman and Fiske, 1995; Bull and Brandon, 1998; Bull, 2004). Procedures include recording the general presence of lichen growth, the dominant species, and measuring the five largest lichen diameters for further analysis.

GPS was also used to record the locations of trees exhibiting visual evidence of rock-fall activity (figure 15). The type and number of visible defects were then recorded. By identifying trees impacted by rock falls, I can map the spatial extent of rock-fall

activity. Selected trees may be sampled for further dendrochronological applications.

The spatial distribution of trees sampled is given in figure 16.

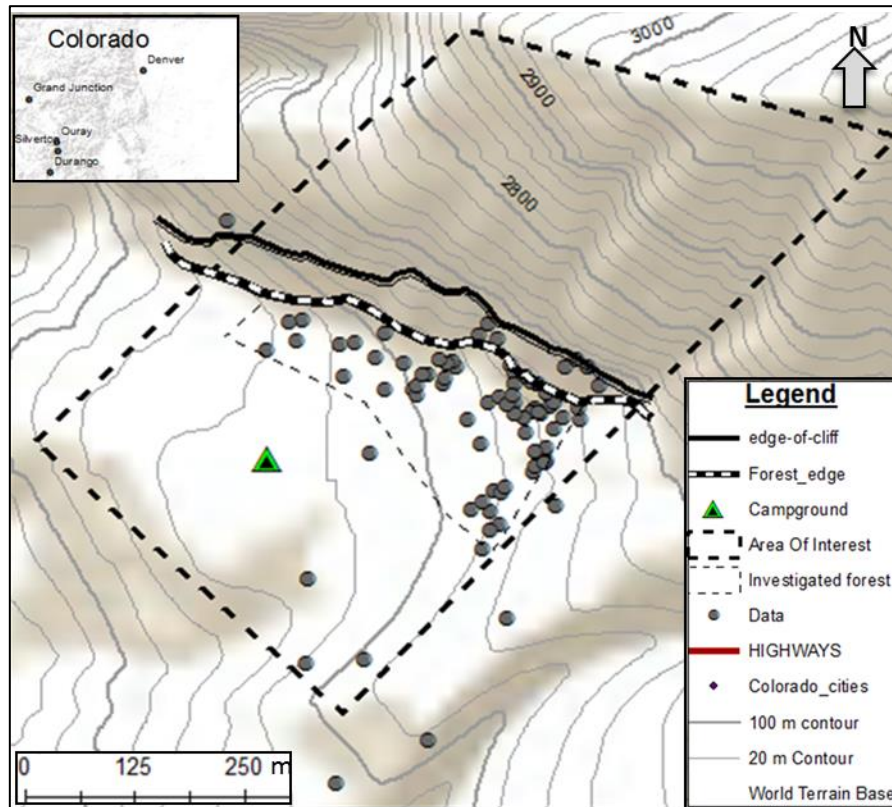


Figure 15 Visualized locations of data samples.



Figure 16 Imagery displaying the location of sampled trees. Yellow circles represent sampling locations.

Establishing a temporal chronology requires a view of past activity. This perspective can be obtained through the use of tree rings of trees impacted by rock falls. Selected trees were sampled by carefully extracting tree cores ~5 mm in diameter using an “increment borer” (figure 17). The cores are visually and statistically analyzed later in the lab to assess tree-ring growth responses to rock-fall activity and construct a rock fall chronology.



Figure 17 Core extracted from an injured tree using an ‘increment borer’ (Photo by Author)

This study employed a dendrogeomorphic approach (Fitts, 1976, 1971; Grissino-Mayer, 2001, 2003; Stokes and Smiley, 1968; and Speer, 2010; Shroder, 1978, 1980), tailored for rock-fall analysis (Stoffel et al., 2005; Stoffel & Bollschweiler, 2008; Stoffel, 2006). Existing literature primarily focuses on modeling the physical response of rock-fall events, whereas this study will investigate the cause-effect response and the dynamic variables associated with rock-fall hazard assessment.

Stoffel et al. (2005), Grissino-Mayer (2003), and Speer (2010) outline procedures for individual core extraction based on targeting trees with visible defect. Cores typically are taken from the up and down-slope sides (figure 18, A & D). When visible injuries or growth defects are present, additional cores may be taken perpendicular to slope and within or near wounds and into the overgrowth callus tissue (figure 18, C & B) (Stoffel & Bollschweiler, 2008; Stoffel et al. 2005; Stoffel, 2006; Trappmann and Stoffel, 2013).

After a core has been extracted from a tree, it is placed in a (plastic or paper) straw for protection during transportation. All tree cores are labeled according to site specifications and a site identification card is completed for each location (Shroder, 1980).

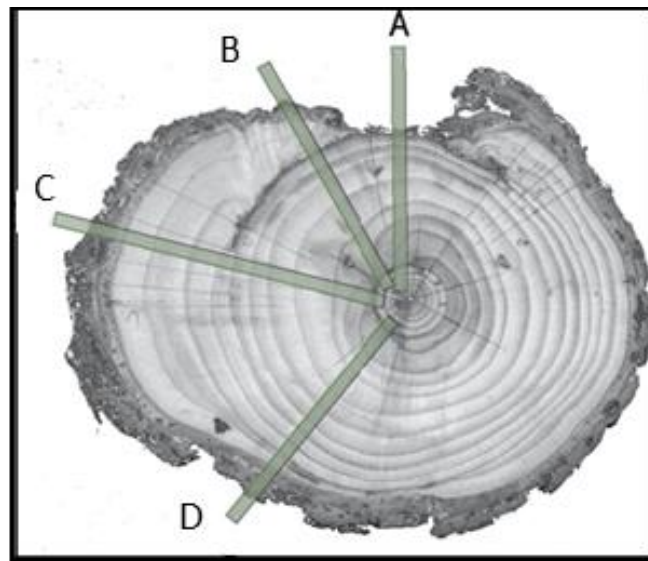


Figure 18 Cross-section of scarred tree with ideal sampling positions A-D (Modified from Stoffel and Bollschweiler, 2008)

4.3 Lab Methods

To construct a rock-fall chronology, the tree cores annual growth rings were dated and measured. Prior to analysis, the samples were prepared for further analysis. All core samples were dried and glued to wooden core mounts to be sanded using progressively finer sand paper (40 to 400 grit), to reveal the cellular structure of the tree rings. Annual ring growth can be altered where the sequence is missing a ring or contains a false ring if normal growing conditions are interrupted (Schweingrober,

1988). To rectify this, the cores were cross-dated using skeleton plots (Stokes and Smiley, 1968; Speer, 2010) and or the listing technique (Yamaguchi, 1991). This approach was used to visually indicate drastic changes of climate or geomorphic events, because they are recorded in the trees growth patterns (Winchester et al., 2007). Precise measurement of annual tree-ring widths (or the latewood-earlywood transitions) was accomplished using a binocular stereomicroscope and a sliding-stage micrometer interfaced with the recording software “Measure J2X” (Robinson and Evans, 1980; Speer, 2010). The accuracy of the cross dating was be verified statistically using the software COFECHA (Grissino-Mayer, 2001; Holmes, 1983; Speer, 2010) (APPENDIX E).

In consideration of ring-width variations resulting from climate change, many dendrochronologist apply a corrective procedure called standardization (Fritts, 1971, 1976). Standardization corrects for the decrease of annual ring width as the tree ages and grows wider. Standardization will correct for the ring growth variation of the youngest rings to a normalized ring width variations, as the variation in ring width for the younger growing rings will be drastic because of the fast rate of growth. Additional fluctuations to tree growth can be related to abrupt GD caused by falling rocks. Figure 14 shows variations of tree-ring width measurements as a trees response to rock-fall induced GD. Analysis of the initiation, duration, and termination of these growth defects (GD) are used to establish a rock-fall chronology.

Recurrence intervals of rockfalls within the forest stand were then calculated by dividing the age of a tree at DBH by the total number of dated GD for the tree (Stoffel et

al., 2005b). This step allowed for the visualization of absolute values of rockfall frequency at the tree level.

Rockfalls typically consist of single falling, bouncing or rolling rocks which may only impact trees along their limited trajectories and constrained by the size of the clast (Dorren et al., 2007; Schneuwly and Stoffel, 2008a; Stoffel et al., 2011). The recurrence interval of rockfalls may, however, overestimate the more recent injuries and underestimate the older events clouding the historical distribution of areas with preferred rockfall trajectories. This is because as trees grow, their thick stem makes them a larger target for rockfall impacts than smaller trees and thus are more likely to record GD. To compensate for this, we used a yearly rockfall “rate” (Stoffel et al, 2005b), expressed as the number of rockfall events per meter width of all tree surfaces present per year:

(1)

$$RR_n = \sum \frac{GD_n}{\sum ED_n}$$

where GD_n stands for the number of reconstructed GD (or injuries) in year n, and ED_n represents the sum of all DBH (in meters) values of the sampled trees (i.e. exposed diameter, ED) existing at the beginning of year n. To calculate ED values, yearly DBH increment of each tree and each year were determined by dividing the DBH at sample year by the tree age. The rockfall “rate” was then obtained by dividing the yearly sum of reconstructed GD by the ED. Rockfall rate is expressed as rockfall events $m^{-1} yr^{-1}$ assuming constant increment rate and disregarding juvenile and aging trends (Stoffel et al., 2005b; Stoffel et al., 2011).

To add to the rockfall chronology, a third approach, adapted from (Trappmann and Stoffel, 2013; Trappmann et al., 2013) classifies impact wounds or injuries of *Abies concolor* (White fir) into age categories by visual inspection of wound recovery and closure. A reference data set was created, listing actual impact ages from core samples matched with relative visual examples of the wounds recovery stage. For each tree exhibiting an injury or scar, the tree size, the scar size, and notes regarding the position and condition of neighboring trees were considered.

Digital data are visualized using Arcgis 10.3[®] and GoogleEarth[®] (ESRI, 2015; Google, 2015). Colorado county and state data were downloaded as shapefiles from the US Census Bureau website (<http://www.census.gov/geo/maps-data/>). A Digital Elevation Model (DEM) with 10 m resolution was downloaded (Coughenour et al., 2015). The DEM was then clipped to only encompass the city and the slopes surrounding the Amphitheater (DEM1). Spatial visualization of the tree-ring data were investigated using the ESRI ArcGIS 10.3 software (ESRI, 2015). Tree locations were converted to geo-objects and included the following data attributes: “tree coordinates, tree age; number, year and type of GD, DBH, injury heights, injury age classification, as well as information on ground vegetation and crown condition, clast size and lithology, and lichenometry measurements and species type”. Return periods (recurrence intervals) were visualized using ArcGIS 10.3 Geostatistical Analyst software extension (ESRI, 2015) to examine the special relationship between data points. Surfaces were interpolated with an Ordinary Kriging model, using five neighboring trees.

CHAPTER V

ANALYSIS

This chapter presents the results of the tree-ring assessment and initial analysis of the spatial extent of rockfalls and a minimum rockfall time-series. The finding presented will answer the questions: (i) where spatially is the slope subjected to rockfall activity and what are the magnitude and frequency of events? Also, (ii) will reconstructing a rockfall chronology using a dendrogeomorphic methodology of *Abies concolor* (White fir) help identify potential triggering mechanisms?

5.1 Tree Rings-Master Chronology

A master chronology was created using increment cores from 32 trees, so that samples could be cross dated accurately. Results from COFECHA show an interseries correlation to the master is .669 with an average mean sensitivity of .374. The master series dates span from 1800 to 2015 (APPENDIX E)

5.2 Rockfall History

This analysis used 28 of the 60 samples collected from the study site were used to generate a preliminary rockfall chronology, and 20 of the 28 dated samples were used for rockfall analysis. Unfortunately, 2 samples were destroyed in transit from the study site, and 2 were undateable due to abnormal growth defects.

5.3 Visible Defects and Growth Responses to Rockfall Activity

Field investigation identified 152 visible defects on 64 *Abies concolor* (White fir), 6 *Pseudotsugamenziesii* (Douglas fir), and 1 *Quercus gambelii* (Gambel oak or Oak brush) (Table 3). As illustrated in Table 4, recent to overgrown injuries (scars) was

predominate visible defect identified in 97 cases (63.8%), followed by 20 cases of ‘broken crown’ (13.2%), 19 trees with tilted stems (12.5%), and 16 cases of decapitated trees (10.5%).

Table 3 Number of trees and injuries sampled

	<i>Abies concolor</i> (White fir)	<i>Pseudotsuga menziesii</i> (Douglas fir)	<i>Quercus gambelii</i> (Gambel oak or Oak brush)	<i>Total</i>
Number of trees	64	6	1	71
Number of visible injuries	135	14	3	152

Table 4 Overview of visible defects used to determine rockfall events

		%
Injuries (scars)	97	63.8%
Broken crown	20	13.2%
Tilted stem	19	12.5%
Decapitation	16	10.5%
Total	152	100.0%

The analysis of 28 cores revealed a total of 121 GD as result of rockfall activity (Table 5). GD identified in multiple cores of the same tree, caused by the same impact were omitted from these results. Injuries and callus tissue were the predominate GDs, observed in 37(30.6%) and 29(24.0%) cases respectively. Abrupt growth suppression occurred in 25 cases (20.7%), and growth release occurred in 26 cases (21.5%). Reaction wood could only be found in 3 samples (2.5%). Traumatic resin ducts (TRD) was only identified in 1 sample (0.8%).

Table 5 Overview of growth disturbances used to determine rockfall events

Growth disturbances	Number	%
Injuries	37	30.6%
Callus tissue	29	24.0%
Growth suppression	25	20.7%
Growth release	26	21.5%
Reaction wood	3	2.5%
Traumatic resin ducts (TRD)	1	0.8%
All reconstructed events	121	100

5.4 Spatial Distribution of Growth Disturbances

The spatial distribution of reconstructed rock-fall activity varied considerably along the investigated forest stand. Analysis of rockfall recurrence intervals reveals rockfall activity is highest in the north-northwestern section of the study area, which is closest to the source of rockfalls. The record of rockfall disturbances decreases away from the forest edge because of the protective nature of the forest as neighboring trees above act as a shield to falling, bouncing and rolling rocks. The recurrence intervals at the stem level are listed in APPENDIX C, and the spatial distribution of interpolated recurrence intervals are illustrated in Figure 19. Both datasets point to the fact that areas with preferred rockfall trajectories generally record higher return periods of rockfalls (decadal scale), whereas lower return periods of rockfalls are recorded on sampled trees protected by neighboring trees or located in a topographically favorable area.

Based on visual inspection of the extent of healing of injuries or corrosion, consistent with results from core samples, scarred trees were placed into scar age classifications based on sages of recovery. As mentioned previously, the extent of the

wounds healing is highly dependent of the annual increment rate, tree age, and scar size (Stoffel et al., 2010), so to minimize error, three age categories were established to satisfy these conditions.

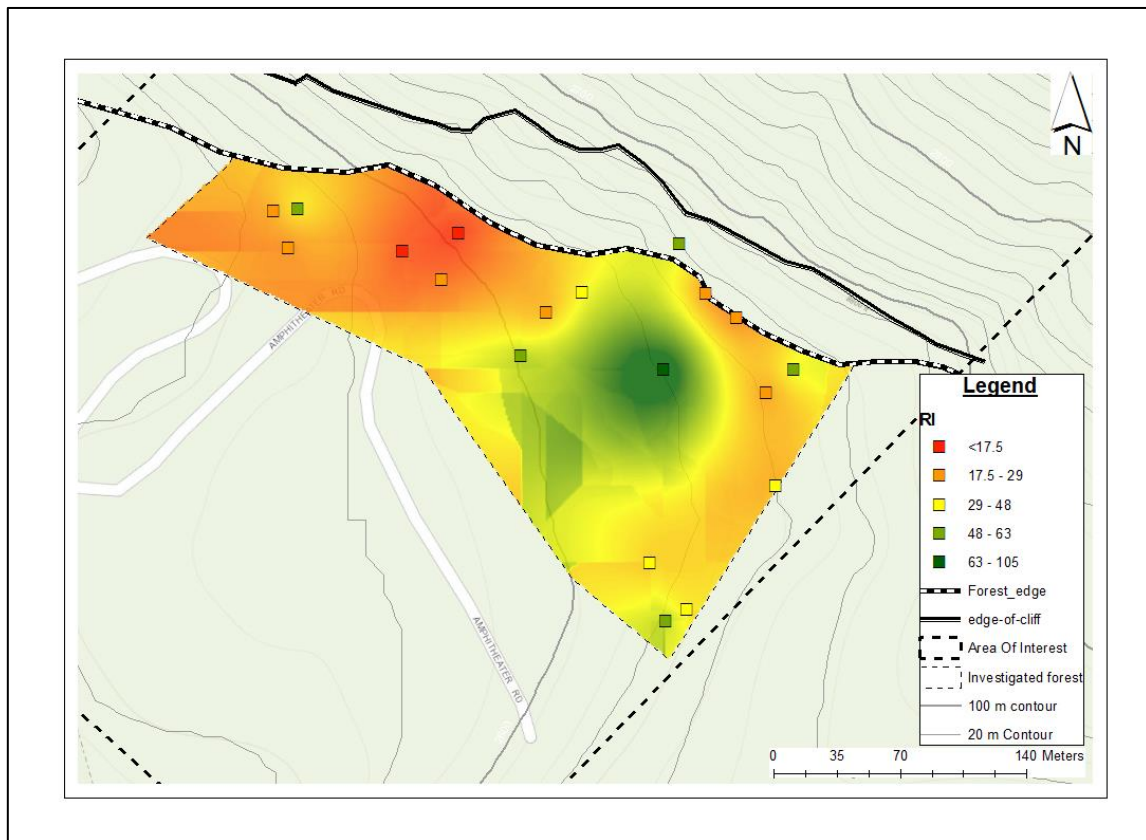


Figure 19 Reconstructed rockfall return intervals.

For this thesis, I used *Abies concolor* (White fir) trees, of which there is little to no existing literature when used for dendro methods. I created a reference data set from tree cores to establish an estimated rate of recovery, and then placed trees based on visual examination of wounds recovery stage into one of three categories. Analysis

shows that for an 105 year old *Abiesconcolor* (White fir) tree with a 24 cm (9.44 in) in diameter scar, an average of 66 years are needed for complete overgrowth and closure of the scar. As suggested by Trappmann and Stoffel, (2013) and Trappmann et al., (2013) relative dating based on visual inspection of wound closure and recovery presents considerable error, however, it is a viable means of relative dating to be used as a quality control (QC).

Abies concolor (White fir) trees exhibiting fresh injuries or corrosion with little to no recovery growth on healthy trees were considered to have occurred within the last 15 years and placed into ‘Age Category 1’. Wounds of early to late stage of recovery exhibiting partial closure from callus tissue overgrowth were placed into ‘Age Category 2’ for impacts occurring before 2000 but after 1950. Completely overgrown injuries or scars in the late stages of recovery are placed in “Age Category 3’ representing old rockfall events occurring before 1950.

Table 6 Injured trees categorized by relative recovery state

Age Category	Number	%
1 (2000-2015)	15	27.3%
2 (1950-2000)	20	36.4%
3 (<1950)	20	36.4%
All visible injuries	55	100

Table 6 shows the number of trees scared within each category. Figures 20, 21, & 22 visualizes the spatial extent of trees for the three-age categories. Here you can see the closed circles representing the location of the samples for each category. From this I was able to delineate areas with favorable rockfall trajectories through time.

Injuries of trees in groups 1 and 2 are primarily concentrated near the interface of the encroaching forest and talas slope which is between 30 and 60 m (100 and 200 ft). Injuries to trees in age-group 3 are more spatially diverse than trees in groups 1 and 2. Without knowing the nature of the investigated forest stands condition, difficulties arise when attempting to constrain forest stand presence past 1910.

The analysis shows that the areas to the upper left of the investigated forest are less active as compares to the areas of the upper right. Also, because we can see many of the same samples with recurring injuries through time this tells us that rockfalls have been continuous for the time of investigation and no large-scale mass-movement event occurred as the present trees would have been destroyed.

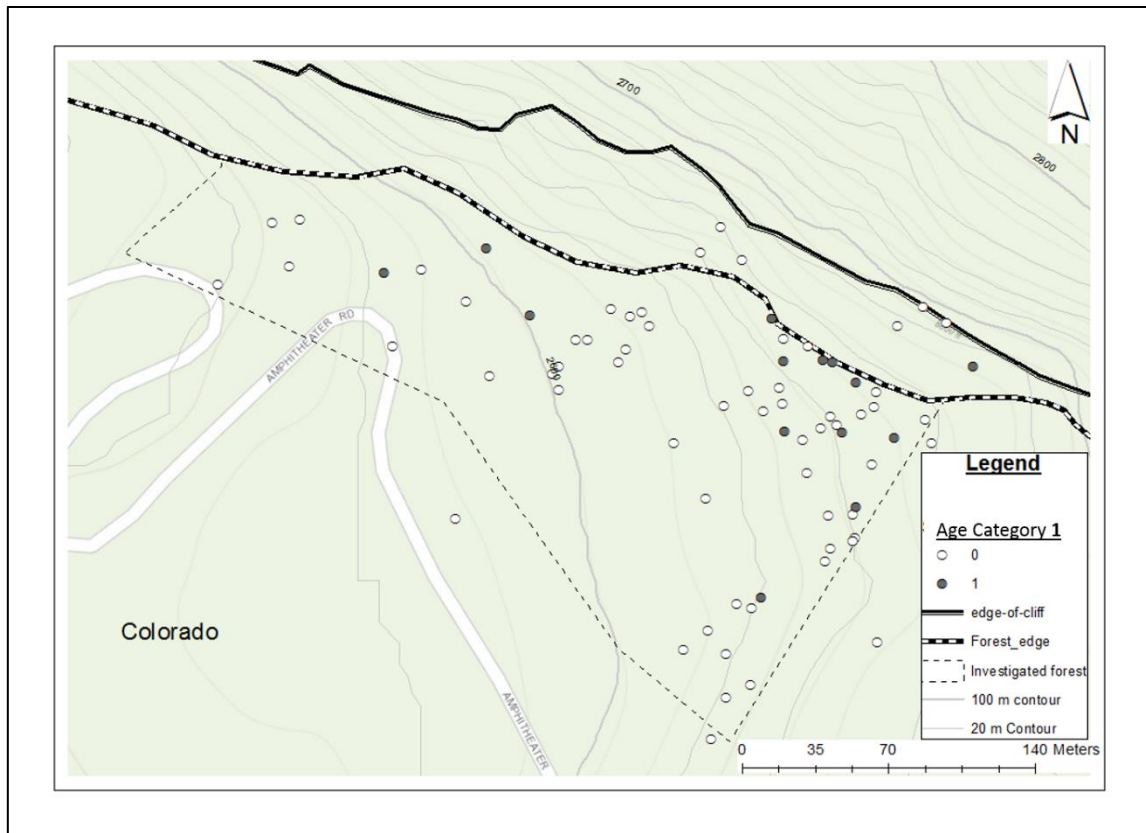


Figure 20 Location of fresh or recent injuries of ‘category 1’ (filled circles). Open circles denote all visible rockfall induced injuries

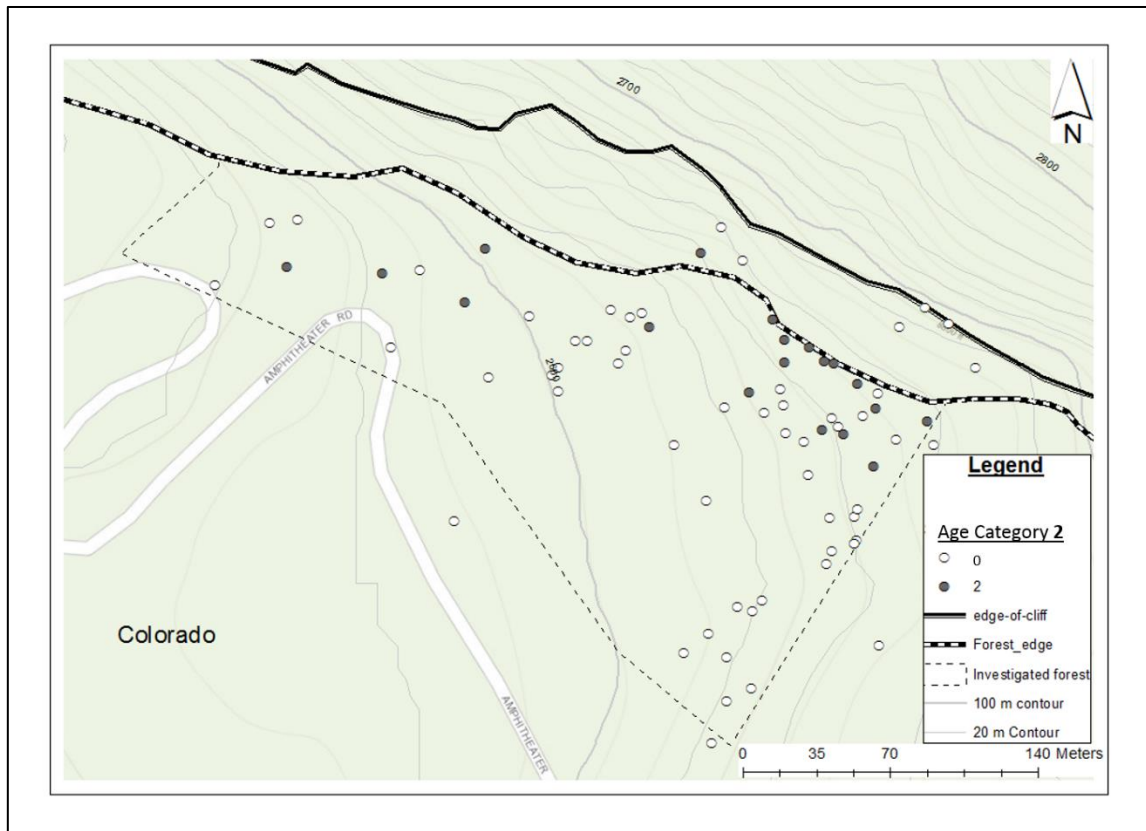


Figure 21 Location of partially recovered tree scars of 'category 2' (filled circles). Open circles denote all visible rockfall induced injuries

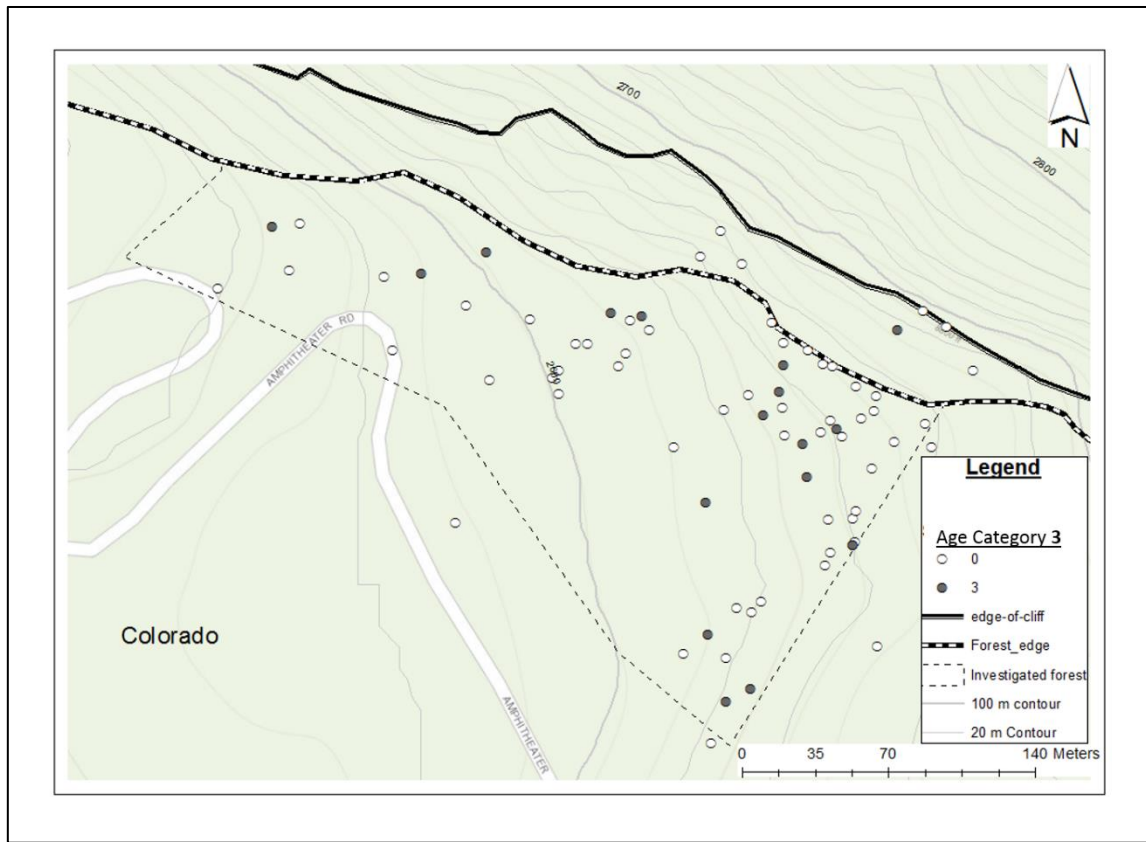


Figure 22 Location of old scars and injuries of ‘category 3’ (filled circles). Open circles denote all visible rockfall induced injuries

Rockfall deposits were categorized into five categories based on clast size (table 7). Figure 23 illustrates the spatial extent of the sampled rockfall deposits. Larger clasts are located near the upper limit of the forest where they are better sorted.

Table 7 Classification of rockfall deposits based on sample diameters.
Grain size adapted from International grain size scale (ISO 14688-1: 2002)

category	classification	clast diameter (in)	clast diameter (mm)	count
1	soils	< 2.4	< 63	12
2	cobbles	2.4-7.8	63-200	19
3	small boulders	7.8-24.8	200-630	12
4	large boulders	24.8-60	630-1530	5
5	very large boulders	>60	>1530	5

The largest boulders traveled the farthest into the forest, however they are usually isolated and surrounded by soils (figure 24 A). The red line in figure 23, annotates the lower edge of the mapped talus and rockfall deposits and on average is about 70 m (230 ft) from the forest edge and about 100 m (328 ft) from the base of the cliff (figure 23). The exception to this is where flowing water has scoured channels in the forest floor and transported a heterogeneous mixture of debris downslope (figure 24 B, APPENDIX B4). Trees in direct contact with these debris flows were disregarded from this analysis.

Lichen cover was used to provide a separate, independent assessment of rockfall activity (table 8). The percent of cover of lichen on independent rock-fragment faces was amassed. The assumption is based on the saying “a rolling rock contains no moss”. In other words, if a rock fragment remains in place for an extended period of time, it will be covered with lichen. The lichen coverage can then be used as a surrogate for stability. Lichen growth is more extensive in the western part of the forest and generally is less abundant to the east (figure 25). Lichen growth can at time be sensitive to direct sunlight or extensive shade, however analysis of the sun’s movement and sunlight phases (Aqafonkin, 2009) indicate uniform sunlight spatially across the study area.

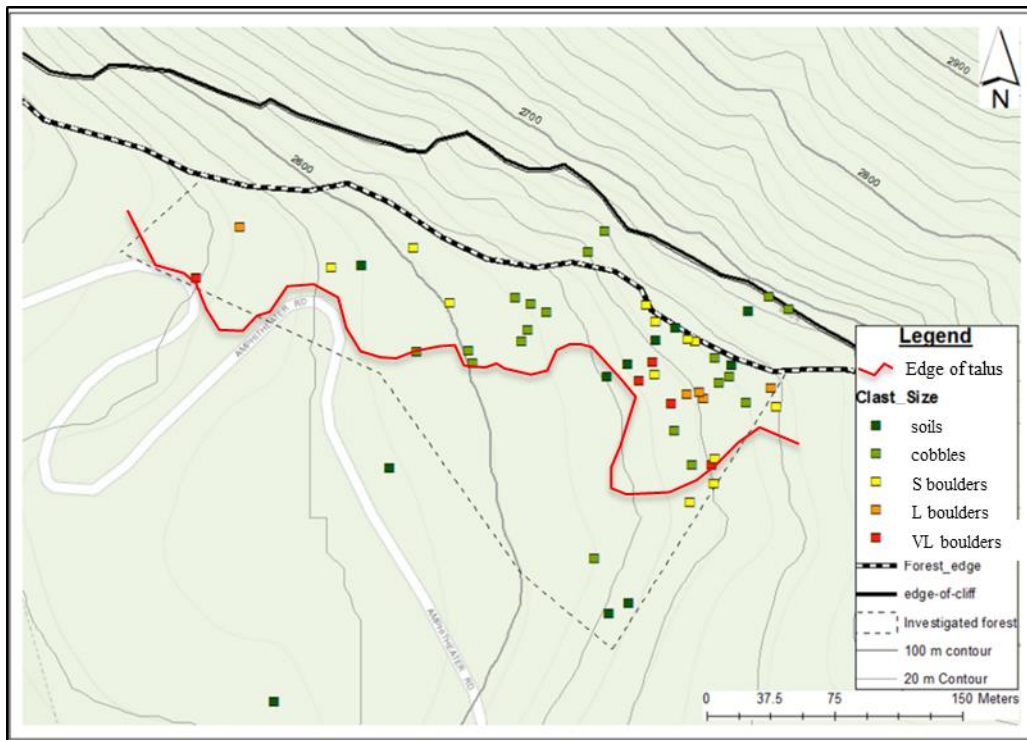


Figure 23 Locations of rockfall deposits subdivided into clast sizes (see Table 7 for more detail)

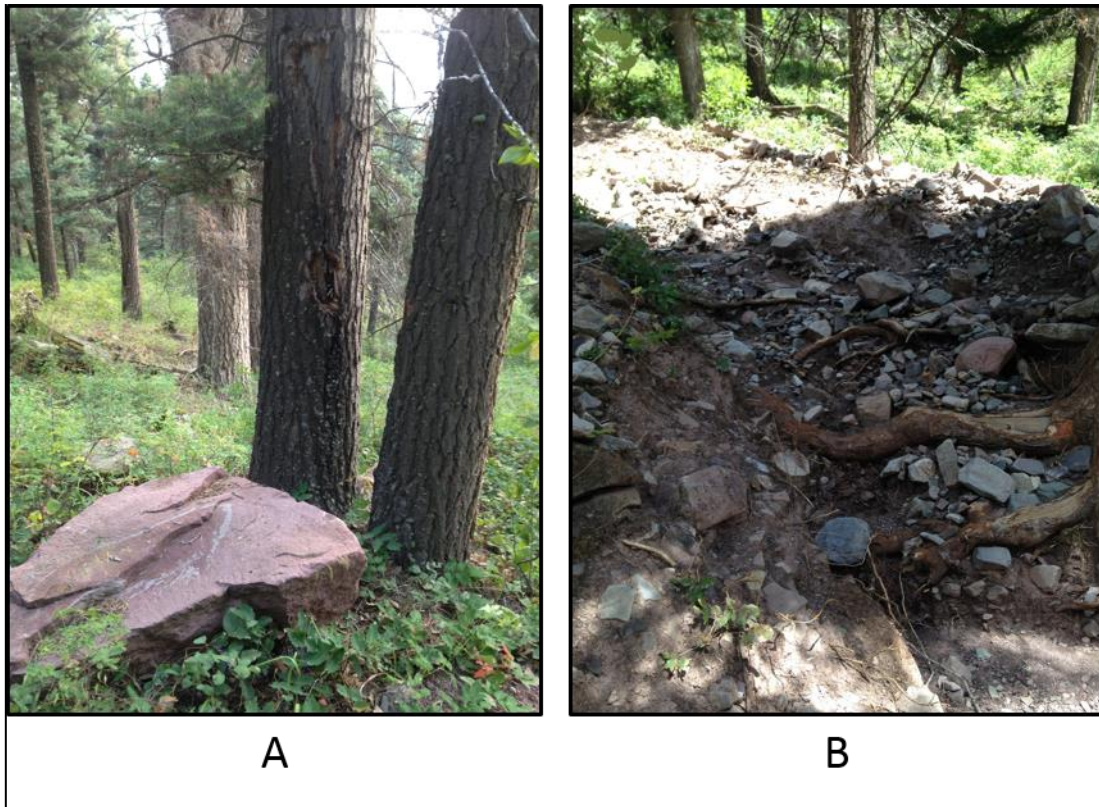


Figure 24 (A) Large isolated disc shaped boulder surrounded by vegetation/soil, and (B) active scouring of the slope transporting varying clast sizes down slope (Photos by Author)

Table 8 Classification of lichen colonization into three age categories based on relative age and percent coverage

category	classification	lichenometry (age)	description	count
1	young/recent	<15	little to no lichen growth	10
2	mixed	-	random distribution of clasts with >50% lichen cover, mixed with fresh blocks	16
3	old	>65	clasts with >50%	15

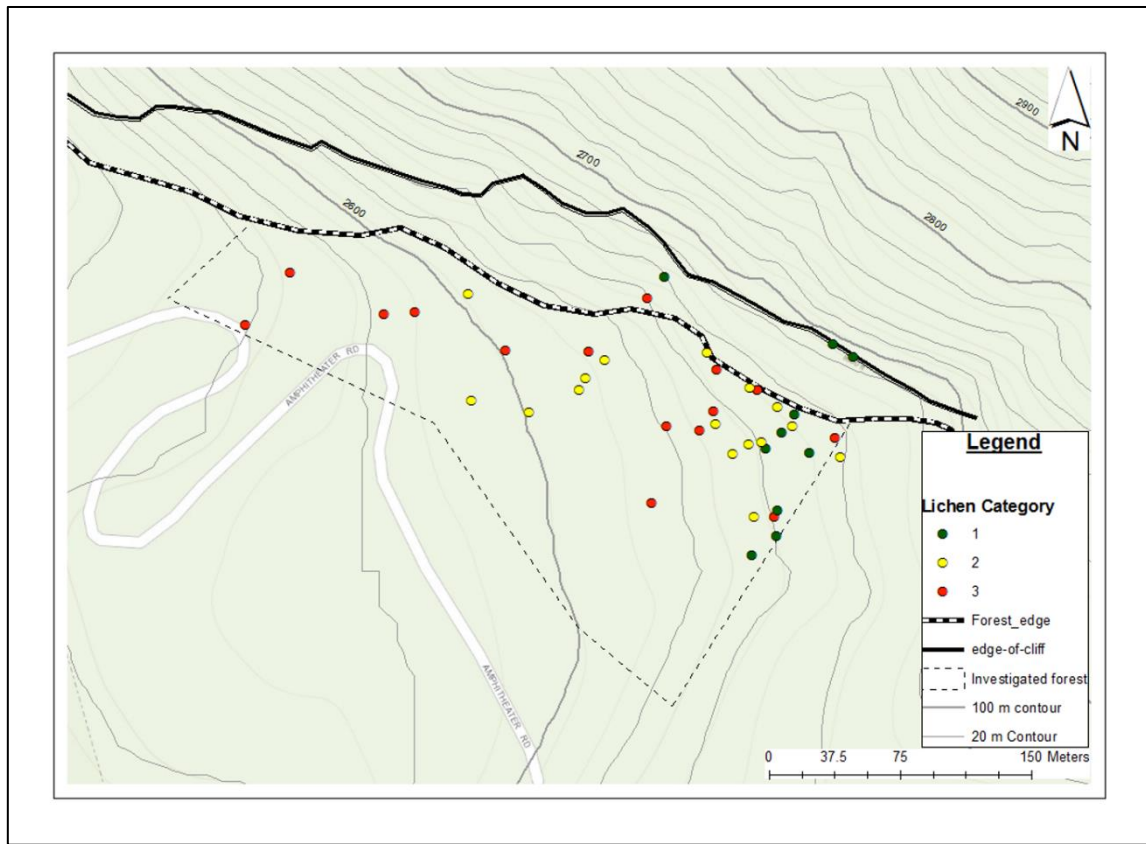


Figure 25 The spatial distribution of the lichen categories (see Table 8 for more details)

5.5 Rockfall Magnitude and Frequencies

During the period 1885-2015, rockfall activity continuously induced GD in the trees analyzed. Whereas multiple rockfall-induced GDs occurred during the same year, analysis of the sampled trees suggest rockfall activity consists of low magnitude-high frequency events for the time period.

5.6 Annual Variations in Rockfall Activity

Annual variability of rockfall was examined for the period 1885 to 2015 and, 121 GD, and an average of .93 GD year⁻¹ in 20 trees (figure 26) was found. Additional

growth disturbances were identified in samples from older trees, however, because of the limited sample number of older trees, these were omitted from the analysis.

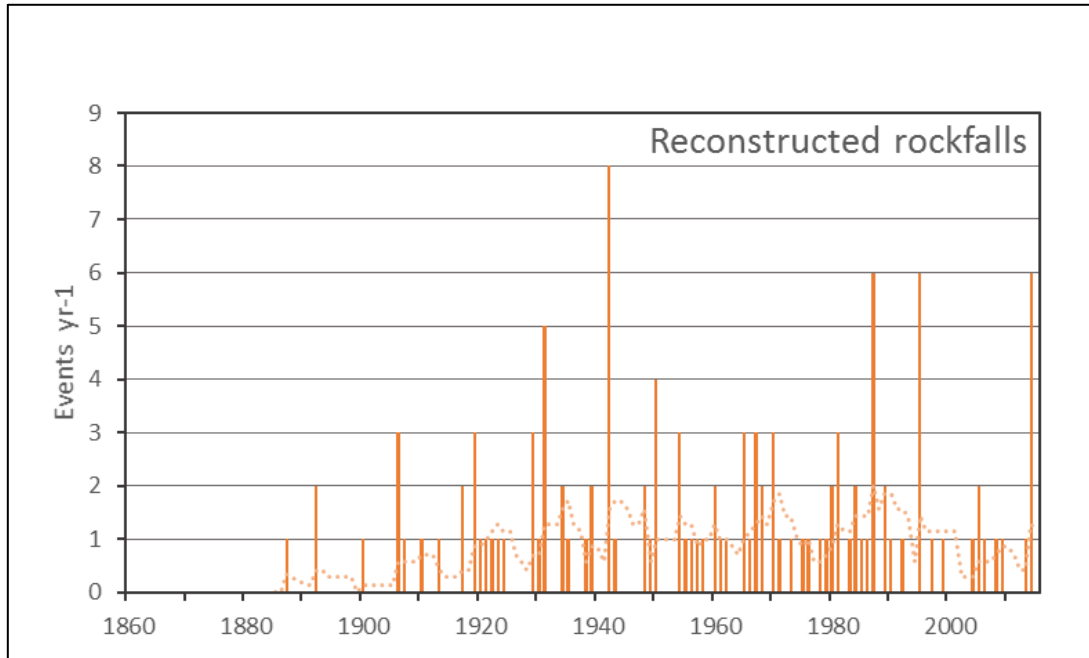


Figure 26 Reconstructed rockfalls based on analysis of GDs identified in tree cores (dashed line represents 7-year moving average)

Reconstruction of rockfall activity was limited to the last 105 years (1910-2015), as the number of samples were too small for the comparison of rockfall events prior to 1910. Investigation of yearly rockfall “rate” yielded an average of $0.30 \text{ events m}^{-1} \text{ y}^{-1}$ between 1910 and 2015 (STDEV: $.45 \text{ events m}^{-1} \text{ y}^{-1}$) ranging from zero to almost 5 events $\text{m}^{-1} \text{ y}^{-1}$. Rockfall rates are slightly less continuous for the period of 1910-1925 as fewer trees existed, and the trees that did were younger with less exposed surface to record rockfall impacts (figure 27). The years during the period of 1926-1950 that are

perceived as having higher rockfall “rates” is a result of the limited number and nature of the trees sampled in this study. The absolute values of reconstructed rockfalls (figure 28) will provide better indication of the rockfall activity before 1951. As the tree ages, the increase in diameter makes the tree more likely to be impacted. This is demonstrated from the increased frequency of yearly rockfall “rates” after 1951. This result is similar to the results from (Stoffel et al., 2005b).

During the period 1926-1950 fewer years of rockfall activity were recorded; however, when present, several years experienced higher rockfall “rates”. The number of years with rockfall events increased after 1951. The seven-year moving average, light-gray line shown in figure 28 does not show any significant trend, but rather demonstrates the continuous pattern of rockfall activity. Rockfall activity was difficult to detect at the turn of the 21st century and its implications will be discussed in more detail in the following chapter. Years with notable rockfall activity are 1931, 1942, 1950, 1960, 1965, 1970, 1981, 1987, 1995, 2005, and 2014.

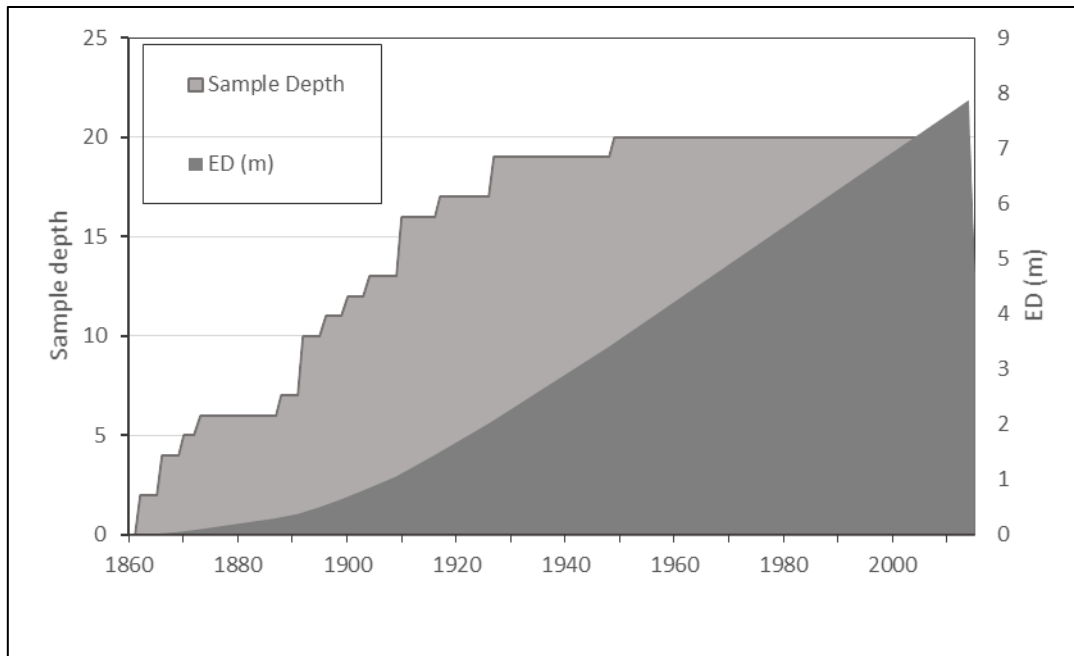


Figure 27 The light gray represents the available sample depth per year and the dark gray represents the exposed diameter for each year under investigation

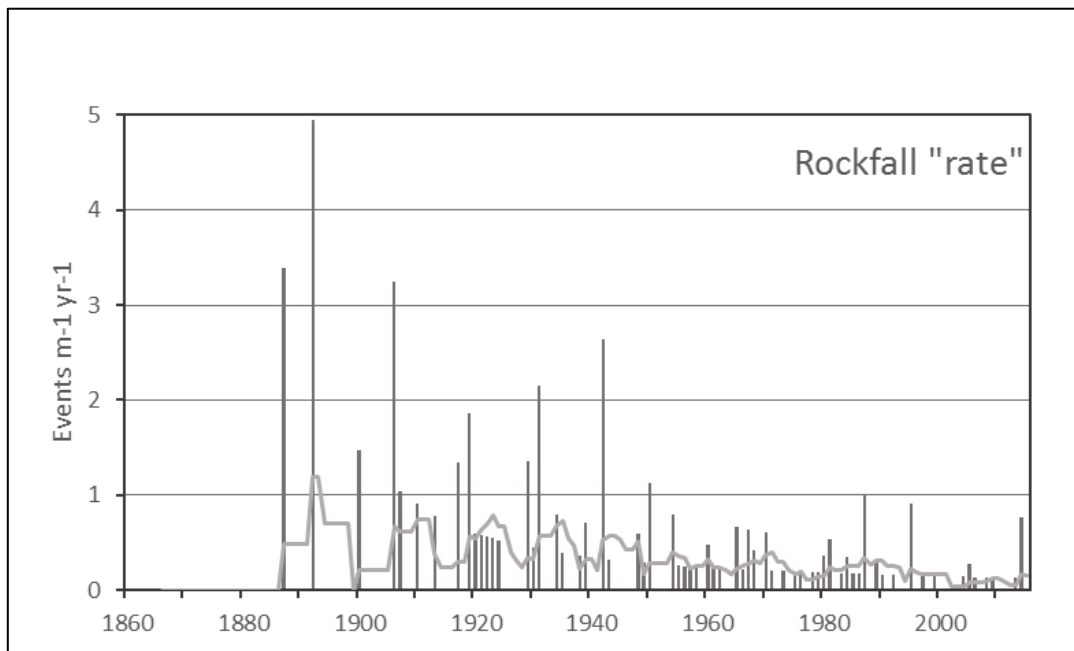


Figure 28 Rockfall 'rate' illustrated by the number of events $m^{-1} yr^{-1}$ (light-gray line represents 7-year moving average)

CHAPTER VI

DISCUSSION

This chapter recaps the analysis and discuss additional findings. The results are evaluated using all available published resources. In addition, this chapter discusses what the analysis means for the area and its potential application to similar areas.

6.1 Rockfall Chronology

A temporal chronology of rockfall activity was created using tree-core data. Rockfall activity was reconstructed from the GD observed in the tree-ring series of *Abies concolor* and a few *Pseudotsuga menziesii*.

6.1.1 Limitations

The predominate GD observed in the tree cores were injuries and the presence of adjacent callus tissue. These GD were easy to identify on fresh or recent injuries; however, it was more difficult on masked wounds and on recovered or overgrown scars. When older injuries have sufficient time to heal, they are difficult to detect on the exterior of the stem (Stoffel and Perret, 2006; Zielonka and Dubaj, 2009).

In addition, abrupt growth suppression and release was a common occurrence throughout the samples. This fact is likely because *Abies concolor* is highly responsive to annual climate fluctuations (Hurteau et al., 2007) and can create difficulties distinguishing annual increment responses from climate of geomorphic events (Tardif et al., 2003). The sensitivity of *Abies concolor* to climate might account for its limited use in dendrogeomorphic studies. In order to compensate for this issue, abrupt growth changes were only considered to be GD as response to rockfall, where unique growth

change was observed in years that it was uncharacteristic. Other studies of *Pinus sp.* and *Pinus hartwegii* also reported annual ring growth sensitivities to climate (Stoffel et al., 2008; Bollschweiler et al., 2010; Biondi, 2001; Biondi et al., 2003; Stoffel et al., 2011), however still proved to be an effective tree species for dendrogeomorphic use.

Identification of reaction wood was limited, likely because of how fast the energy is transferred from the impacting rock to the tree (fraction of a second) (Schneuwly and Stoffel, 2008). Another reaction to rockfalls that is not characteristic of *Abies concolor*, but has proved to be particularly reliable in rockfall studies is the timing of the formation of traumatic resin ducts (TRD) (Bollschweiler et al., 2008; Stoffel and Hitz, 2008; Schneuwly et al., 2009a; Stoffel and Corona, 2014). One TRD was observed in the 3 samples of *Pseudotsuga menziesii* (Douglas fir), however, four more were observed in the older section outside the period of analysis for this study and, therefore, were disregarded. This thesis demonstrates that, aside from prior noted limitations, *Abies concolor* (White fir) can be used in dendrogeomorphic assessments of rockfall activity.

The period for which rockfalls can be reconstructed is dependent on sample depth and the presence of visible or inferred injuries and associated GD. Rockfall reconstructions are therefore limited to the past 105 years and cannot provide a complete record for events that may have occurred earlier. Additionally, the number of rockfall reconstructions for the investigated study area represents an absolute minimum frequency. One reason for this is rock trajectories may or may not impact a tree during its descent thus only alluding to a partial record.

This study was conducted under strict reserve for the investigated forest. The number of trees to be sampled with an increment borer was limited and the extraction of cross-sections from standing tree stems or from felled trees or snags was not permitted. This restricted methodology prevented large sample number for a more detailed analysis of rockfall activity both spatially and temporally.

6.1.2 Evaluating Rockfall Activity

Rockfall activity is expressed at the rockfall “rate” which allows for a comparative assessment of the most recent events, when the exposed surface was the greatest, to earlier events when smaller DBH of younger trees made them less likely to be hit by a rockfall. The continuous nature of these GD for the period of 1910-2015 suggests low magnitude-high frequency rockfall events similar to the findings of (Stoffel et al., 2005b; Perret et al., 2006; Schneuwly and Stoffel, 2008; Stoffel et al., 2011). The injuries occurred primarily during different years suggesting they formed by separate isolated stones, which fell sporadically, rather than a large-scale event affecting many trees.

Low-magnitude high-frequency rockfall activity is typical of freeze-thaw cycles. Patterns of lichen cover showed a similar distribution (table 8). Climate data from the two data stations in Ouray show typical cycles during the Fall and Spring when temperatures drop below freezing followed by a brief warming period before returning to freezing conditions (APPENDIX D). This activity coupled with precipitation as either rain or snow facilitates the steep slopes and cliffs as prime areas for frost wedging and subsequent rockfall.

6.1.3 Notable Rockfall Activity

Notable years exhibiting abnormally high rockfall activity must then be examined as a result of some external factor ‘promoting’ and/or ‘triggering’ the rockfall event (i.e., abnormally high frost-thaw cycles, heavy rainfall or rapid snowmelt, extreme daily temperature fluctuations, winter storms or high wind events, earthquakes, ect.) (figure 29).

Years with notable rockfall activity are 1931, 1942, 1950, 1960, 1965, 1970, 1981, 1987, 1995, 2005, and 2014. When the exact triggering mechanism is unknown, investigation into significant documented events may provide more information on rockfall activity for that year. APPENDIX A contains the daily temperature and precipitation data for the notable years that occurred since 1965.

Weather data are unavailable for 1931 and 1942; however, the 1978 Floodplain Information Report for Ouray County reported flooding in 1931 (Ouray County, 2013). Rockfall activity in 1950 was denoted by suppression and injuries. Reports from SHELDUS show rapid snowmelt caused flooding. Runoff from meltwater could potentially dislodge rocks from the cliffs and slopes as either primary or secondary rockfall.

The largest recorded earthquake in Colorado’s history occurred in the Montrose-Ridgeway area on October 11, 1960, as a magnitude 5.5. Damages were recorded in many of the surrounding cities, including Ouray. The intense shaking may have dislodged rocks or boulders on the steep slopes and cliffs surrounding Ouray and may be responsible for the injuries identified in this study. The GDs of 1965 can most likely be

attributed to the July cloudburst along Portland and Cascade Creeks (APPENDIX A2), which resulted in large debris flows and considerable flooding (Ouray County, 2013). In 1970, a small earthquake occurred on February 3, 1970, in San Miguel County, South of Norwood, as well as abnormally high precipitation during September of that year (APPENDIX A4). The years of 1980 and 1981 appeared to be ideal conditions for rockfall activity as considerable drought during the winter of 1980-1981 resulted in extremely dry soil and arid surface conditions. The dry and hard solid surface increased surface runoff when the area experienced a series of intense cloudbursts during the summer of 1981 (APPENDIX A5-A8). This resulted in extensive flooding and debris flows (Ouray, 2013). Rockfall analysis revealed numerous suppression and injuries in 1987 which is consistent with the type of growth response associated with large winter storm events such as those of that year (APPENDIX A9-A10). Significant events during 1995 include winter storms and the end of drought (APPENDIX A11-A12). Heavy rainfall on August 10 and 11, 2005, produced large-volume debris flows, and extensive flooding across Ouray (Ouray County, 2013). The year 2005 also experienced severe winter storms with temperatures nearly -10°. A massive rockslides was reported in January of 2014, which completely buried a portion of US 550, just outside of Ouray. The generally consistent growth release of healthy trees suggests decrease in competition as neighboring trees may be suffering from beetle infestation.

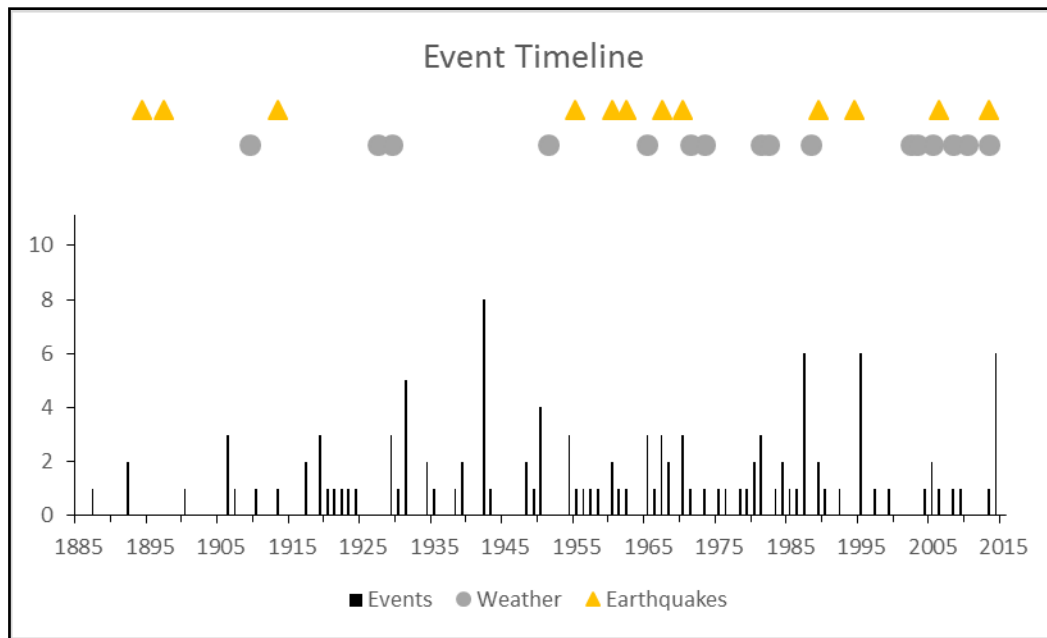


Figure 29 Event Timeline for rockfall occurrences and triggering mechanisms

6.2 Spatial Extent of Rockfall Activity

6.2.1 Rockfall Distribution

Analysis of recurrence intervals identified areas of preferred rockfall trajectories generally recording higher return periods of rockfalls (figure 30), and lower return periods on sampled trees protected by neighboring trees or located in a topographically favorable area. The number of trees affected by rockfall activity also decreases in a distant direction from the source highlighting the standard protective nature of the forest (Brang *et al.*, 2001) (APPENDIX B3). Recurrence intervals also align up with our mapped edge of our talus (figure 30).

One explanation for areas with higher recurrence intervals is the size and number of trees along the upper boundary of the forest edge. Those trees are likely to record the

highest number of impacts as compared to those down slope, thus rightfully named “Centurion trees”. Areas with higher recurrence intervals also correspond to areas with debris flows. These areas are down slope from major gullies as gullies can act as a major conduit for rockfall debris (APPENDIX B5).

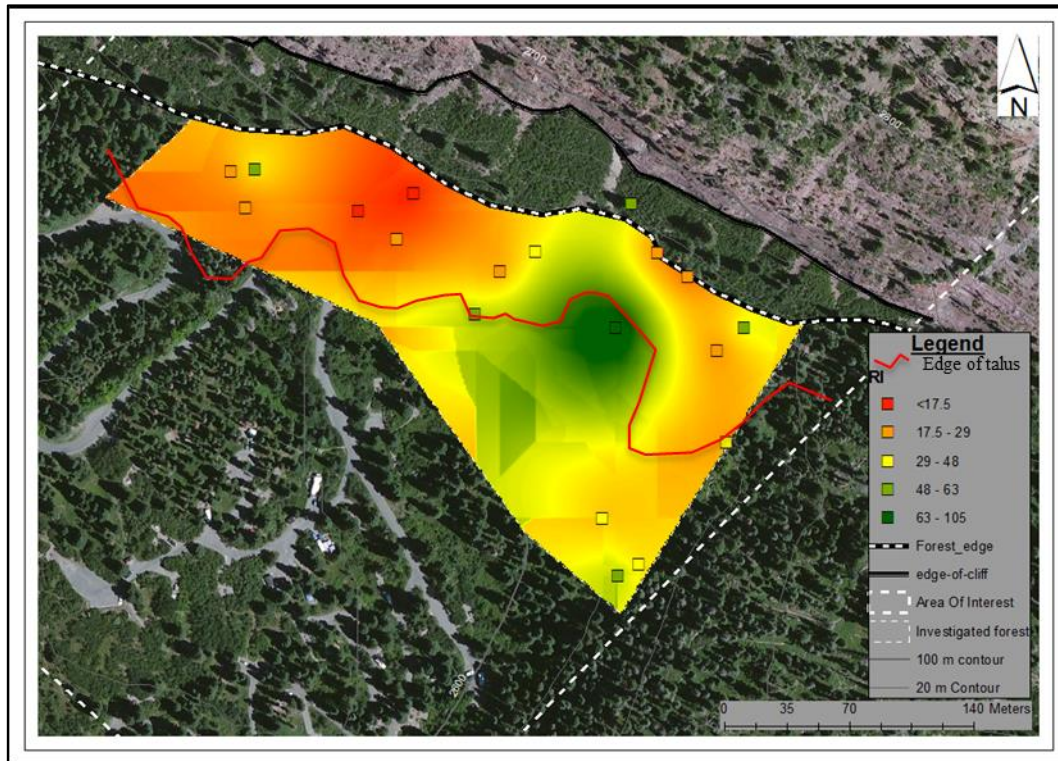


Figure 30 Distribution of return periods for rockfalls with interpolated values. The red line indicates the mapped lower edge of talus and rockfall deposits.

The distribution of clast size and sorting reflected the variable nature of a random rockfall process. Many of the largest boulders came to rest at the base of trees, which ended its downward momentum after being slowed by decapitated trees upslope. The

injuries visible from these impacts were used to help gage the frequency of rocks that make in deeper into the protective forest stand.

Figure 31 is a histogram of the number of total injuries binned into distances from forest edge. There is a strong negative correlation, and notice the abrupt brake between the 60 and 80 m which fits with the 70 m previously identified. This illustrates that the number of rockfall injuries will be the highest towards the leading edge of the forest as more rocks will impact trees before coming to a rest. The larger rocks that travel farther may impact multiple trees along its path thus demonstrating the frequency of recorded rockfall impacts with distance into the forest and not the number of individual rockfall events.

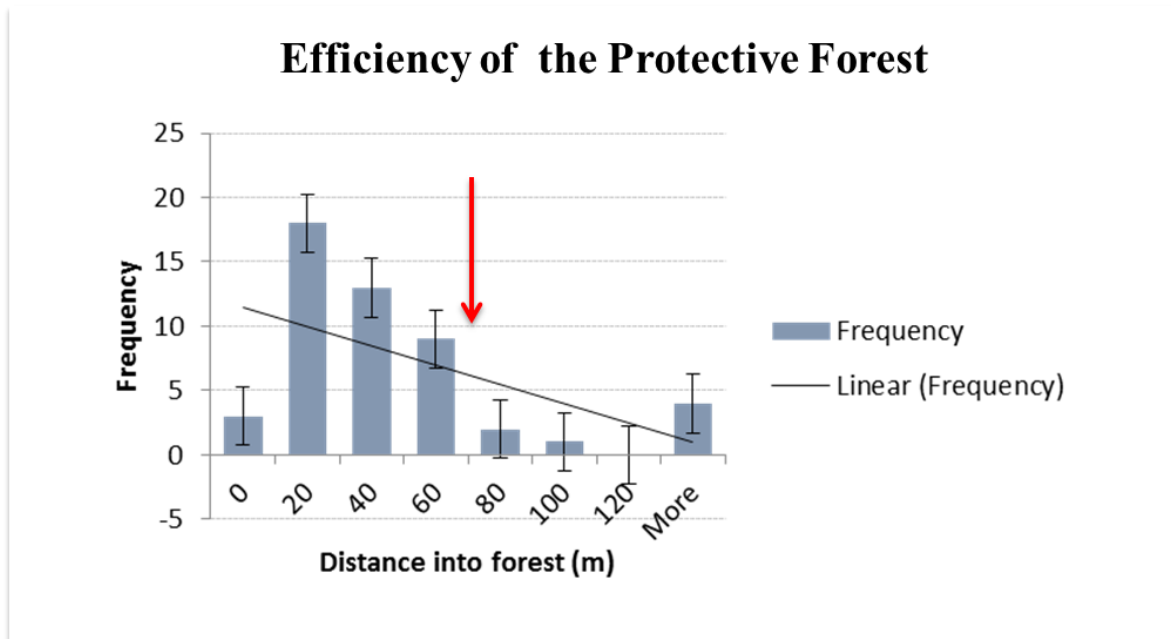


Figure 31 Histogram of number of total injuries binned into distances from forest edge. This illustrates that the farther into the forest, away from the source, the fewer impacts will be recorded as rocks are more likely to come to rest upslope (error bars and linear trend annotated)

6.2.2 *Broader Impacts*

For the past three years, the *Abies concolor* surrounding Ouray have been subjected to an engraver beetle infestation. Rapid removal of the forest will remove vital protective cover. This study can serve as a basis for planners who may want to create an educational program through awareness. Trees that are closely spaced will act as a protective barrier to rockfall, however, the higher density of trees in an area may also promote the spread of engraver beetles. Future work should place controls on tree spacing for optimal forest protection and limiting beetle outbreak.

CHAPTER VII

CONCLUSION

7.1 Conclusions and Recommendations

A US forest service campground is positioned below a large bedrock escarpment and is subjected to rockfall hazards. This research answers the question: What are the spatial and temporal characteristics of rockfall? To answer this question, two objectives were established. (i) delineate the spatial patterns of rockfall activity and (ii) establish a temporal chronology of rockfall activity. By visually analyzing rockfall deposits, rockfall induced tree injuries and associated growth disturbances to *Abies concolor* (White fir) trees, this study was able to delineating areas of varying rockfall hazard potential. The findings identify the area with the greatest hazard to rockfall activity is the area located below the gullies of the overlying cliffs and steep slopes. Additionally, the area from the base of the cliff to the forest edge, often called the scree slope, is especially subjected to rockfalls. Rockfalls activity continue into the adjacent forested zone, however, rockfall deposits were observed to rarely travel greater than 70 m once they enter the protective forest boundary, suggesting that the current spacing and density of the forest acts as an effective protective forest to rockfalls.

This study also demonstrates that tree-ring records of *Abies concolor* (White fir) can be used in geomorphic analysis to infer spatial and temporal patterns of rockfall event. This may be beneficial to other alpine areas where *Abies concolor* is the dominant tree species in the forest. Analysis of growth defects identified from *Abies concolor* tree cores allowed for the reconstruction of a rockfall chronology. This reconstruction

alluded to the observation of rockfall activity being dominated by low magnitude, high frequency events. Also, for the time period of investigation (1910-2015), no large mass movement event occurred within the study area. Based on the previous observations, we interpret the recorded rockfalls as attributed to annual freeze and thaw activity.

Although there were no observations of a large-scale mass movement event, several years recorded abnormally high rockfall rates, as determined from the reconstructed rockfall chronology. Years with abnormal rockfall activity include 1931, 1942, 1950, 1960, 1965, 1970, 1981, 1987, 1995, 2005, and 2014. Notable years exhibiting abnormally high rockfall activity are a result of some additional external factor ‘promoting’ and/or ‘triggering’ the rockfall event. Such external factors observed include heavy rainfall, rapid snow melt, earthquakes, among others.

Future work should include a hazard rating systems such as the “RHRS” which can be modified to categorize hazardous slope conditions on the steep slopes and cliffs above the campground. Maps can be produced using GIS software to visualize which lithologies and specific areas present the greatest hazard to slope failure.

Those hazards can then be used as a tool in rockfall modeling softwares to model rockfall trajectories based on expected release zones. Further work can also be used to predict rockfall velocities, and bounce heights using tree scar heights, and clast size, shape, and composition.

REFERENCES

Alestalo, J., 1971. Dendrochronological interpretation of geomorphic processes. *Fennia* 105, 1–139.

Andrew, R., 1994. The Colorado Rockfall Hazard Rating System. Colorado Department of Transportation. Report # CTI-CDOT-2-94.

Andrew, R., Hume, H., Bartingale, R., Rock, A., and Zhang, R., 2012. *CRSP-3D User's Manual-Colorado Rockfall Simulation Program*. Federal Highway Administration (FHWA), Federal Lands Highway (FLH) division. Publication No. FHWA-CFL/TD-12-007

Aqafonkin, V., 2009. SunCalc. <http://suncalc.net/> Accessed: May 20, 2016

Bathke, D., 2016. National Drought Mitigation Center, <http://droughtmonitor.unl.edu/> Accessed: January 14, 2016

Berger F., & Dorren L., 2006. Objective comparison of models using real size experimental data, Interpraevent 2006, 8 pp.

Berger, F., Larcher, V., Simoni, S., Pasquazzo, R., Strada, C., Zampedri, G., 2013. WP6 guidelines -Rockfall and Forecast systems. Paramount. Alpine Space: European Territorial Cooperation. 84 pp

Bjerrum, L., Jørstad, F., 1968. Stability of rock slopes in Norway. Norwegian Geotechnical Institute Publication 79:1– 11

Bozzolo, D., and Pamini, R., 1986. Simulation of rock falls down a valley side. *ActaMechanica* 63,113–30.

Brang, P., Gardner, B., Ott, E., Schönenberger, W., 2001. Forests as protection from natural hazards. In: EVANS, J. (ed.), *The Forests Handbook Volume 2*. Blackwell Science, Oxford, pp. 53–81.

Bull, W., Brandon, M., 1998. Lichen dating of earthquake-generated regional rockfall events, Southern Alps, New Zealand. *Geological Society of America Bulletin* 110, 60–84.

Bull, W., 2004. Sierra Nevada earthquake history from Lichens on rockfall blocks. *Sierra Nature Notes*, Vol. 4, 2004

Caine, N., 1974. The geomorphic processes of the alpine environment. In: Ives, J., Barry, R. (eds.): Arctic and Alpine Environments. Methuen, London, 721–748.

Carrara, P., and Andrews, J., 1973. Problems and application of lichenometry to geomorphic studies, San Juan Mountains, Colorado. Arctic and Alpine Research 5, p. 373-384

Chang, W., 1998. The effect of surface roughness on dynamic friction between neolite and quarry tile. Safety Science 29(2), 89–108. Colorado Earthquake Evaluation Report. www.dola.state.co.us/dem/mitigation/plan_2007/2007_plan.htm.

Collins, B., and Stock, G., 2016. Rockfall triggering by cyclic thermal stressing of exfoliation fractures. Nature Geoscience 9(5): 395-400.

Colorado Division of Emergency Management (CDEM), 2013. State of Colorado Natural Hazards Mitigation Plan. <http://www.dhsem.state.co.us/emergency-management/mitigationrecovery/mitigation/state-colorado-natural-hazards-mitigation-plan>.

Colorado Earthquake Information. Colorado Geological Survey, 2013. <http://geosurvey.state.co.us/hazards/Earthquakes/Pages/Earthquakes.aspx>.

Corona, C., Morel, P., Stoffel, M., Trappmann, D., 2015. Defining sample size and sampling strategy for dendrogeomorphic rockfall reconstructions. *Geomorphology* 236, 79-89.

Coughenour, M., Gao, W., and Stohlgren, T., 2015. Coloradoview.org. 10 meter resolution DEM.
<http://coloradoview.org/cwis438/websites/ColoradoView/Data.php?DefaultTab=Aerial>

Coutard J-P., Francou B., 1989. Rock temperature measurements in two alpine environments: implications for frost shattering. *Artic Alpine Res* 1989;21(4):399–416.

Cross, Whitman, and Spencer, A. C, 1900. Geology of the Rico Mountains, Colorado: U.S. Geological Survey 21st Annual Report, Pt. 2, p. 7-165

Cross, Whitman, Howe, Ernest, and Irving, J.D., 1907. Description of the Ouray quadrangle [Colorado]: U.S. Geological Survey Geologic Atlas, Folio 120, 20 p.

Dorren, L., 2003. A review of rockfall mechanics and modelling approaches. *Progress in Physical Geography* 27(1), 69–87.

Dorren, L., Berger, F., Jonnson, M., Krautblatter, M., Moelk, M., Stoffel, M., Wehrli, A., 2007. State of the art in rockfall – forest interactions.

SchweizerischeZeitschriftfürForstwesen 158: 128–141.

Douglas, G., 1980. Magnitude frequency study of rockfall in Co. Antrim, N. Ireland.

Earth Surface Processes and Landforms 5(2), 123–129.

Drought and Water Supply Assessment, 2004,

http://cwcb.state.co.us/Conservation/Drought/Drought_Water/index_DWSA.html

ESRI 2015. ArcGIS Desktop: Release 10.3 Redlands, CA: Environmental Systems Research Institute.

Franczyk, K., 1993. Measured section of the Pennsylvanian Hermosa Group near Ouray, Colorado: U.S. Geological Survey Open-File Report 93-712, 25 p.

Fritts, H., 1971. Dendroclimatology and dendroecology. Quaternary Research 1: 419-449

Fritts, H., 1976. Tree Rings and Climate, Academic Press, London. P 94

Giardino, J., (in review). Modeling The Face of Earth: Principle and Applications in Engineering Geology, Elsevier Science Series.

Google., 2015. Google Earth (Version 7) [Computer program]. Available at <http://www.google.com/earth/download/ge/agree.html>

Grissino-Mayer, H., 2001. Evaluating crossdating accuracy: a manual and tutorial for the computer program COFECHA. *Tree-Ring Research* 57:205-221.

Grissino-Mayer, H., 2003. A Manual and Tutorial for the Proper Use of an Increment Borer. *Tree Ring Research* 59: 63-79.

Gunzburger, Y., Merrien-Soukatchoff, V., & Guglielmi, Y., 2005. Influence of daily surface temperature fluctuations on rock slope stability: case study of the Rochers de Valabresslope (France). *Int. J. Rock Mech. Min. Sci.* 42,331–349

Guzzetti, F., Reichenbach, P., Wieczorek, G., 2003. Rockfall hazard and risk assessment in the Yosemite Valley, California, USA: *Natural Hazards and Earth System, Sciences*, v. 3, p.491-503, www.nat-hazards-earth-syst-sci.net/3/491/2003/

Hale, M., 1967. *The Biology of Lichens*. Edward Arnold Ltd., London

Hast, N., 1969. The state of stress in the upper part of the earth's crust.

Tectonophysics, 8, 169-211

Hazard Mitigation Planning and Hazard Mitigation Grant Program. Federal Register.

Interim Final Rule. February 26, 2002.

www.fema.gov/plan/mitplanning/interim_final_rules.shtm.

Hegg, C., and Kienholz, H., 1995. Determining paths of gravity-driven slope processes – the ‘Vector Tree Model’. In Carrara, A. and Guzetti, F., editors, Geographic information systems in assessing natural hazards. Dordrecht: Kluwer Academic Publishers, 79–92.

Hurteau, M., Zald, H., and North, M., 2007. Species-specific response to climate reconstruction in upper-elevation mixed-conifer forests of the western Sierra Nevada, California. Can. J. For. Res. 37, 1681–1691.

Ishikawa, M., Kurashige, Y., and Hirakawa, K., 2004. Analysis of crack movements observed in an alpine bedrock cliff. Earth Surface Processes and Landforms 29(7), 883–891.

"ISO 14688-1: 2002. Geotechnical investigation and testing – Identification and classification of soil – Part 1: Identification and description". International Organization for Standardization (ISO).

Jaboyedoff, M., and Labiouse, V., 2003. Preliminary assessment of rockfall hazard based on GIS data. ISRM2003 - Technology roadmap for rock mechanics, SouthAfrican Institute of Mining and Metallurgy.

Jochim, C., 1986. Debris-Flow Hazard in the Immediate Vicinity of Ouray, Colorado. Colorado Geological Survey Department of Natural Resources. Special Publication 30. 1986.

Lee, F., Odum, J., and Lee, J., 1997. Slope failures in northern Vermont, USA. *Enviornmental and Engineering Geoscience*. 3:161-82.

Luckman, B.H., 1976. Rockfalls and rockfall inventory data; some observations from the Surprise Valley, Jasper National Park, Canada. *Earth Surface Processes and Landforms* 1, 287–298.

Luckman, B., and Fiske, C., 1995. Estimating long term rockfall accretion rates by lichenometry. In: Slaymaker, O., (ed.), *Steepland Geomorphology*. Wiley, Chichester, UK, pp. 233–255.

Luedke, R., and Burbank, W., 1962. Geology of the Ouray Quadrangle, Colorado: U.S. Geological Survey Geologic Quadrangle Map GQ-152, scale 1:24,000.

Luedke, R., and Burbank, W., 1994. Measured Stratigraphic Sections In The Ouray Area, Western San Juan Mountains, Colorado: U.S. Geological Survey Open-File Report 94-583, 28 p.

Matsuoka, N., 2008. Frost weathering and rock wall erosion in the southeastern Swiss Alps: long term (1994-2006) observations. *Geomorphology* 99,353–368.

Matsuoka, N., and Sakai, H., 1999. Rockfall activity from an alpine cliff during thawing periods. *Geomorphology* 28, 309–328.

Nesje, A., Dahl, S., Løvlie, R. and Sulebak, J., 1994. Holocene glacier activity at the southeastern part of Hardangerjøkulen, central-southern Norway: evidence from lacustrine sediments. *The Holocene* 4, 377, 82.

NOAA's National Weather Service, 2013, Ouray Colorado.

<https://nwschat.weather.gov/p.php?pid=201302272011-KGJT-NOUS45-PNSGJT>

Nyberg, R., 1991. Geomorphic processes at snowpatch sites in the Abisko Mountains, northern Sweden. *Zeitschrift für Geomorphologie* 35(3),321–343.

Ouray County Multi-Hazard Mitigation Plan (Ouray), 2008, 2013. Hazard Mitigation and Emergency Management Programs.

Patrick, A., and Manitou-Alvarez, E., 2008. Using GIS data and mapping techniques to delineate areas most prone to hazardous rockfall in the state of Colorado.

Petrides, G., and Petrides, O., 1992. A Field Guide To Western Trees : Western United States And Canada. George A. Petrides ; Illustrated By Olivia Petrides, n.p.: Boston : Houghton Mifflin Co., 1992

Reed, J., 2013. Analysis Of The Mechanics Of The Ouray, CO Landslide. Honors and Undergraduate Research Thesis: Texas A&M University.

Ritter, D., Kochel, G., and Miller, J., 2002. Process geomorphology. McGraw-Hill, New York (4th edition).

Rizzo, D., and Harrington, T., 1988. Root movement and root damage of red spruce and balsam fir on subalpine sites in the White Mountains, New Hampshire. Canadian Journal of Forest Research, 18, 991–1001.

Russell, C., 2005. *Modification to the Colorado Rockfall Hazard Rating System*. Prepared for the Colorado Department of Transportation.

Russell, C., Santi, P., and Higgins, J., 2008. *Modification and Statistical Analysis of the Colorado Rockfall Hazard Rating System*. Prepared for the Colorado Department of

Transportation-Dtd Applied Research and Innovation Branch. Report No. CDOT-2008-7.

Schneuwly, D., and Stoffel, M., 2008a. Spatial analysis of rockfall activity, bounce heights and geomorphic changes over the last 50 years – a case study using dendrogeomorphology. *Geomorphology* 102:522–531.

Schneuwly, D., Stoffel, M., and Bollschweiler, M., 2009a. Formation and spread of callus tissue and tangential rows of resin ducts in *Larix decidua* and *Picea abies* following rockfall impacts. *Tree Physiol.* 29:281–289.

Schneuwly, D., Stoffel, M., Dorren, L., and Berger, F., 2009b. Three-dimensional analysis of the anatomical growth response of European conifers to mechanical disturbance. *Tree Physiol.* 29:1247–1257

Schuster, R., and Krizek, R., 1978. *Landslides, analysis and control*, Transportation Research Board Special Report No. 176., Washington: National Academy of Sciences.

Schweingruber, F., 1988. *Tree Rings; Basics and Applications of Dendrochronology*. D. Reidel Publishing Co., Dordrecht, the Netherlands. 276 pp.

Sharpe, C., 1960. *Landslides and related phenomena; a study of mass-movements of soil and rock*, Paterson N.J., Pageant Books

Shroder, J., 1978. Dendrogeomorphology: review and new techniques of tree-ring dating. *Progress in Physical Geography* 1980 4: 161

Skempton, A., and Weeks, A., 1976. The Quaternary History of the Lower Greensand Escarpment and Weald Clay Vale near Sevenoaks, Kent. In Turner, A., and Schuster, R., 1996. *Landslides: investigation and mitigation*, Transportation Research Board, Special Report 247, Washington, DC: National Academy Press.

Spatial Hazard Events and Losses Database for the United States. *SHELDUS*. 2015. University of South Carolina Hazards Research Lab. <http://hvri.geog.sc.edu/SHELDUS/>

State of Colorado Drought Mitigation and Response Plan. 2010 and 2013.
<http://cwcbweblink.state.co.us/WebLink/ElectronicFile.aspx?docid=145453&searchid=8b0c8c76-e047-4f46-8e09-7237713bddeb&dbid=0>

Stoffel, M., 2006. A review of studies dealing with tree rings and rockfall activity: the role of dendrogeomorphology in natural hazard research. *Nat. Hazards* 39, 51–70.

Stoffel, M., and Bollschweiler, M., 2008. Tree-ring analysis in natural hazards research—an overview. *Nat. Hazards Earth Syst. Sci.* 8, 187–202.

Stoffel, M., and Perret, S., 2006. Reconstructing past rockfall activity with tree rings: some methodological considerations. *Dendrochronologia* 24, 1–15

Stoffel, M., Schneuwly, D., Bollschweiler, M., Lièvre, I., Delaloye, R., Myint, M., and Monbaron, M., 2005a. Analyzing rockfall activity (1600–2002) in a protection forest – A case study using dendrogeomorphology. *Geomorphology* 68:224–241.

Stoffel, M., Lievre, I., Monbaron, M., and Perret, S., 2005b. Seasonal timing of rockfall activity on a forested slope at Täschgufer (Swiss Alps) – A dendrochronological approach. *Zeitschrift für Geomorphologie* 49:89–106.

Stoffel, M., Bollschweiler, M., Butler, D., and Luckman, B., 2010. *Tree Rings and Natural Hazards – A State-of-the-art*. Springer: Dordrecht; New York.

Stoffel, M., Bollschweiler, M., Vazquez-Selem, L., Franco-Ramos, O., and Palacios, D., 2011. Dendrogeomorphic dating of rockfalls on low-latitude, high-elevation slopes: Rodadero, Iztaccíhuatl volcano, Mexico. *Earth Surface Processes and Landforms* 36:1209–1217

Stoffel, M., Butler, D., and Corona, C., 2013. Mass movements and tree rings: a guide for dendrogeomorphic field sampling and dating. *Geomorphology* 200, 106–120.

Stokes, M., and Smiley, T., 1968. *An Introduction to Tree-Ring Dating*. University of Chicago Press, Chicago, Illinois.

Storm Events Database. National Climatic Data Center.

<http://www.ncdc.noaa.gov/stormevents/>. *Assessed: Febuary 4,2014.*

Strunk, H., 1997. Dating of geomorphological processes using dendrogeomorphological methods. *Catena* 31, 137–151

Tardif, J., Camarero, J., Ribas, M., and Gutie´rrez, E., 2003. Spatiotemporal variability in tree growth in the Central Pyrenees: climatic and site influences. *Ecological Monographs*, 73, 241–257.

Terzaghi, K., 1950. Mechanism of landslides. In *Application of geology to engineering practice*, pp. 83-1123. Ed. By S. Paige. Geol. Soc. America Berkey Vol.

Terzaghi, K., and Peck, R., 1967. *Soil Mechanics in Engineering Practice*. John Wiley & Sons, New York, pp. 425 – 426. In Turner, A., and Schuster, R., 1996. *Landslides: investigation and mitigation*, Transportation Research Board, Special Report 247, Washington, DC: National Academy Press.

Trappmann, D., and Stoffel, M., 2013. Counting scars on tree stems to assess rockfall hazards: a low effort approach, but how reliable? *Geomorphology* 180–181: 180–186.

Trappmann, D., Corona, C., and Stoffel, M., 2013. Rolling stones and tree rings: a state of research on dendrogeomorphic reconstruction of rockfall. *Prog. Phys. Geogr.* 37 (5), 701–716.

Turner, A., and Schuster, R., 1996. *Landslides: investigation and mitigation*, Transportation Research Board, Special Report 247, Washington, DC: National Academy Press.

US Census Bureau. (<http://www.census.gov/geo/maps-data/>). Assessed: November 19, 2015.

Varnes, D., 1978. Slope movements: types and processes. In: Schuster, R., and Krizek, R., (Eds.), 1978. *Landslide analysis and control*. Transportation Research Board, Special Report 176, Washington D.C., pp. 11–33.

Western Regional Climate Center (WRCC). 2016. Cooperative Climatological Data Summaries. Retrieved from <http://www.wrcc.dri.edu/climatedata/climsum/>

Whalley, W., 1974. Rock glaciers and their formation as part of a glacier debris-transport system. Geographical Papers, University of Reading, Department of Geography, 24.

Whalley, W., 1984. Rockfalls. In: Brundsdon, D., Prior, D.B., (eds.), Slope instability. London, Wiley, pp. 217–256.

White, J., and Wait, T., 2008. Rockfall in Colorado, Rock Talk. Colorado Geological Survey (CGS). Vol 11. No. 2

Winchester, V., Gartner, H., and Bezzi, M., 2007. Dendrogeomorphological applications. In: Kalvoda, J., Goudie, A., (eds), Geomorphological Variations. Prague: Nakladatelstvi P3K, pp. 183–203.

Yamaguchi, D., 1991. A simple method for cross-dating increment cores from living trees. Canadian Journal of Forest Research 21: 414-416.

Zaruba, Q., and Mencl, V., 1982. *Landslides and Their Control*. In Turner, A., and Schuster, R., 1996, *Landslides: investigation and mitigation*, Transportation Research Board, Special Report 247, Washington, DC: National Academy Press.

Zielonka, T., and Dubaj, N., 2009. A tree-ring reconstruction of geomorphologic disturbances in cliff forests in the Tatra Mts. *Landform Analysis* 11: 71–76.

APPENDIX A

DAILY TEMPERATURE AND PRECIPITATION

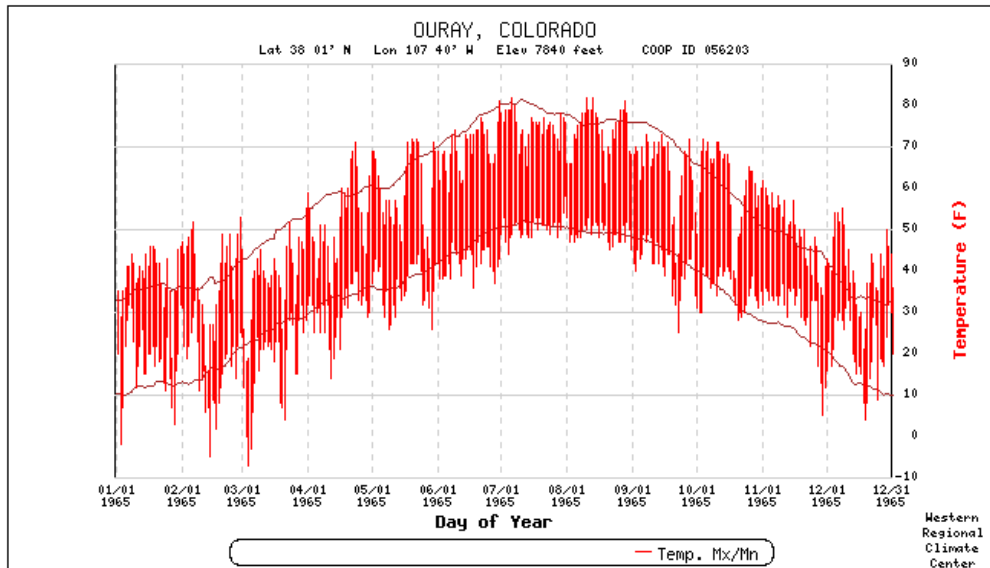


Figure A1: Daily temperature (F°) for 1965 (Source: Western Regional Climate Center)

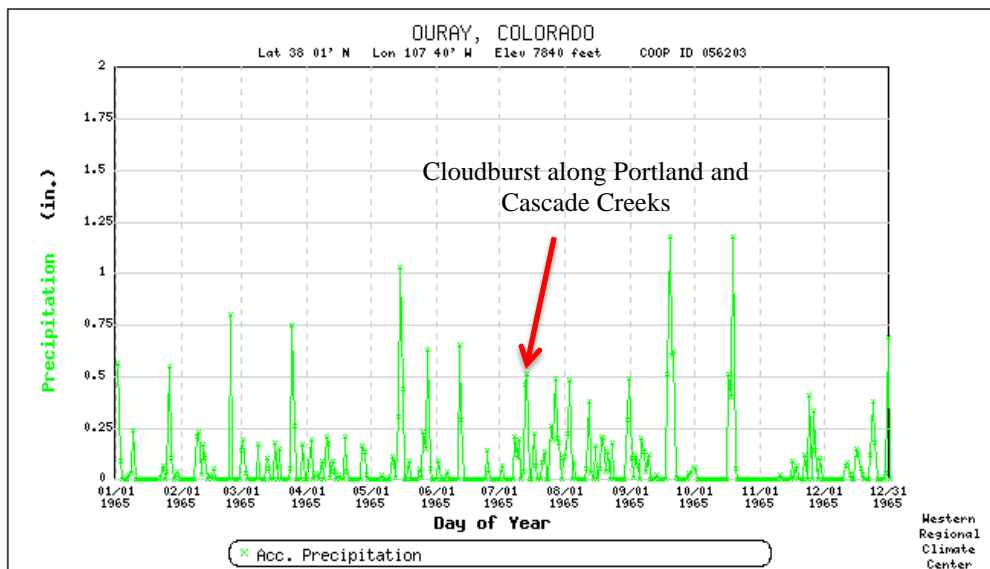


Figure A2: Daily precipitation (in) for 1965 (Source: Western Regional Climate Center)

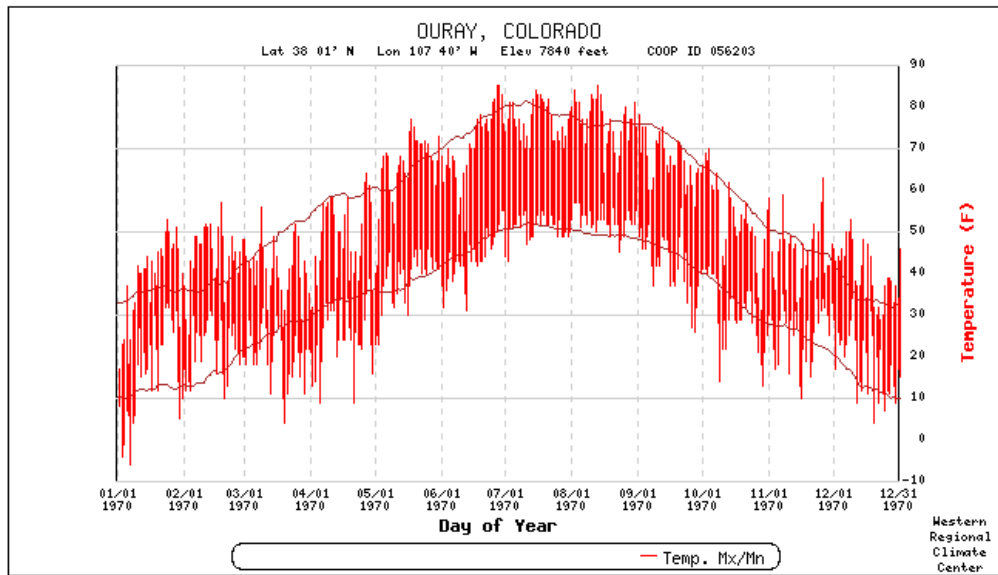


Figure A3: Daily temperature (F°) for 1970 (Source: Western Regional Climate Center)

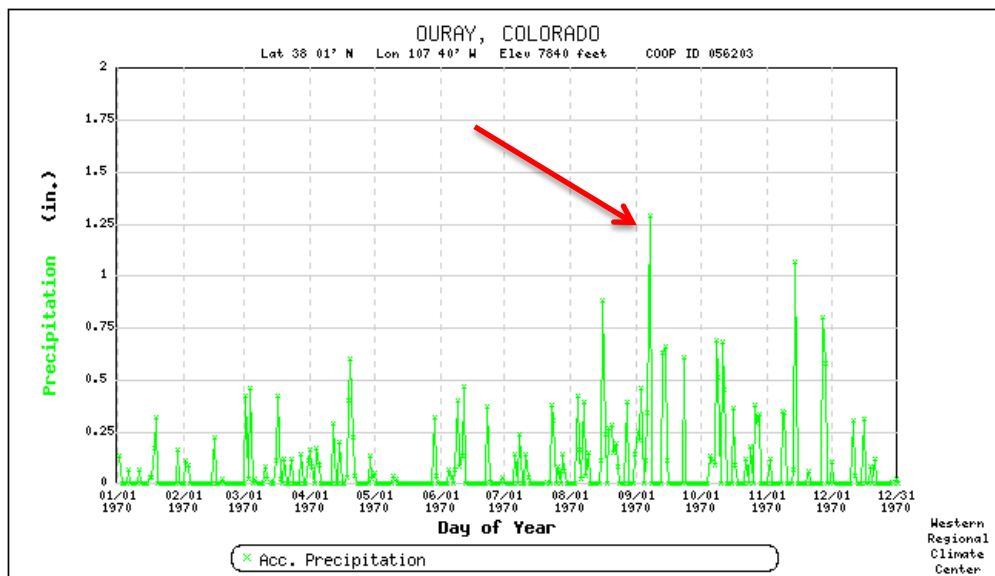


Figure A4: Daily precipitation (in) for 1970 (Source: Western Regional Climate Center)

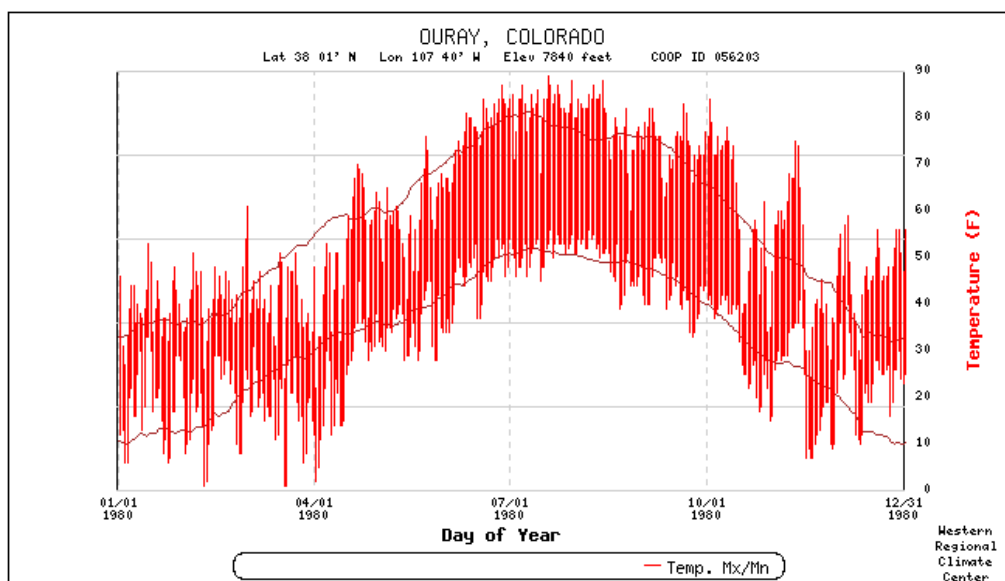


Figure A5: Daily temperature (F°) for 1980 (Source: Western Regional Climate Center)

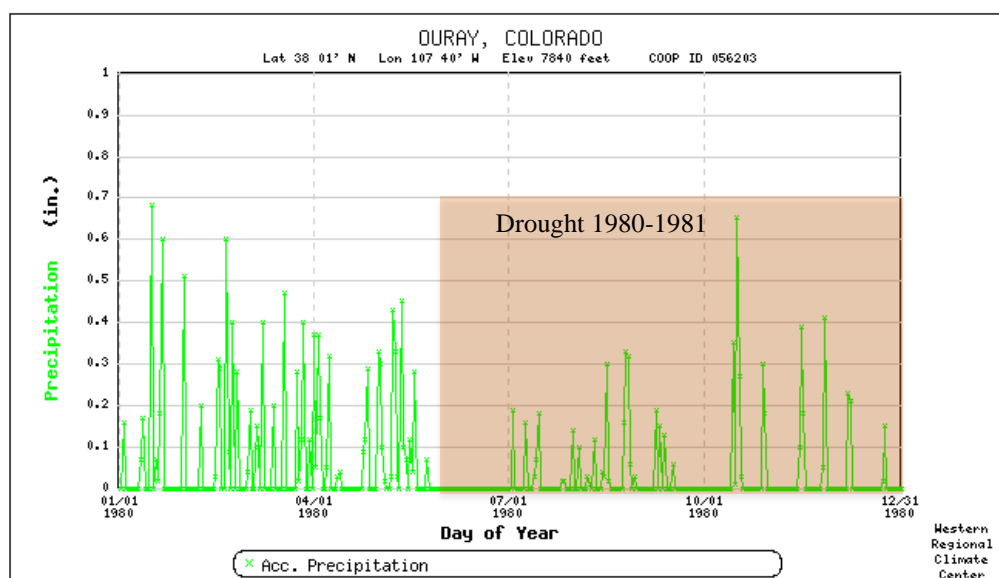


Figure A6: Daily precipitation (in) for 1980 (Source: Western Regional Climate Center)

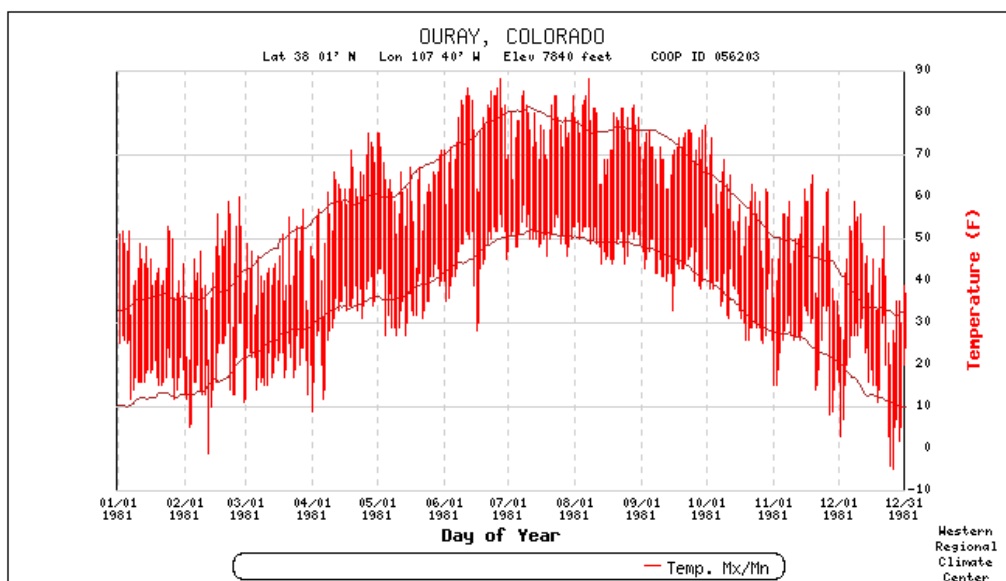


Figure A7: Daily temperature (F°) for 1981 (Source: Western Regional Climate Center)

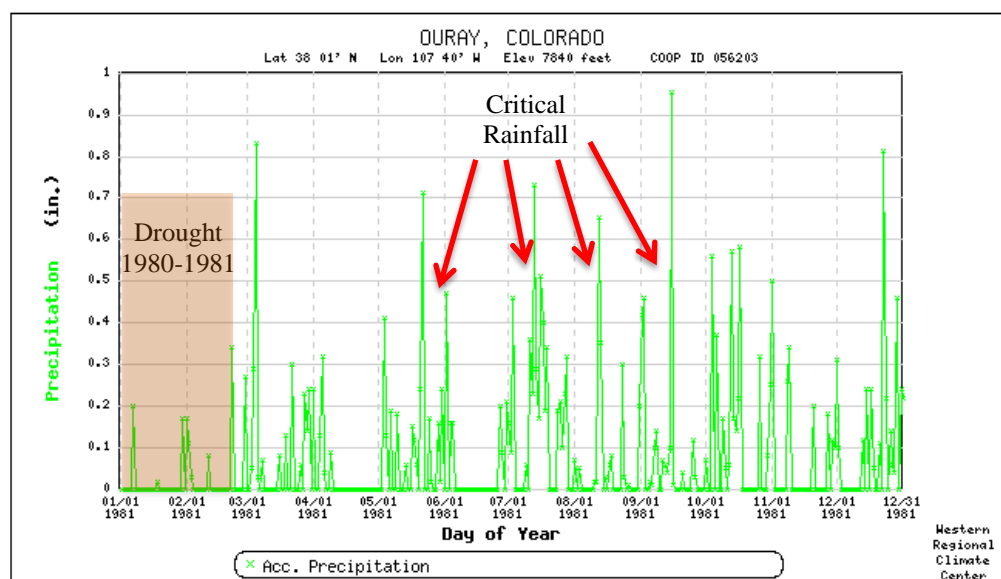


Figure A8: Daily precipitation (in) for 1981 (Source: Western Regional Climate Center)

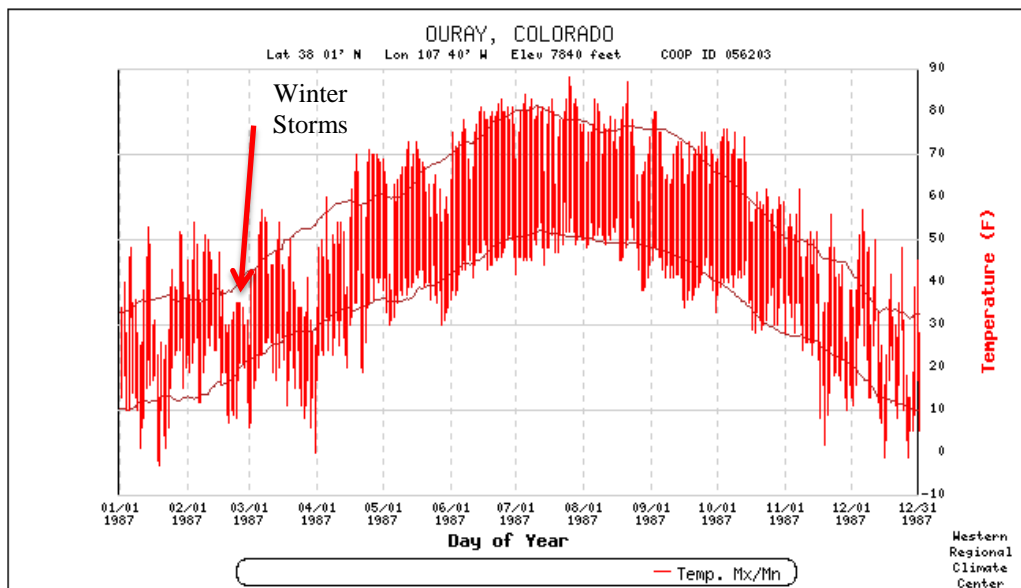


Figure A9: Daily temperature (F°) for 1987 (Source: Western Regional Climate Center)

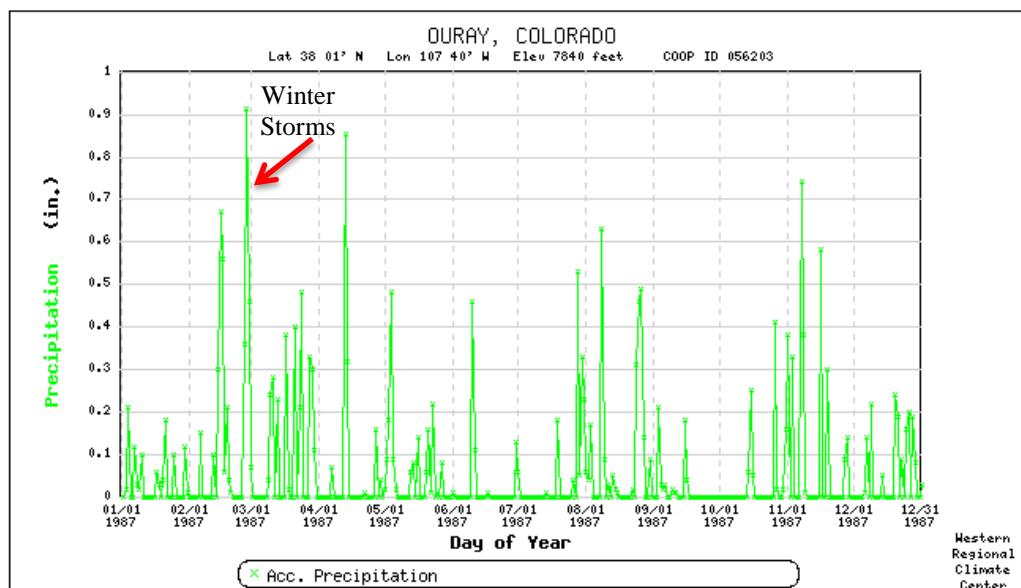


Figure A10: Daily precipitation (in) for 1987 (Source: Western Regional Climate Center)

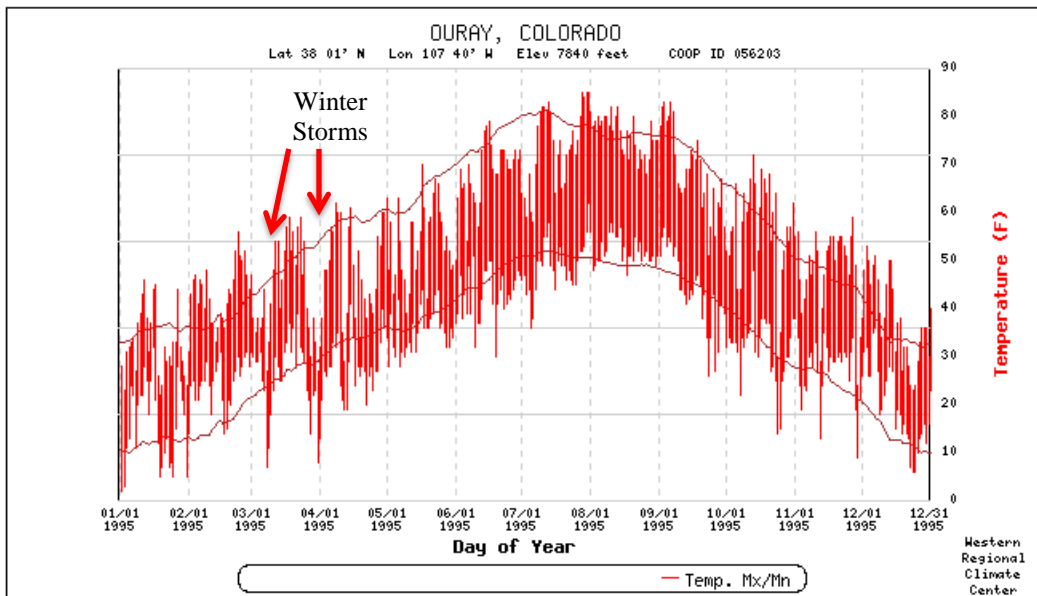


Figure A11: Daily temperature (F°) for 1995 (Source: Western Regional Climate Center)

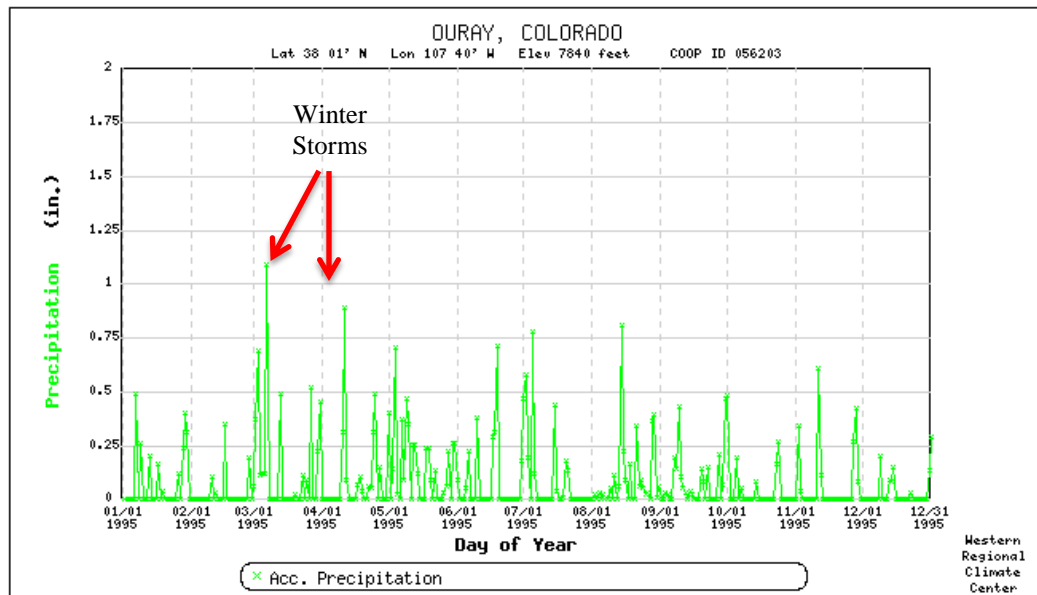


Figure A12: Daily precipitation (in) for 1995 (Source: Western Regional Climate Center)

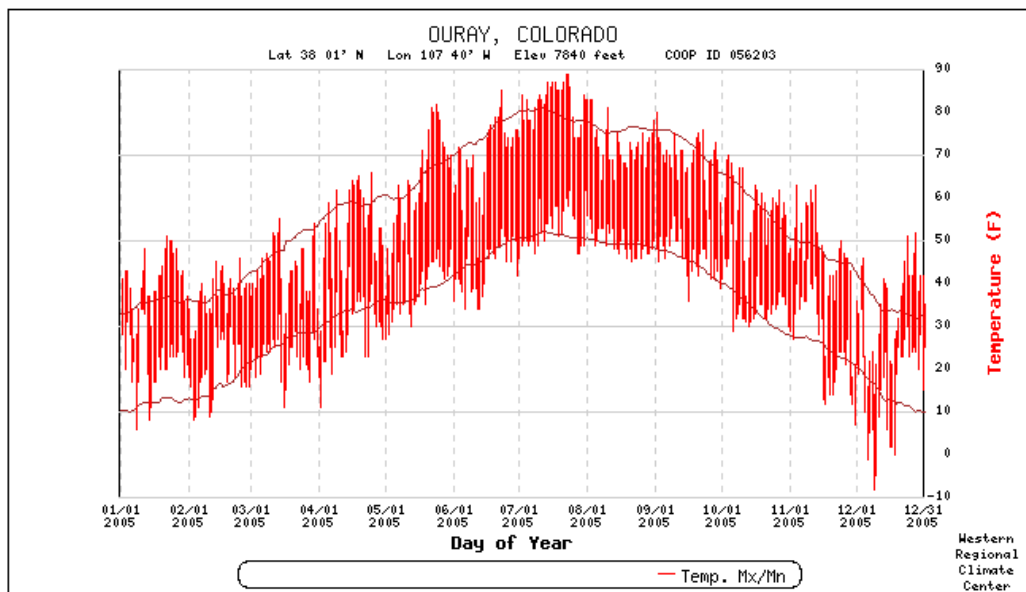


Figure A13: Daily temperature (F°) for 2005 (Source: Western Regional Climate Center)

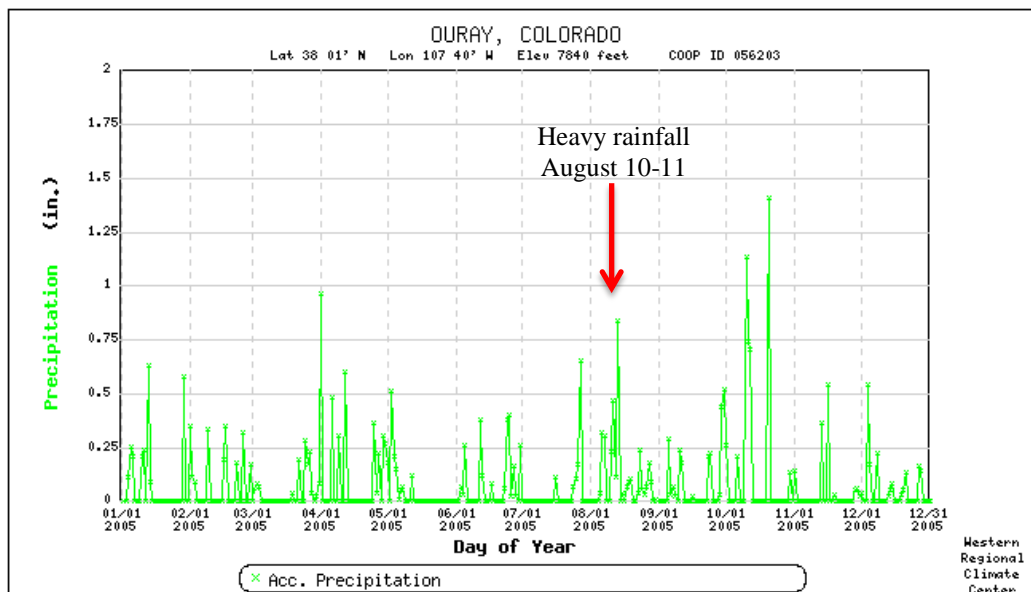


Figure A14: Daily precipitation (in) for 2005 (Source: Western Regional Climate Center)

APPENDIX B

ADDITIONAL FIGURES

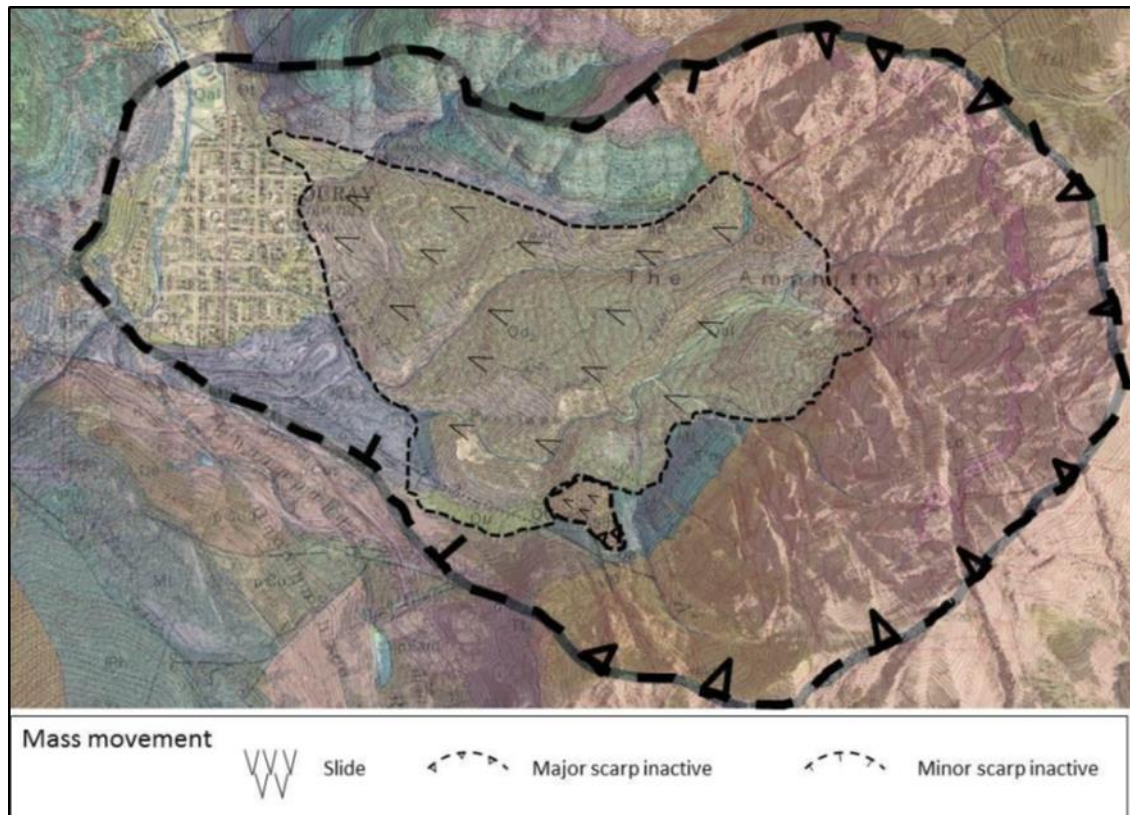


Figure B1: Ouray Amphitheater landslide deposits from (from Reed, 2013)



Figure B2: Mosaic of injured trees (Photos by author)

Table B1: Average rockfall distance from forest edge in each category

Age Category	Average distance (m)
1 (2000-2015)	29.2
2 (1950-2000)	18.8
3 (<1950)	56.8
Total average	~35

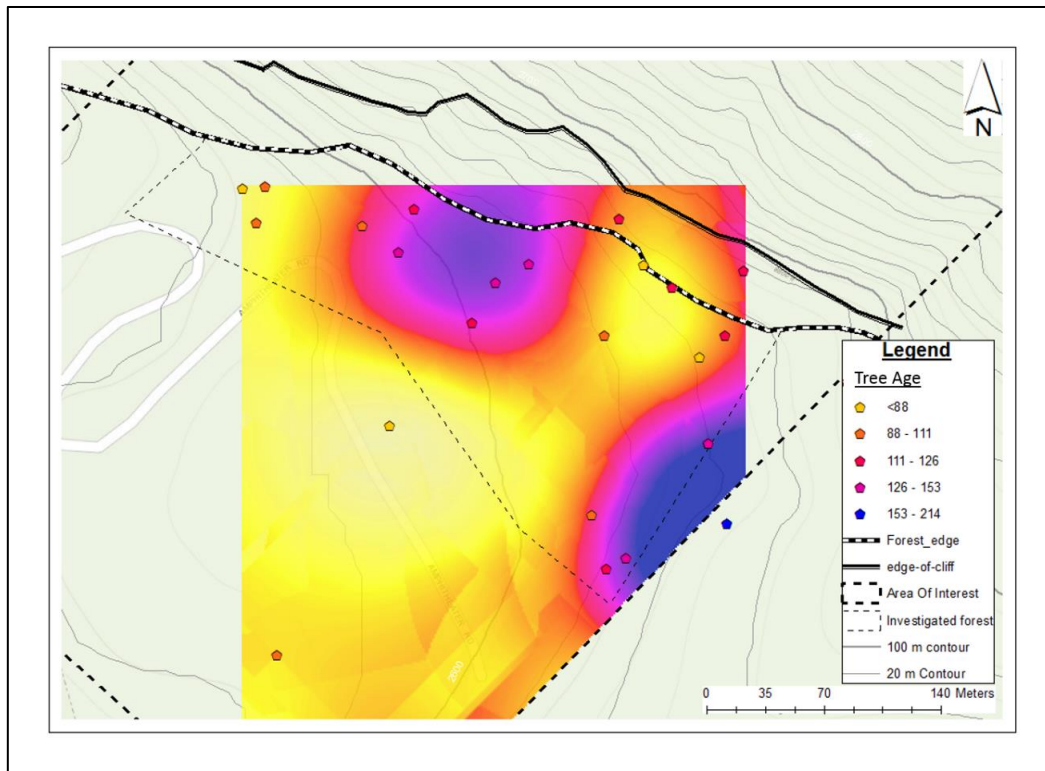


Figure B3: Visualization of tree ages with interpolated values

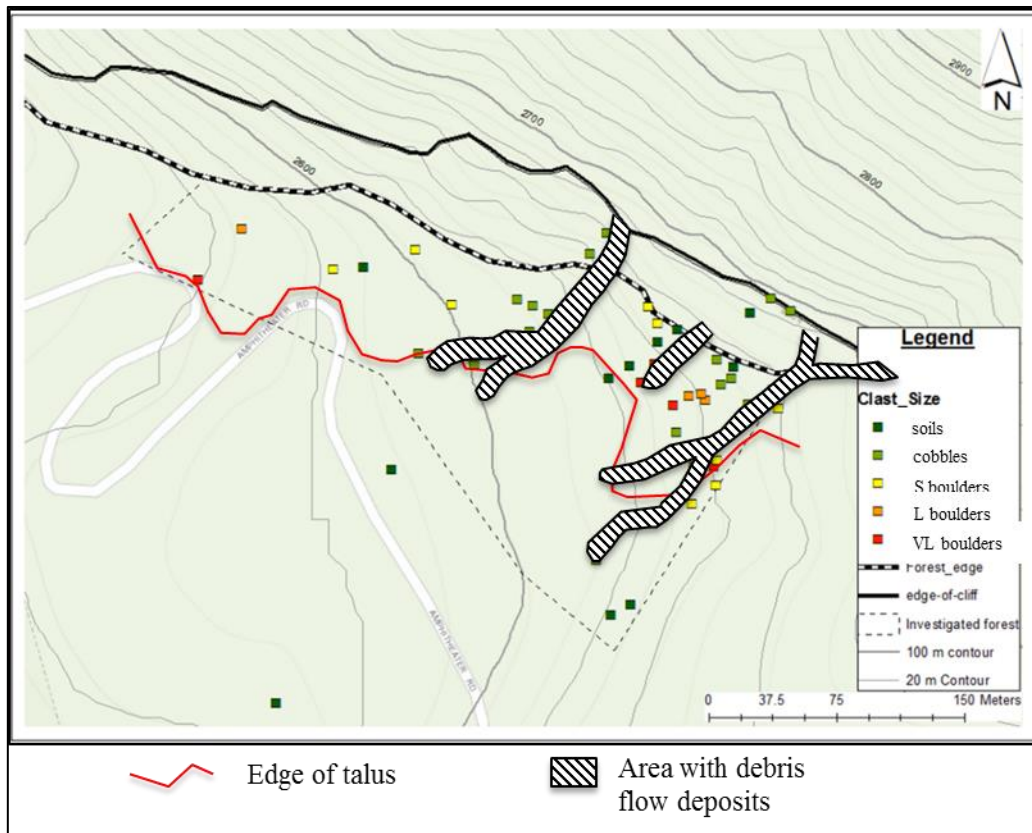


Figure B4: Locations of rockfall deposits subdivided into clast sizes. Redline annotates the lowed edge of the mapped talus debris. Areas with debris flows are also shown.

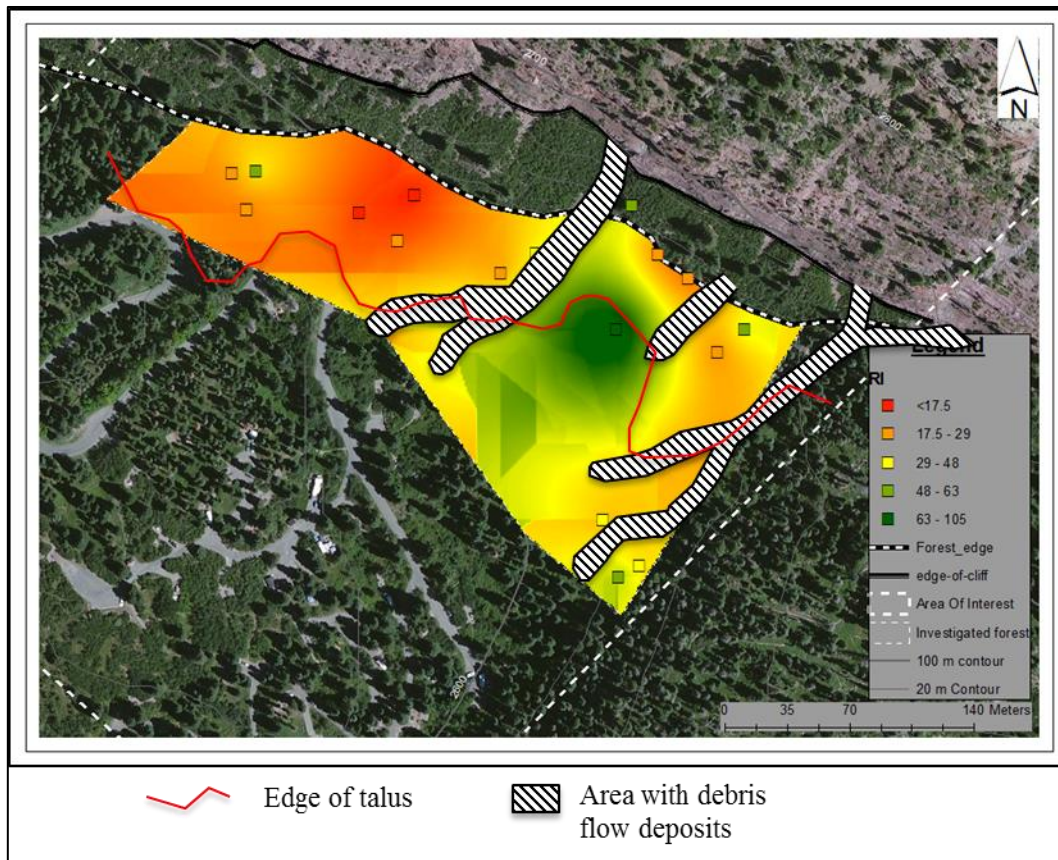


Figure B5: Distribution of return periods for rockfalls with interpolated values. Redline annotates the lowered edge of the mapped talus debris. Areas with debris flows are also shown.

APPENDIX C

RETURN PERIOD DATA

Table C1: Estimation of return periods of rockfalls, depending on the availability of growth disturbances in trees

Tree	First ring	Age (years)	Tree diameter	Impacts	Return period (years)
O1501	1904	111	21.3	2	55.5
O1502	-	-	27.4	-	-
O1503	1910	105	57.9	3	35.0
O1504	-	-	-	-	-
O1505	1900	115	48.8	2	57.5
O1506	-	-	12.2	-	-
O1507	1890	125	61.0	1	-
O1508	1892	123	39.6	6	20.5
O1509	1949	66	30.5	3	22.0
O1510	1892	123	48.8	2	61.5
O1511	1873	142	30.5	5	28.4
O1512	1910	105	48.8	1	105.0
O1513	-	-	-	-	-
O1514	1927	88	30.5	4	22.0
O1515	1892	123	48.8	9	13.7
O1516	1917	98	27.4	4	24.5
O1517	1862	153	15.2	7	21.9
O1518	1910	105	30.5	6	17.5
O1401	1900	114	32.0	4	-
O1402	1910	104	57.9	2	-
O1403	1928	86	54.9	2	-
O1404	1800	214	57.9	3	-
O1405	1866	148	31.1	6	24.7
O1406	1866	148	31.1	4	37.0
O1407	1870	144	64.0	3	48.0
O1408	1896	118	57.9	2	59.0
O1409	1927	87	16.5	3	29.0
O1410	1936	78	63.1	-	-
O1411	1909	105	63.1	4	-
O1412	1916	98	48.8	4	-
O1413	1862	152	37.8	4	38.0
O1414	1888	126	68.0	2	63.0
Total	-	-	-	98	-
Mean	-	118.0	42.1	3.6	39.2
Note: Return periods were obtained by dividing tree age (years) by the number of reconstructed impacts. Tree diameter (cm) taken at breast height.					

APPENDIX D

ADDITIONAL WEATHER DATA

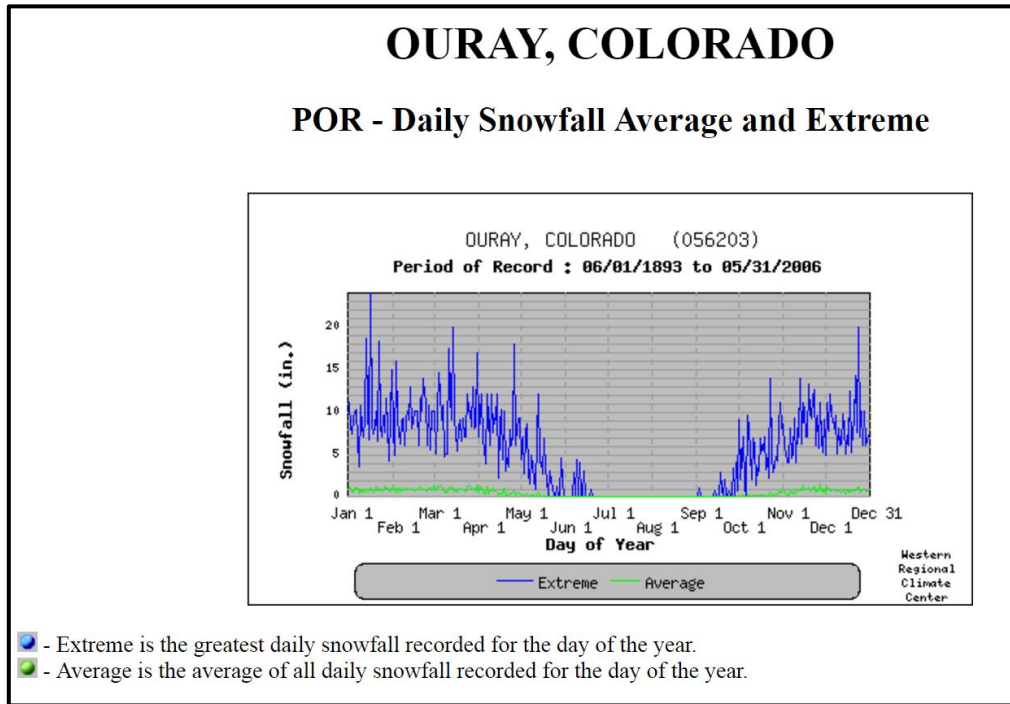
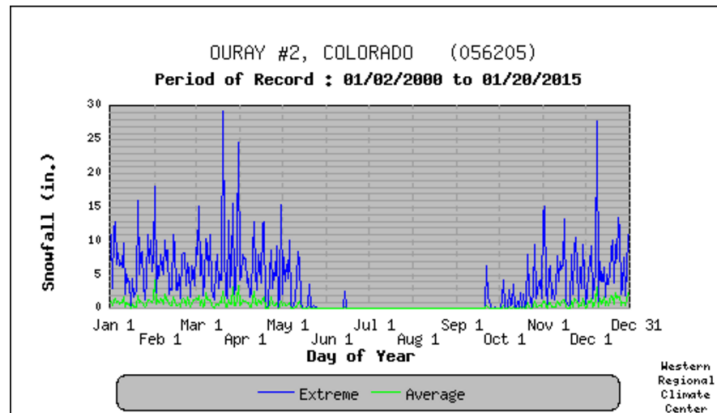


Figure D1: Ouray, Co., daily snowfall average and extreme (1893-2006) (Source: Western Regional Climate Center)

OURAY #2, COLORADO

POR - Daily Snowfall Average and Extreme



- - Extreme is the greatest daily snowfall recorded for the day of the year.
- - Average is the average of all daily snowfall recorded for the day of the year.

Figure D2: Ouray, Co., daily snowfall average and extreme (2000-2015) (Source: Western Regional Climate Center)

OURAY, COLORADO

POR - Daily Snowfall Average

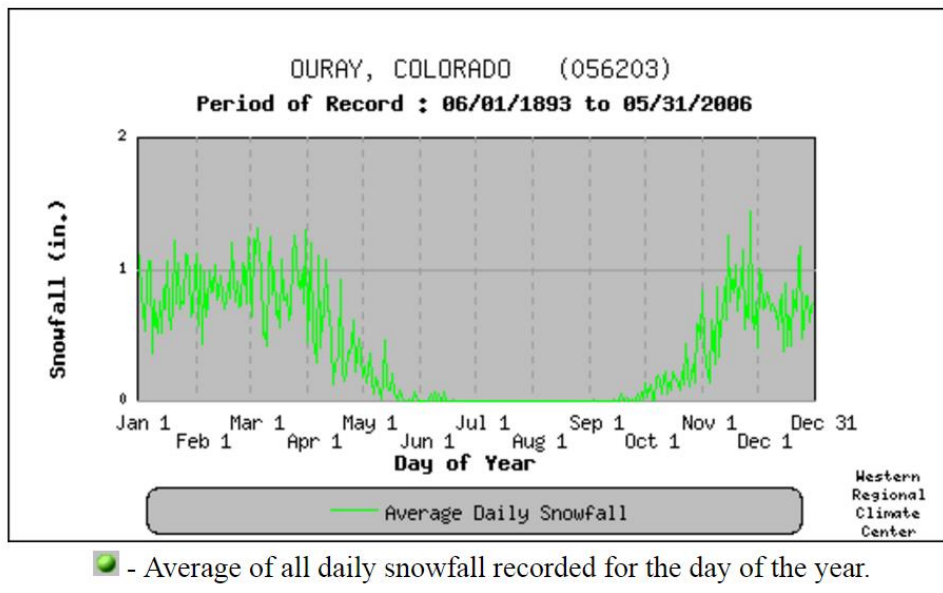


Figure D3: Ouray, Co., daily snowfall average (1893-2006) (Source: Western Regional Climate Center)

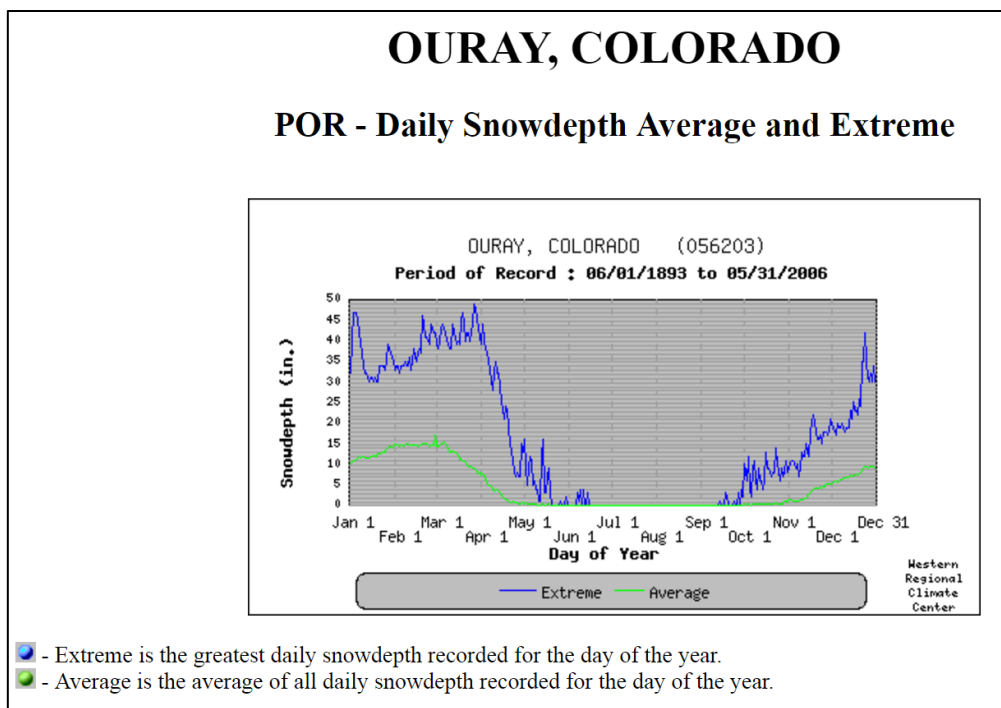


Figure D4: Ouray, Co., daily snowdepth average and extreme (1893-2006) (Source: Western Regional Climate Center)

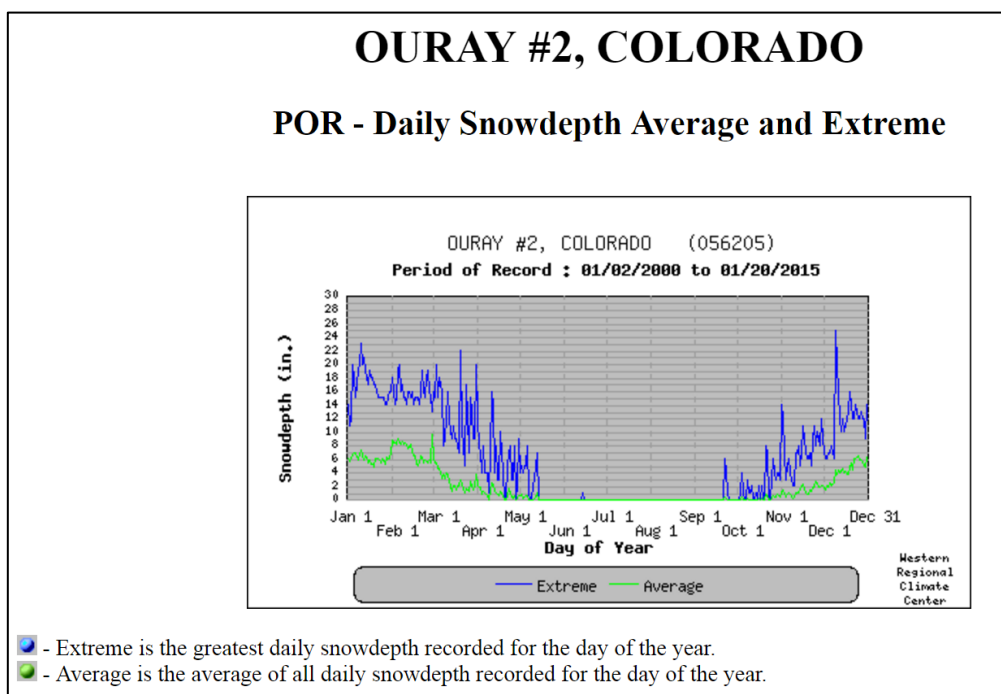


Figure D5: Ouray, Co., daily snowdepth average and extreme (2000-2015) (Source: Western Regional Climate Center)

OURAY, COLORADO

POR - Daily Snowdepth Average

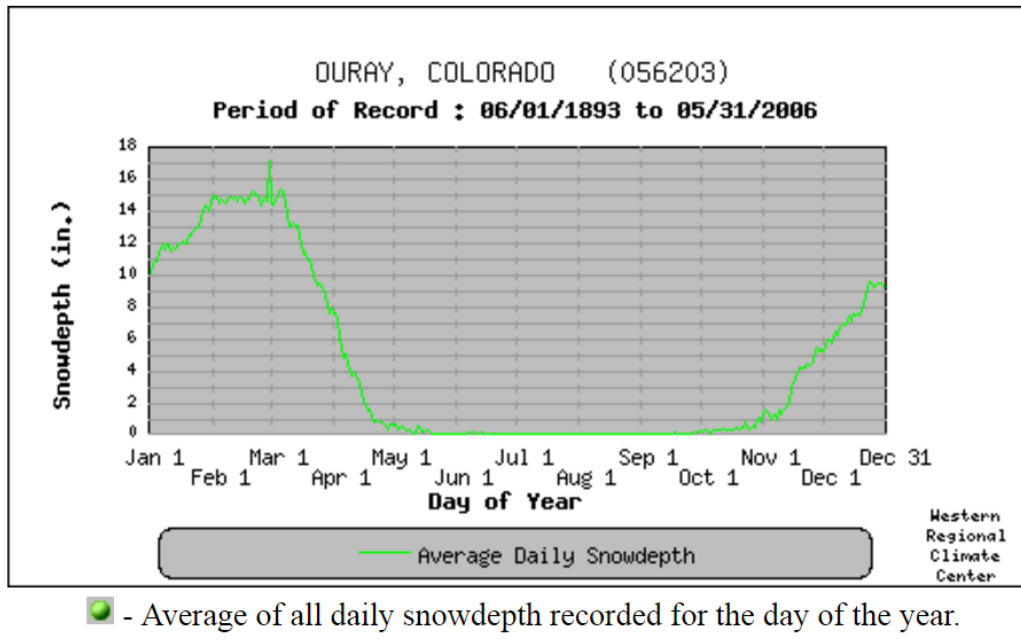
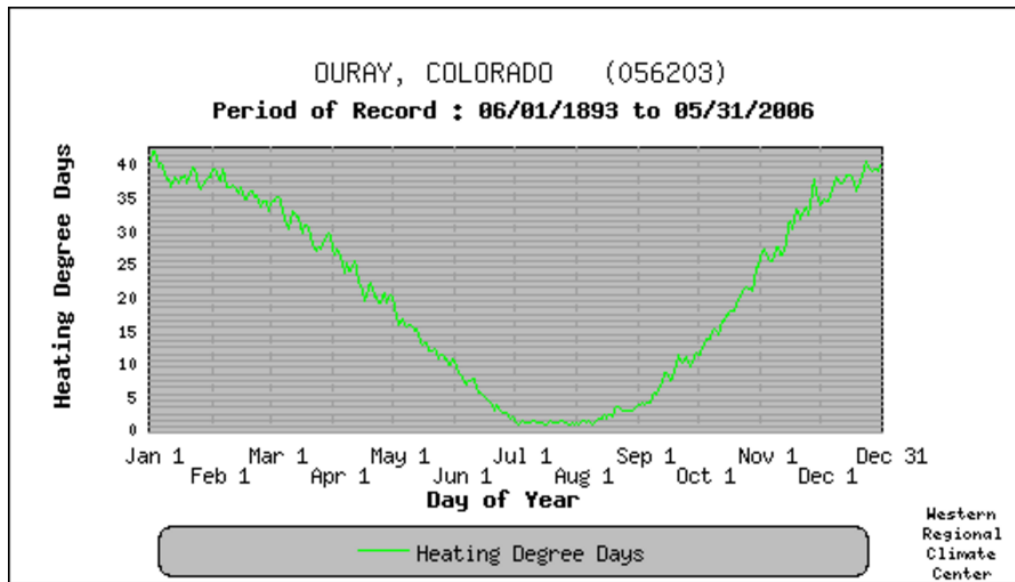


Figure D6: Ouray, Co., daily snowdepth average (1893-2006) (Source: Western Regional Climate Center)

OURAY, COLORADO

POR - Heating Degree Days (Base 65)

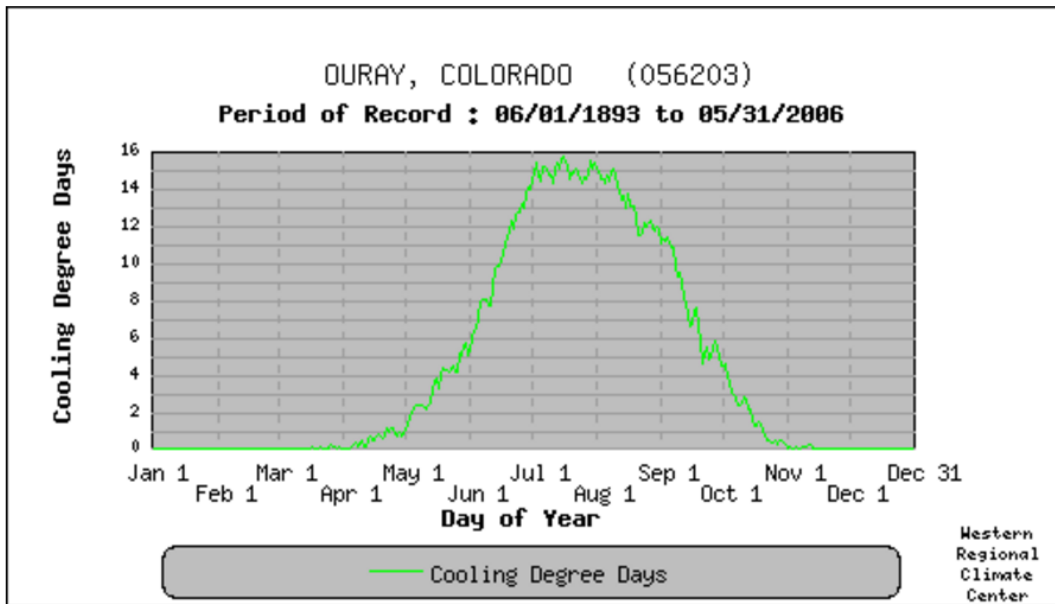


■ - Average of all heating degree day units recorded for the day of the year.

Figure D7: Ouray, Co., heating degree days (1893-2006) (Source: Western Regional Climate Center)

OURAY, COLORADO

POR - Cooling Degree Days



■ - Average of all cooling degree day units recorded for the day of the year.

Figure D8: Ouray, Co., cooling degree days (1893-2006) (Source: Western Regional Climate Center)

APPENDIX E

COFECHA RESULTS

```
[ ] DENDROCHRONOLOGY PROGRAM LIBRARY                      Run CORE8
Program COF  21:33  Fri 25 MAR 2016  Page   1
[ ]
[ ] P R O G R A M          C O F E C H A
Version 3.00P      29671
```

QUALITY CONTROL AND DATING CHECK OF TREE-RING MEASUREMENTS

Title of run: cores8 omitted

File of DATED series: Cores8

CONTENTS:

- Part 1: Title page, options selected, summary, absent rings by series
- Part 2: Histogram of time spans
- Part 3: Master series with sample depth and absent rings by year
- Part 4: Bar plot of Master Dating Series
- Part 5: Correlation by segment of each series with Master
- Part 6: Potential problems: low correlation, divergent year-to-year changes, absent rings, outliers
- Part 7: Descriptive statistics

RUN CONTROL OPTIONS SELECTED

VALUE

1	Cubic smoothing spline 50% wavelength cutoff for filtering	32 years
2	Segments examined are	50 years lagged successively by
25 years		
3	Autoregressive model applied	A Residuals are used in master
dating series and testing		
4	Series transformed to logarithms	Y Each series log-transformed
for master dating series and testing		
5	Critical correlation, 99% confidence level	.3281
6	Master dating series saved	N
7	Ring measurements listed	N
8	Parts printed	1234567
9	Absent rings included in master series	N

Time span of Master dating series is 1800 to 2015 216 years
Continuous time span is 1800 to 2015 216 years
Portion with two or more series is 1862 to 2015 154 years

```
>> WARNING: Year 1800 absent in 1 of 1 series; Master Series value -.037
>> WARNING: Year 1952 absent in 1 of 40 series; Master Series value .285
>> WARNING: Year 1953 absent in 1 of 40 series; Master Series value .689
>> WARNING: Year 1955 absent in 1 of 41 series; Master Series value .321
>> WARNING: Year 1957 absent in 1 of 41 series; Master Series value .998
>> WARNING: Year 1958 absent in 2 of 41 series; Master Series value .743
>> WARNING: Year 1959 absent in 2 of 41 series; Master Series value -.331
>> WARNING: Year 1960 absent in 2 of 41 series; Master Series value .315
>> WARNING: Year 1962 absent in 2 of 41 series; Master Series value .498
>> WARNING: Year 1965 absent in 1 of 41 series; Master Series value 1.331
>> WARNING: Year 1966 absent in 1 of 42 series; Master Series value .253
>> WARNING: Year 1968 absent in 1 of 42 series; Master Series value .681
>> WARNING: Year 1969 absent in 1 of 42 series; Master Series value .306
>> WARNING: Year 1970 absent in 1 of 42 series; Master Series value .092
>> WARNING: Year 1974 absent in 1 of 42 series; Master Series value .924
```

```
>> WARNING: Year 1975 absent in 1 of 41 series; Master Series value .996
>> WARNING: Year 1983 absent in 1 of 41 series; Master Series value 1.444
>> WARNING: Year 1984 absent in 1 of 41 series; Master Series value 1.077
>> WARNING: Year 1994 absent in 1 of 40 series; Master Series value -.341
>> WARNING: Year 1995 absent in 1 of 40 series; Master Series value .862
>> WARNING: Year 1996 absent in 2 of 40 series; Master Series value .034
>> WARNING: Year 1998 absent in 1 of 40 series; Master Series value .052
>> WARNING: Year 1999 absent in 2 of 40 series; Master Series value .768
>> WARNING: Year 2000 absent in 2 of 40 series; Master Series value .058
>> WARNING: Year 2001 absent in 2 of 40 series; Master Series value -.258
>> WARNING: Year 2003 absent in 3 of 39 series; Master Series value .179
>> WARNING: Year 2004 absent in 2 of 39 series; Master Series value .728
>> WARNING: Year 2005 absent in 2 of 39 series; Master Series value 1.204
>> WARNING: Year 2006 absent in 5 of 39 series; Master Series value .164
>> WARNING: Year 2007 absent in 3 of 38 series; Master Series value .626
>> WARNING: Year 2009 absent in 1 of 38 series; Master Series value .661
```

```
*****
*C* Number of dated series      42 *C*
*O* Master series 1800 2015  216 yrs *O*
*F* Total rings in all series  4187 *F*
*E* Total dated rings checked  4125 *E*
*C* Series intercorrelation    .669 *C*
*H* Average mean sensitivity   .374 *H*
*A* Segments, possible problems  7  *A*
*****
```

ABSENT RINGS listed by SERIES:
by year)

(See Master Dating Series for absent rings listed

```
D1_2_1B      1 absent rings:  1993
3_32Aab      1 absent rings:  2003
D1_52A       5 absent rings:  1958  1959  1960  1961  1962
D1_21C       3 absent rings:  1994  1995  1996
```

S&L 1	3 absent rings:	1981	1983	1984									
S&L 4A	3 absent rings:	2006	2007	2008									
L 4A	1 absent rings:	2006											
L 4B	1 absent rings:	2006											
S4A	2 absent rings:	1974	1975										
S&L5B	3 absent rings:	1991	1992	1993									
S&L6D	20 absent rings:	1951	1952	1953	1954	1955	1956	1957	1958	1959	1960		
1961 1962	1963 1964 1965	1966											
		1967	1968	1969	1970								
34Aab	1 absent rings:	1800											
4234B	11 absent rings:	1999	2000	2001	2002	2003	2004	2005	2006	2007	2008		
2009													
4234A	11 absent rings:	1998	1999	2000	2001	2002	2003	2004	2005	2006	2007		
2008													
41_33Bab	1 absent rings:	1996											
	67 absent rings	1.600%											

PART 2: TIME PLOT OF TREE-RING SERIES: cores8 omitted
 21:33 Fri 25 MAR 2016 Page 2

1000					1100					1200					1300					1400					1500					1600					1700					1800														
1900					2000					Beg					End																																							
Ident					Seq					year					year					Yrs																																		
:					:					:					:					:					:					:					:					:					:									
:					:					:					:					:					:					:					:					:					:									
.													
<=====					41_32Aab					1					1909					2014					106																													
.													
<=====					4235Aabc					2					1898					2014					117																													
.													
<=====					D1_2_1B					3					1907					2014					108																													
.													
.					<=====					1_33Aab					4					1928					2014					87																								
.								
<=====					3_3_1_A					5					1885					2013					129																													
.													
<=====					3_32Aab					6					1900					2014					115																													
.													
.					<=====					4131Aabc					7					1936					2014					79																								
.													
.					<=====					D1_52A					8					1930					2010					81																								
.													
<=====					D1_21C					9					1906					2014					109																													
.													
.					<=====					D3_33A					10					1927					2010					84																								
.													
.					<=====					> D3_33B					11					1929					2006					78																								
.													
.					<=====					42_35B					12					1954					2014					61																								
.													

<=====	BC	13	1904	2015	112
.	<=====	L1	A	14	1932	2015	84
.	<=====	S&L	1	15	1939	2014	76
.	.	<=====	L3	16	1966	2015	50
<=====	S4	B	17	1892	2015	124
.	<=====	S&L	4A	18	1949	2015	67
.	<=====	S&L	4B	19	1949	2002	54
.	<=====	S&L	4C	20	1951	2013	63
.	<=====	L	4A	21	1925	2015	91
<=====	L	4B	22	1893	2015	123
<=====	L5	23	1873	2015	143
.	<=====	OK	1A	24	1917	2015	99
.	<=====	OK	1B	25	1910	2015	106
<=====	Basecamp	26	1904	2015	112
<=====	S4A	27	1904	1986	83
.	<=====	Pb1A	28	1917	2015	99
.	<=====	Pb1B	29	1927	2015	89

.
.	<==>	.	S&L5A	.	30	1940	1974	35
.	<=====	.	S&L5B	.	31	1927	2015	89
<=====	.	.	S&L6A	.	32	1901	2015	115
.	<=====	.	S&L6B	.	33	1926	2015	90
<=====	.	.	S&L6C	.	34	1904	2014	111
<=====	.	.	S&L6D	.	35	1908	2015	108
.	<=====	.	S5B	.	36	1913	2011	99
<=====	34Aab	.	37	1800	2014	215
.	<=====	.	4133Aab	.	38	1916	2012	97
.	<=====	.	4234B	.	39	1862	2014	153
.	<=====	.	4234A	.	40	1917	2014	98
.	<=====	.	D135Aab	.	41	1866	2014	149
.	<=====	.	41_33Bab	.	42	1916	2014	99
:	:	:	:	:	:	:	:	:	:	:	:	:	:	:	:	:	:	:	:
:	:	:	:	:	:	:	:	:	:	:	:	:	:	:	:	:	:	:	:
1000	1100	1200	1300	1400	1500	1600	1700	1800											
1900	2000																		

PART 3: Master Dating Series: cores8 omitted
 21:33 Fri 25 MAR 2016 Page 3

Year	Value	No Ab	Year	Value	No Ab	Year	Value	No Ab	Year	Value	No Ab	
Year	Value	No Ab	Year	Value	No Ab							
1900	-.155	9	1950	-.739	39	1800	-.037	1	1850	1.134	1	
1901	.150	10	1951	-1.958	40	1801	.148	1	1851	-3.274	1	
1902	-1.704	10	1952	.285	40	1802	1.099	1	1852	.292	1	
1903	.431	10	1953	.689	40	1803	.662	1	1853	.475	1	
1904	-.627	14	1954	-2.035	41	1804	.870	1	1854	.830	1	
1905	-.668	14	1955	.321	41	1805	.581	1	1855	.145	1	
1906	.650	15	1956	-1.184	41	1806	-.554	1	1856	-1.207	1	
1907	1.270	16	1957	.998	41	1807	1.185	1	1857	.232	1	
1908	.176	17	1958	.743	41	1808	1.262	1	1858	1.100	1	
1909	.370	18	1959	-.331	41	1809	-.614	1	1859	.572	1	
1910	-.334	19	1960	.315	41	1810	-1.382	1	1860	-1.141	1	
1911	.795	19	1961	-1.277	41	1811	-.225	1	1861	-2.850	1	

1912	.826	19	1962	.498	41	2<<	1812	-1.153	1	1862	.007	2
1913	.136	20	1963	-1.392	41	1	1813	-.928	1	1863	-.473	2
1914	.542	20	1964	-.454	41	1	1814	1.026	1	1864	1.311	2
1915	-.540	20	1965	1.331	41	1<<	1815	1.575	1	1865	-.106	2
1916	-2.015	22	1966	.253	42	1<<	1816	1.062	1	1866	1.469	3
1917	-.428	25	1967	-.450	42	1	1817	-.016	1	1867	.581	3
1918	-.105	25	1968	.681	42	1<<	1818	.720	1	1868	.201	3
1919	-.540	25	1969	.306	42	1<<	1819	1.177	1	1869	.399	3
1920	-.371	25	1970	.092	42	1<<	1820	.953	1	1870	.278	3
1921	1.059	25	1971	.920	42		1821	-.379	1	1871	-3.122	3
1922	-.413	25	1972	-1.302	42		1822	-2.455	1	1872	.635	3
1923	-.071	25	1973	1.129	42		1823	.312	1	1873	.440	4
1924	.036	25	1974	.924	42	1<<	1824	-2.083	1	1874	-1.250	4
1925	.538	26	1975	.996	41	1<<	1825	.009	1	1875	-.242	4
1926	.684	27	1976	-.868	41		1826	-2.159	1	1876	.362	4
1927	.709	30	1977	-2.114	41		1827	.564	1	1877	.395	4

1928	.957	31	1978	.261	41	1828	1.813	1	1878	1.335	4
1929	.997	32	1979	.694	41	1829	-.246	1	1879	-.305	4
1930	.714	33	1980	-.852	41	1830	-1.762	1	1880	-1.187	4
1931	-.716	33	1981	-1.386	41	1831	.905	1	1881	-.792	4
1932	-.069	34	1982	.714	41	1832	.131	1	1882	.352	4
1933	-.970	34	1983	1.444	41	1833	-.661	1	1883	.477	4
1934	-2.957	34	1984	1.077	41	1834	-.336	1	1884	.035	4
1935	-.540	34	1985	.809	41	1835	1.504	1	1885	1.404	5
1936	-.642	35	1986	.554	41	1836	.594	1	1886	.786	5
1937	.160	35	1987	-.340	40	1837	1.783	1	1887	-.370	5
1938	.587	35	1988	-.493	40	1838	1.762	1	1888	-.441	5
1939	-.137	36	1989	-1.143	40	1839	.247	1	1889	.587	5
1940	-.101	37	1990	-.974	40	1840	.284	1	1890	-.613	5
1941	.810	37	1991	-.709	40	1841	.388	1	1891	.489	5
1942	.401	37	1992	-.545	40	1842	-1.484	1	1892	.427	6
1943	.821	37	1993	-.699	40	1843	.802	1	1893	-.784	7

1944	-.372	37	1994	-.341	40	1<<	1844	-3.361	1	1894	-.888	7
1945	.332	37	1995	.862	40	1<<	1845	-.915	1	1895	.226	7
1946	-.167	37	1996	.034	40	2<<	1846	.221	1	1896	-.345	7
1947	.841	37	1997	.424	40		1847	-1.164	1	1897	.140	7
1948	1.011	37	1998	.052	40	1<<	1848	.517	1	1898	.315	8
1949	1.222	39	1999	.768	40	2<<	1849	1.681	1	1899	-1.776	8

PART 3: Master Dating Series: cores8 omitted
 21:33 Fri 25 MAR 2016 Page 4

Year	Value	No Ab	Year	Value	No Ab	Year	Value	No Ab	Year	Value	No Ab
Year	Value	No Ab	Year	Value	No Ab						
2000	.058	40	2<<								
2001	-.258	40	2<<								
2002	-2.154	40	2								
2003	.179	39	3<<								
2004	.728	39	2<<								
2005	1.204	39	2<<								
2006	.164	39	5<<								
2007	.626	38	3<<								
2008	-.825	38	3								
2009	.661	38	1<<								
2010	-.502	38									
2011	.563	36									
2012	-.651	35									
2013	-1.187	34									
2014	1.017	32									
2015	1.014	17									

PART 4: Master Bar Plot: cores8 omitted
 21:33 Fri 25 MAR 2016 Page 5

Year Rel value	Year Rel value	Year Rel value	Year Rel value	Year Rel value	Year Rel value
1900----a	1950--c			1800----@	1850-----
1901-----A	1951h			1801-----A	1851m
A 1902g	1952-----A			1802-----D	1852-----
-B 1903-----B	1953-----C			1803-----C	1853-----
---C 1904--c	1954h			1804-----C	1854-----
A 1905--c	1955-----A			1805-----B	1855-----
1906-----C	1956-e			1806--b	1856-e
A 1907-----E	1957-----D			1807-----E	1857-----
----D 1908-----A	1958-----C			1808-----E	1858-----
--B 1909-----A	1959---a			1809--b	1859-----
----	----			----	----
1910---a	1960-----A			1810-f	1860-e
1911-----C	1961-e			1811---a	1861k
1912-----C	1962-----B			1812-e	1862----@

1913-----A	1963-f
-----E 1914-----B	1964---b
1915--b	1965-----E
-----F 1916h	1966-----A
--B 1917---b	1967---b
A 1918----@	1968-----C
-B 1919--b	1969-----A
----	----
----	----
A 1920---a	1970-----@
1921-----D	1971-----D
--C 1922---b	1972-e
-B 1923----@	1973-----E
1924----@	1974-----D
1925-----B	1975-----D
-A 1926-----C	1976--c
-B 1927-----C	1977h
-----E 1928-----D	1978-----A

1813-d	1863---b
1814-----D	1864-----
1815-----F	1865----@
1816-----D	1866-----
1817----@	1867-----
1818-----C	1868-----
1819-----E	1869-----
----	----
1820-----D	1870-----
1821---b	18711
1822j	1872-----
1823-----A	1873-----
1824h	1874-e
1825----@	1875---a
1826i	1876-----
1827-----B	1877-----
1828-----G	1878-----

1929-----D	1979-----C			1829---a	1879---a
----	----	----	----	----	----
1930-----C	1980--c			1830g	1880-e
1931--c	1981-f			1831-----D	1881--c
-A	1932----@	1982-----C		1832-----A	1882-----
-B	1933-d	1983-----F		1833--c	1883-----
1934l	1984-----D			1834---a	1884----@
-----F	1935--b	1985-----C		1835-----F	1885-----
---C	1936--c	1986-----B		1836-----B	1886-----
1937-----A	1987---a			1837-----G	1887---a
1938-----B	1988--b			1838-----G	1888---b
--B	1939----a	1989-e		1839-----A	1889-----
----	----	----	----	----	----
1940----@	1990-d			1840-----A	1890--b
--B	1941-----C	1991--c		1841-----B	1891-----
-B	1942-----B	1992--b		1842-f	1892-----
1943-----C	1993--c			1843-----C	1893--c

1944---a	1994---a
A	1945-----A 1995-----C
1946----a	1996----@
A	1947-----C 1997-----B
-A	1948-----D 1998----@
1949-----E	1999-----C

1844m	1894-d
1845-d	1895-----
1846-----A	1896---a
1847-e	1897-----
1848-----B	1898-----
1849-----G	1899g

PART 4: Master Bar Plot: cores8 omitted
21:33 Fri 25 MAR 2016 Page 6

	Year Rel value	Year Rel value	Year Rel value	Year Rel value	Year Rel value	Year Rel value	Year Rel value
value	Year Rel value	Year Rel value	Year Rel value	Year Rel value	Year Rel value	Year Rel value	Year Rel value
2000	----	@					
2001	---	a					
2002	i						
2003	-----	A					
2004	-----	C					
2005	-----	E					
2006	-----	A					
2007	-----	C					
2008	--	c					
2009	-----	C					
	----		----		----		----
	----		----				
2010	--	b					
2011	-----	B					
2012	--	c					
2013	-	e					
2014	-----	D					
2015	-----	D					

Correlations of 50-year dated segments, lagged 25 years
 Flags: A = correlation under .3281 but highest as dated; B = correlation higher at
 other than dated position

Seq	Series	Time_span	1850	1875	1900	1925	1950	1975
			1899	1924	1949	1974	1999	2024
1	41_32Aab	1909 2014			.68	.75	.76	.78
2	4235Aabc	1898 2014		.75	.76	.85	.87	.83
3	D1_2_1B	1907 2014			.73	.73	.77	.77
4	1_33Aab	1928 2014				.76	.84	.82
5	3_3_1_A	1885 2013		.69	.73	.85	.84	.86
6	3_32Aab	1900 2014			.40	.78	.86	.74
7	4131Aabc	1936 2014				.68	.83	.80
8	D1_52A	1930 2010				.39	.40	.69
9	D1_21C	1906 2014			.78	.80	.69	.66
10	D3_33A	1927 2010				.57	.74	.59
11	D3_33B	1929 2006				.24B	.47	.53
12	42_35B	1954 2014					.80	.72
13	BC	1904 2015			.66	.74	.85	.78
14	L1 A	1932 2015				.79	.88	.85
15	S&L 1	1939 2014				.57	.55	.53
16	L3	1966 2015					.66	
17	S4 B	1892 2015		.65	.75	.76	.73	.78
18	S&L 4A	1949 2015				.71	.70	.59
19	S&L 4B	1949 2002				.83	.83	.68
20	S&L 4C	1951 2013					.79	.55
21	L 4A	1925 2015				.84	.89	.71
22	L 4B	1893 2015		.59	.65	.84	.91	.74

23	L5	1873	2015	.56	.58	.73	.73	.80	.74
24	OK 1A	1917	2015			.83	.88	.89	.91
25	OK 1B	1910	2015			.82	.93	.92	.92
26	Basecamp	1904	2015			.63	.75	.86	.78
27	S4A	1904	1986			.54	.71	.63	
28	Pb1A	1917	2015			.71	.78	.67	.64
29	Pb1B	1927	2015				.81	.76	.71
30	S&L5A	1940	1974				.75		
31	S&L5B	1927	2015				.77	.69	.43
32	S&L6A	1901	2015			.79	.88	.89	.90
33	S&L6B	1926	2015				.71	.71	.75
34	S&L6C	1904	2014			.74	.66	.65	.67
35	S&L6D	1908	2015			.29A	.42	.43	.69
36	S5B	1913	2011			.34B	.44	.66	.48
37	34Aab	1800	2014	.23B	.40	.62	.85	.79	.67
38	4133Aab	1916	2012			.79	.85	.79	.66
39	4234B	1862	2014	.65	.78	.78	.82	.79	.58
40	4234A	1917	2014			.79	.81	.70	.56
41	D135Aab	1866	2014	.26B	.14B	.19B	.40	.50	.53
42	41_33Bab	1916	2014			.77	.84	.78	.74

 For each series with potential problems the following diagnostics may appear:

- [A] Correlations with master dating series of flagged 50-year segments of series filtered with 32-year spline,
 at every point from ten years earlier (-10) to ten years later (+10) than dated
- [B] Effect of those data values which most lower or raise correlation with master series
- [C] Year-to-year changes very different from the mean change in other series
- [D] Absent rings (zero values)
- [E] Values which are statistical outliers from mean for the year

=====
 =====
 41_32Aab 1909 to 2014 106 years
 Series 1

[B] Entire series, effect on correlation (.732) is:
 Lower 1972 -.010 1910 -.010 1928 -.010 1958 -.008 Higher 1934 .024
 1963 .010 1977 .008 1965 .007

4235Aabc 1898 to 2014 117 years
Series 2

[B] Entire series, effect on correlation (.809) is:
Lower 2008 -.018 1944 -.011 1939 -.006 1915 -.006 Higher 1934 .016
2002 .010 1902 .007 1963 .006

[E] Outliers 1 3.0 SD above or -4.5 SD below mean for year
2008 +3.2 SD

=====
=====

D1_2_1B 1907 to 2014 108 years
Series 3

[B] Entire series, effect on correlation (.742) is:
Lower 1911 -.011 1931 -.010 1967 -.009 1971 -.008 Higher 1954 .020
1977 .008 1916 .006 1983 .005

[D] 1 Absent rings: Year Master N series Absent
1993 -.699 40 2

=====
=====

1_33Aab 1928 to 2014 87 years
Series 4

[B] Entire series, effect on correlation (.774) is:
Lower 1930 -.024 2000 -.011 1945 -.009 1950 -.008 Higher 1977 .012
2002 .008 1954 .007 1934 .006

[E] Outliers 1 3.0 SD above or -4.5 SD below mean for year
 1943 +3.0 SD

=====

3_3_1_A 1885 to 2013 129 years
 Series 5

[B] Entire series, effect on correlation (.772) is:
 Lower 1916 -.015 1891 -.010 1889 -.008 1944 -.007 Higher 1934 .021
 2002 .011 1977 .007 1902 .007

[E] Outliers 1 3.0 SD above or -4.5 SD below mean for year
 1916 +3.3 SD

=====

3_32Aab 1900 to 2014 115 years
 Series 6

[B] Entire series, effect on correlation (.626) is:
 Lower 2003 -.028 1902 -.028 1916 -.026 1907 -.022 Higher 1934 .040
 1954 .024 2002 .013 1977 .011

[D] 1 Absent rings: Year Master N series Absent
 2003 .179 39 3 >> WARNING: Ring is not usually
 narrow

[E] Outliers 6 3.0 SD above or -4.5 SD below mean for year
 1902 +4.0 SD; 1907 -4.5 SD; 1916 +4.4 SD; 1917 +3.4 SD; 1934 -5.8 SD;
 2003 -5.9 SD


```
=====
=====
```

```
4131Aabc 1936 to 2014      79 years
Series    7
```

```
[B] Entire series, effect on correlation ( .699) is:
      Lower  1944  -.060   1936  -.028   1938  -.011   2003  -.010   Higher  1951   .018
1977   .016   1965   .011   1972   .010
```

```
[E] Outliers      2    3.0 SD above or -4.5 SD below mean for year
      1936 +4.6 SD;    1944 -6.5 SD
```

```
=====
=====
```

```
D1_52A    1930 to 2010      81 years
Series    8
```

```
[B] Entire series, effect on correlation ( .546) is:
      Lower  1958  -.099   1963  -.028   1954  -.017   1962  -.016   Higher  2002   .037
1983   .013   1934   .012   1977   .011
```

```
[D]    5 Absent rings: Year  Master  N series Absent
                        1958    .743    41      2 >> WARNING: Ring is not usually
narrow
                        1959   -.331    41      2 >> WARNING: Ring is not usually
narrow
                        1960    .315    41      2 >> WARNING: Ring is not usually
narrow
                        1961   -1.277   41      2
                        1962    .498    41      2 >> WARNING: Ring is not usually
narrow
```

[E] Outliers 3 3.0 SD above or -4.5 SD below mean for year
 1951 +3.1 SD; 1954 +3.3 SD; 1958 -5.0 SD

=====

D1_21C 1906 to 2014 109 years
 Series 9

[B] Entire series, effect on correlation (.714) is:
 Lower 1981 -.017 1995 -.016 2002 -.013 1963 -.011 Higher 1934 .028
 1954 .015 1977 .009 1916 .006

[D]	3 Absent rings:	Year	Master	N series	Absent	
		1994	-.341	40	1	>> WARNING: Ring is not usually
narrow						
		1995	.862	40	1	>> WARNING: Ring is not usually
narrow						
		1996	.034	40	2	>> WARNING: Ring is not usually
narrow						

[E] Outliers 2 3.0 SD above or -4.5 SD below mean for year
 1916 -6.7 SD; 1981 +3.4 SD

=====

D3_33A 1927 to 2010 84 years
 Series 10

[B] Entire series, effect on correlation (.512) is:
 Lower 1929 -.051 1931 -.028 1997 -.023 1942 -.019 Higher 1954 .055
 1972 .027 1977 .026 1965 .013

[E] Outliers 4 3.0 SD above or -4.5 SD below mean for year
 1929 -6.8 SD; 1931 +3.3 SD; 1940 +3.2 SD; 1954 -4.6 SD

=====

D3_33B 1929 to 2006 78 years
 Series 11

[A] Segment	High	-10	-9	-8	-7	-6	-5	-4	-3	-2	-1	+0	+1	+2	+3	
+4	+5	+6	+7	+8	+9	+10										
-----	-----	-----	-----	-----	-----	-----	-----	-----	-----	-----	-----	-----	-----	-----	-----	
---	---	---	---	---	---	---	---	---	---	---	---	---	---	---	---	
1929	1978	9	.03	.20	.33	.14	-.08	-.01	-.20	-.13	-.13	-.44	.24	-.15	.12	.02
.05	.23	-.20	-.16	.05	.37*	.01										

[B] Entire series, effect on correlation (.311) is:
 Lower 1934 -.044 1941 -.044 1942 -.032 1981 -.016 Higher 2002 .049
 1972 .044 1954 .029 1965 .024
 1929 to 1978 segment:
 Lower 1941 -.059 1934 -.059 1942 -.041 1933 -.021 Higher 1972 .068
 1954 .045 1965 .039 1976 .034

[E] Outliers 4 3.0 SD above or -4.5 SD below mean for year
 1934 +5.8 SD; 1940 +3.4 SD; 1964 +3.7 SD; 1977 +3.1 SD

=====

42_35B 1954 to 2014 61 years
 Series 12

[B] Entire series, effect on correlation (.768) is:

	Lower	2008	-.037	2000	-.020	1979	-.008	2003	-.007	Higher	1972	.014
1963	.012	2002	.012	1957	.007							

[E] Outliers 1 3.0 SD above or -4.5 SD below mean for year
2008 +3.6 SD

=====

BC 1904 to 2015 112 years
Series 13

[B] Entire series, effect on correlation (.726) is:

	Lower	1934	-.013	2002	-.011	2006	-.008	1949	-.008	Higher	1972	.009
1963	.007	1965	.007	1977	.006							

[E] Outliers 1 3.0 SD above or -4.5 SD below mean for year
1916 -5.1 SD

=====

L1 A 1932 to 2015 84 years
Series 14

[B] Entire series, effect on correlation (.790) is:

	Lower	1933	-.023	1944	-.009	2003	-.008	2007	-.006	Higher	2002	.011
1977	.010	1951	.009	1972	.009							

[E] Outliers 1 3.0 SD above or -4.5 SD below mean for year
1933 +3.3 SD

=====

S&L 1 1939 to 2014 76 years
Series 15

[B] Entire series, effect on correlation (.628) is:
 Lower 1983 -.060 1950 -.025 1984 -.024 1975 -.014 Higher 2002 .035
1954 .034 1951 .017 1963 .014

[D] 3 Absent rings: Year Master N series Absent
 1981 -1.386 41 1
 1983 1.444 41 1 >> WARNING: Ring is not usually
narrow
 1984 1.077 41 1 >> WARNING: Ring is not usually
narrow

[E] Outliers 3 3.0 SD above or -4.5 SD below mean for year
 1950 +3.0 SD; 1983 -5.2 SD; 1984 -4.6 SD

=====

L3 1966 to 2015 50 years
Series 16

[B] Entire series, effect on correlation (.659) is:
 Lower 1972 -.063 1976 -.034 1988 -.023 2010 -.017 Higher 1977 .044
2002 .035 1981 .016 1980 .014

[E] Outliers 2 3.0 SD above or -4.5 SD below mean for year
 1972 +3.8 SD; 1988 +3.2 SD

=====

S4 B 1892 to 2015 124 years
Series 17

[B] Entire series, effect on correlation (.705) is:
 Lower 1899 -.031 1900 -.030 1917 -.013 1989 -.009 Higher 1934 .029
 1954 .014 2002 .012 1951 .011

[C] Year-to-year changes diverging by over 4.0 std deviations:
 1899 1900 -4.1 SD

[E] Outliers 4 3.0 SD above or -4.5 SD below mean for year
 1895 +3.7 SD; 1899 +4.4 SD; 1917 +3.9 SD; 1934 -4.7 SD

=====

S&L 4A 1949 to 2015 67 years
Series 18

[B] Entire series, effect on correlation (.618) is:
 Lower 1958 -.032 2006 -.024 2007 -.024 1981 -.020 Higher 1977 .024
 1972 .023 1963 .018 1961 .013

[D] 3 Absent rings: Year Master N series Absent
 2006 .164 39 5 >> WARNING: Ring is not usually
 narrow
 2007 .626 38 3 >> WARNING: Ring is not usually
 narrow
 2008 -0.825 38 3

[E] Outliers 4 3.0 SD above or -4.5 SD below mean for year
 1981 +3.0 SD; 2001 +3.1 SD; 2002 +3.0 SD; 2007 -4.8 SD

```

=====
S&L 4B      1949 to 2002      54 years
Series 19

```

```

[B] Entire series, effect on correlation ( .676) is:
      Lower 2002 -.152 1960 -.014 1950 -.013 1981 -.008 Higher 1954 .032
1977 .023 1963 .019 1972 .018

```

```

[E] Outliers      1      3.0 SD above or -4.5 SD below mean for year
      2002 +7.2 SD

```

```

=====
S&L 4C      1951 to 2013      63 years
Series 20

```

```

[B] Entire series, effect on correlation ( .618) is:
      Lower 2013 -.042 2004 -.034 2002 -.027 2012 -.019 Higher 1951 .022
1963 .016 1983 .013 1977 .012

```

```

[E] Outliers      2      3.0 SD above or -4.5 SD below mean for year
      1954 +3.5 SD;      2013 +4.9 SD

```

```

=====
L 4A        1925 to 2015      91 years
Series 21

```

```

[B] Entire series, effect on correlation ( .783) is:

```

	Lower	2006	-.054	1933	-.007	1972	-.007	2002	-.007	Higher	1934	.027
1977	.008	1963	.006	1973	.005							

[D] 1 Absent rings: Year Master N series Absent
2006 .164 39 5 >> WARNING: Ring is not usually
narrow

[E] Outliers 1 3.0 SD above or -4.5 SD below mean for year
2006 -5.8 SD

=====

L 4B 1893 to 2015 123 years
Series 22

[B] Entire series, effect on correlation (.705) is:
Lower 1915 -.032 2006 -.031 1894 -.020 1896 -.013 Higher 1916 .012
1951 .010 1934 .010 1977 .009

[D] 1 Absent rings: Year Master N series Absent
2006 .164 39 5 >> WARNING: Ring is not usually
narrow

[E] Outliers 3 3.0 SD above or -4.5 SD below mean for year
1894 +4.2 SD; 1915 -7.1 SD; 2006 -5.2 SD

=====

L5 1873 to 2015 143 years
Series 23

[B] Entire series, effect on correlation (.669) is:

	Lower	1884	-.033	1961	-.018	1881	-.017	1939	-.016	Higher	1954	.015
1934	.011	1899	.010	1902	.008							

[E] Outliers 4 3.0 SD above or -4.5 SD below mean for year
1881 -5.4 SD; 1884 -4.7 SD; 1961 +4.2 SD; 2004 +3.4 SD

=====

OK 1A 1917 to 2015 99 years
Series 24

[B] Entire series, effect on correlation (.868) is:

	Lower	1918	-.009	1990	-.008	1959	-.008	1919	-.005	Higher	1934	.015
2002	.008	1977	.006	1951	.005							

[E] Outliers 1 3.0 SD above or -4.5 SD below mean for year
1918 +3.1 SD

=====

OK 1B 1910 to 2015 106 years
Series 25

[B] Entire series, effect on correlation (.868) is:

	Lower	1915	-.014	1921	-.012	1910	-.007	1916	-.007	Higher	1934	.011
2002	.007	1954	.006	1951	.004							

=====

Basecamp 1904 to 2015 112 years
Series 26

[B] Entire series, effect on correlation (.715) is:
Lower 1909 -.013 1949 -.013 1934 -.011 2002 -.009 Higher 1972 .009
1963 .009 1965 .007 1983 .005

[E] Outliers 1 3.0 SD above or -4.5 SD below mean for year
1916 -5.1 SD

=====
=====

S4A 1904 to 1986 83 years
Series 27

[B] Entire series, effect on correlation (.568) is:
Lower 1974 -.041 1916 -.041 1908 -.025 1975 -.019 Higher 1934 .075
1954 .028 1951 .014 1973 .011

[D] 2 Absent rings: Year Master N series Absent
1974 .924 42 1 >> WARNING: Ring is not usually
narrow
1975 .996 41 1 >> WARNING: Ring is not usually
narrow

[E] Outliers 4 3.0 SD above or -4.5 SD below mean for year
1908 -5.1 SD; 1916 +4.7 SD; 1934 -5.6 SD; 1975 -4.5 SD

=====
=====

Pb1A 1917 to 2015 99 years
Series 28

[B] Entire series, effect on correlation (.676) is:
 Lower 1977 -.031 1917 -.019 1993 -.013 1931 -.011 Higher 1934 .026
 2002 .022 1972 .013 1954 .008

[E] Outliers 2 3.0 SD above or -4.5 SD below mean for year
 1977 +4.0 SD; 1993 +3.4 SD

=====

Pb1B 1927 to 2015 89 years
 Series 29

[B] Entire series, effect on correlation (.758) is:
 Lower 1940 -.019 1993 -.019 1929 -.015 1992 -.011 Higher 1934 .031
 2002 .014 1954 .010 1977 .008

[E] Outliers 1 3.0 SD above or -4.5 SD below mean for year
 1993 +3.8 SD

=====

S&L5A 1940 to 1974 35 years
 Series 30

[B] Entire series, effect on correlation (.749) is:
 Lower 1950 -.029 1945 -.028 1964 -.023 1956 -.013 Higher 1951 .032
 1963 .027 1954 .023 1957 .010

=====

S&L5B 1927 to 2015 89 years
Series 31

[B] Entire series, effect on correlation (.559) is:
 Lower 2002 -.066 1991 -.023 1992 -.020 1927 -.019 Higher 1954 .021
 1963 .016 1977 .016 1961 .012

[D] 3 Absent rings: Year Master N series Absent
 1991 -.709 40 1
 1992 -.545 40 1
 1993 -.699 40 2

[E] Outliers 4 3.0 SD above or -4.5 SD below mean for year
 1991 -5.3 SD; 1992 -5.5 SD; 1993 -5.3 SD; 2002 +6.2 SD

=====

S&L6A 1901 to 2015 115 years
Series 32

[B] Entire series, effect on correlation (.855) is:
 Lower 1964 -.012 1902 -.011 1930 -.005 1908 -.004 Higher 1934 .013
 1954 .010 2002 .006 1916 .005

=====

S&L6B 1926 to 2015 90 years
Series 33

[B] Entire series, effect on correlation (.728) is:

	Lower	1991	-.022	1939	-.017	1937	-.016	1950	-.012	Higher	2002	.017
1954	.016	1951	.012	1934	.012							

[E] Outliers 2 3.0 SD above or -4.5 SD below mean for year
 1991 +3.9 SD; 1992 +3.8 SD

=====

S&L6C 1904 to 2014 111 years
 Series 34

[B] Entire series, effect on correlation (.703) is:

	Lower	1972	-.016	1927	-.010	1968	-.010	1963	-.009	Higher	1934	.014
1954	.008	1977	.007	1965	.007							

[E] Outliers 1 3.0 SD above or -4.5 SD below mean for year
 2002 -6.0 SD

=====

S&L6D 1908 to 2015 108 years
 Series 35

	[A] Segment	High	-10	-9	-8	-7	-6	-5	-4	-3	-2	-1	+0	+1	+2	+3	
+4	+5	+6	+7	+8	+9	+10											
	-----	----	----	----	----	----	----	----	----	----	----	----	----	----	----	----	
---	---	---	---	---	---	---	---	---	---	---	---	---	---	---	---	---	
	1908	1957	0	-.15	-.19	-.14	-.09	-.05	-.09	.03	.12	.12	.29	.29*	.20	-.01	-.14
	.06	-.09	-.05	-.12	-.08	-.04	-.12										

[B] Entire series, effect on correlation (.456) is:

	Lower	1917	-.056	1931	-.022	1972	-.015	1965	-.013	Higher	2002	.036
1934	.020	1950	.012	1973	.009							
	1908 to 1957 segment:											
	Lower	1917	-.093	1931	-.038	1957	-.019	1937	-.019	Higher	1934	.066
1950	.042	1933	.021	1948	.019							

[C] Year-to-year changes diverging by over 4.0 std deviations:
 1916 1917 -5.4 SD

[D]	20 Absent rings:	Year	Master	N series	Absent	
		1951	-1.958	40	1	
		1952	.285	40	1	>> WARNING: Ring is not usually
narrow						
		1953	.689	40	1	>> WARNING: Ring is not usually
narrow						
		1954	-2.035	41	1	
		1955	.321	41	1	>> WARNING: Ring is not usually
narrow						
		1956	-1.184	41	1	
		1957	.998	41	1	>> WARNING: Ring is not usually
narrow						
		1958	.743	41	2	>> WARNING: Ring is not usually
narrow						
		1959	-.331	41	2	>> WARNING: Ring is not usually
narrow						
		1960	.315	41	2	>> WARNING: Ring is not usually
narrow						
		1961	-1.277	41	2	
		1962	.498	41	2	>> WARNING: Ring is not usually
narrow						
		1963	-1.392	41	1	
		1964	-.454	41	1	
		1965	1.331	41	1	>> WARNING: Ring is not usually
narrow						

narrow	1966	.253	42	1	>> WARNING: Ring is not usually
	1967	-.450	42	1	
narrow	1968	.681	42	1	>> WARNING: Ring is not usually
	1969	.306	42	1	>> WARNING: Ring is not usually
narrow	1970	.092	42	1	>> WARNING: Ring is not usually

[E] Outliers 5 3.0 SD above or -4.5 SD below mean for year
 1913 +3.1 SD; 1916 +3.9 SD; 1917 -7.2 SD; 1931 +4.2 SD; 1972 +4.0 SD

=====

S5B 1913 to 2011 99 years
 Series 36

[A] Segment	High	-10	-9	-8	-7	-6	-5	-4	-3	-2	-1	+0	+1	+2	+3	
+4	+5	+6	+7	+8	+9	+10										
---	---	---	---	---	---	---	---	---	---	---	---	---	---	---	---	
---	---	---	---	---	---	---										
1913	1962	1	-.05	-.25	-.26	.00	-.17	.11	-.06	-.15	.17	-.07	.34	.43*	.01	-.10
.01	.19	-.17	-.05	-.13	-.19	-.10										

[B] Entire series, effect on correlation (.397) is:
 Lower 1934 -.046 1977 -.022 1949 -.022 2004 -.020 Higher 1951 .020
 1972 .018 1954 .017 2002 .014
 1913 to 1962 segment:
 Lower 1934 -.083 1949 -.040 1938 -.031 1931 -.023 Higher 1951 .041
 1954 .037 1950 .015 1956 .014

[C] Year-to-year changes diverging by over 4.0 std deviations:

1933 1934 5.7 SD

[E] Outliers 5 3.0 SD above or -4.5 SD below mean for year
1933 -7.8 SD; 1934 +5.7 SD; 1977 +4.3 SD; 1981 +3.0 SD; 1992 +3.5 SD

=====
=====

34Aab 1800 to 2014 215 years
Series 37

[*] Early part of series cannot be checked from 1800 to 1861 -- not matched by another series

[A] Segment	High	-10	-9	-8	-7	-6	-5	-4	-3	-2	-1	+0	+1	+2	+3		
+4	+5	+6	+7	+8	+9	+10											
-----	-----	-----	-----	-----	-----	-----	-----	-----	-----	-----	-----	-----	-----	-----	-----		
---	---	---	---	---	---	---	---	---	---	---	---	---	---	---	---		
1862	1911	-3	-.27	.08	.14	-.14	.04	-.05	-.09	.27*	.11	-.25	.23	.02	-.02	-.04	-
.09	-.05	.14	-.15	.13	-.15	-.09											

[B] Entire series, effect on correlation (.491) is:
Lower 1871 -.049 1881 -.031 1873 -.017 1862 -.013 Higher 1954 .018
2002 .015 1934 .014 1902 .011
1862 to 1911 segment:
Lower 1871 -.073 1881 -.061 1873 -.030 1862 -.026 Higher 1899 .059
1902 .038 1866 .026 1885 .021

[C] Year-to-year changes diverging by over 4.0 std deviations:
1870 1871 4.4 SD

[D] 1 Absent rings: Year Master N series Absent
1800 -.037 1 1 >> WARNING: Ring is not usually
narrow

>> WARNING: First ring in series is ABSENT

[E] Outliers 9 3.0 SD above or -4.5 SD below mean for year
1800 -5.0 SD; 1862 +3.4 SD; 1867 +3.4 SD; 1871 +6.3 SD; 1881 +7.2 SD;
1899 -6.5 SD; 1916 +3.3 SD;
1917 +3.2 SD; 1993 +4.5 SD

=====
=====

4133Aab 1916 to 2012 97 years
Series 38

[B] Entire series, effect on correlation (.710) is:
Lower 2002 -.020 1999 -.014 2012 -.014 1981 -.011 Higher 1977 .014
1916 .014 1972 .012 1954 .010

=====
=====

4234B 1862 to 2014 153 years
Series 39

[B] Entire series, effect on correlation (.678) is:
Lower 1999 -.026 1862 -.017 1863 -.016 1874 -.015 Higher 1871 .024
1954 .011 1916 .010 1902 .009

[D] 11 Absent rings: Year Master N series Absent
1999 .768 40 2 >> WARNING: Ring is not usually
narrow
2000 .058 40 2 >> WARNING: Ring is not usually
narrow

narrow	2001	-.258	40	2	>> WARNING: Ring is not usually
	2002	-2.154	40	2	
narrow	2003	.179	39	3	>> WARNING: Ring is not usually
narrow	2004	.728	39	2	>> WARNING: Ring is not usually
narrow	2005	1.204	39	2	>> WARNING: Ring is not usually
narrow	2006	.164	39	5	>> WARNING: Ring is not usually
narrow	2007	.626	38	3	>> WARNING: Ring is not usually
	2008	-.825	38	3	
narrow	2009	.661	38	1	>> WARNING: Ring is not usually

[E] Outliers 3 3.0 SD above or -4.5 SD below mean for year
 1864 +3.2 SD; 1874 -4.7 SD; 1891 +3.2 SD

=====

4234A 1917 to 2014 98 years
 Series 40

[B] Entire series, effect on correlation (.667) is:
 Lower 1998 -.038 2005 -.014 1999 -.011 1991 -.010 Higher 1954 .027
 1934 .020 1972 .014 1963 .013

[D] 11 Absent rings: Year Master N series Absent
 1998 .052 40 1 >> WARNING: Ring is not usually
 narrow

narrow	1999	.768	40	2	>> WARNING: Ring is not usually
narrow	2000	.058	40	2	>> WARNING: Ring is not usually
narrow	2001	-.258	40	2	>> WARNING: Ring is not usually
	2002	-2.154	40	2	
narrow	2003	.179	39	3	>> WARNING: Ring is not usually
narrow	2004	.728	39	2	>> WARNING: Ring is not usually
narrow	2005	1.204	39	2	>> WARNING: Ring is not usually
narrow	2006	.164	39	5	>> WARNING: Ring is not usually
narrow	2007	.626	38	3	>> WARNING: Ring is not usually
narrow	2008	-.825	38	3	

=====

=====

D135Aab 1866 to 2014 149 years
Series 41

[A]	Segment	High	-10	-9	-8	-7	-6	-5	-4	-3	-2	-1	+0	+1	+2	+3
+4	+5	+6	+7	+8	+9	+10										
---	---	---	---	---	---	---	---	---	---	---	---	---	---	---	---	---
---	---	---	---	---	---	---	---	---	---	---	---	---	---	---	---	---
.02	1866	1915	3	.16	.13	.09	-.26	.17	-.33	-.01	-.18	-.15	.05	.26	-.07	.03 .32*
.07	.00	.09	.03	.00	.05	-.04										
	1875	1924	-9	.02	.26*	-.13	-.25	.04	-.26	-.01	-.13	-.08	.12	.14	.08	.09 .17
	.07	.13	.14	.20	-.12	-.03	-.17									

1900 1949 -2 -.14 -.04 -.10 -.40 -.26 -.18 -.02 -.05 .28* .24 .19| .25 .17 .10
 .18 -.18 .05 -.14 -.17 .00 -.31

[B] Entire series, effect on correlation (.382) is:
 Lower 1934 -.027 1883 -.026 1905 -.016 1887 -.014 Higher 1871 .038
 1954 .020 1972 .018 1951 .016
 1866 to 1915 segment:
 Lower 1883 -.065 1905 -.041 1887 -.038 1874 -.025 Higher 1871 .177
 1899 .037 1866 .031 1878 .022
 1875 to 1924 segment:
 Lower 1883 -.090 1905 -.049 1887 -.046 1884 -.027 Higher 1899 .066
 1878 .038 1916 .032 1880 .028
 1900 to 1949 segment:
 Lower 1934 -.069 1905 -.049 1935 -.030 1931 -.021 Higher 1916 .038
 1902 .029 1933 .025 1941 .025

[C] Year-to-year changes diverging by over 4.0 std deviations:
 1934 1935 -4.6 SD

[E] Outliers 6 3.0 SD above or -4.5 SD below mean for year
 1871 -5.5 SD; 1874 +3.4 SD; 1887 +4.0 SD; 1905 +5.2 SD; 1934 +5.4 SD;
 1971 +3.7 SD

=====
 =====

41_33Bab 1916 to 2014 99 years
 Series 42

[B] Entire series, effect on correlation (.747) is:
 Lower 1996 -.060 1917 -.017 1921 -.008 1944 -.007 Higher 1934 .015
 1972 .009 1977 .007 1965 .007

[D] 1 Absent rings: Year Master N series Absent

```
1996      .034      40      2 >> WARNING: Ring is not usually
narrow
```

```
[E] Outliers      2      3.0 SD above or -4.5 SD below mean for year
      1917 +4.2 SD;      1996 -7.3 SD
```

```
=====
=====
```

PART 7: DESCRIPTIVE STATISTICS: cores8 omitted
 21:33 Fri 25 MAR 2016 Page 8

```

-----
--- Filtered -----\\
Max      Std      Auto  AR      No.      No.      No.      Corr   //----- Unfiltered -----\\  //-
Seq Series  Interval Years  Segmt  Flags  with  Mean  Max    Std    Auto    Mean
value      dev    corr  ()      -----
--  -----  -----  --
  1 41_32Aab 1909 2014    106      4      0    .732  2.97  7.39  1.349  .557  .377
2.12   .461   .021   1
  2 4235Aabc 1898 2014    117      5      0    .809  1.95  5.54  1.225  .784  .421
2.00   .442  -.035   1
  3 D1_2_1B  1907 2014    108      4      0    .742  1.25  6.19  1.048  .848  .454
2.09   .405   .013   1
  4 1_33Aab  1928 2014     87      3      0    .774  2.53 10.34  1.360  .598  .353
2.06   .350  -.030   1
  5 3_3_1_A  1885 2013    129      5      0    .772  1.54  4.53   .985  .897  .310
2.03   .357  -.020   1
  6 3_32Aab  1900 2014    115      4      0    .626  1.91  4.21   .938  .746  .311
1.80   .253  -.012   1
  7 4131Aabc 1936 2014     79      3      0    .699  3.03  8.12  1.355  .702  .281
1.92   .333  -.037   1
  8 D1_52A   1930 2010     81      3      0    .546  2.34  4.68  1.140  .724  .287
2.06   .362   .017   1
  9 D1_21C   1906 2014    109      4      0    .714  1.55  5.03  1.071  .807  .416
1.97   .341   .033   1
 10 D3_33A   1927 2010     84      3      0    .512  1.21  2.68   .705  .834  .308
1.86   .338  -.055   1

```

11	D3_33B	1929	2006	78	3	1	.311	.51	1.82	.406	.781	.379
2.07	.449	.027	2									
12	42_35B	1954	2014	61	2	0	.768	1.44	3.73	.893	.488	.540
2.05	.536	-.133	1									
13	BC	1904	2015	112	4	0	.726	2.28	5.32	1.032	.626	.321
1.96	.324	-.017	1									
14	L1 A	1932	2015	84	3	0	.790	1.92	4.07	.918	.590	.433
1.91	.388	.002	1									
15	S&L 1	1939	2014	76	3	0	.628	1.87	5.31	1.119	.580	.456
1.94	.365	-.036	1									
16	L3	1966	2015	50	1	0	.659	2.98	4.53	.973	.548	.278
1.88	.444	.043	1									
17	S4 B	1892	2015	124	5	0	.705	1.28	3.13	.634	.711	.389
1.94	.310	.008	1									
18	S&L 4A	1949	2015	67	3	0	.618	.66	1.49	.394	.716	.432
2.02	.530	.022	1									
19	S&L 4B	1949	2002	54	3	0	.676	.72	1.58	.398	.758	.356
2.20	.451	-.054	1									
20	S&L 4C	1951	2013	63	2	0	.618	.75	1.63	.494	.719	.472
2.00	.508	.026	3									
21	L 4A	1925	2015	91	3	0	.783	1.32	3.31	.699	.738	.358
1.85	.337	-.037	1									
22	L 4B	1893	2015	123	5	0	.705	1.56	3.18	.805	.786	.336
1.90	.347	.031	1									
23	L5	1873	2015	143	6	0	.669	.97	2.32	.434	.565	.341
2.17	.385	-.029	1									
24	OK 1A	1917	2015	99	4	0	.868	1.73	3.40	.762	.577	.385
1.92	.382	-.004	1									
25	OK 1B	1910	2015	106	4	0	.868	1.83	3.74	.785	.614	.360
1.90	.359	-.042	1									
26	Basecamp	1904	2015	112	4	0	.715	2.27	5.33	1.028	.638	.322
1.94	.304	-.013	1									
27	S4A	1904	1986	83	3	0	.568	1.51	3.48	.735	.679	.410
1.86	.282	.028	1									

28	Pb1A	1917	2015	99	4	0	.676	1.44	3.87	.797	.701	.405
2.04	.444	.010	1									
29	Pb1B	1927	2015	89	3	0	.758	1.46	3.65	.786	.616	.424
2.03	.353	.011	1									
30	S&L5A	1940	1974	35	1	0	.749	1.69	2.70	.492	.029	.354
2.15	.562	.013	1									
31	S&L5B	1927	2015	89	3	0	.559	.96	2.13	.543	.590	.433
1.94	.413	.115	1									
32	S&L6A	1901	2015	115	4	0	.855	1.83	3.75	.744	.736	.263
1.90	.326	.001	1									
33	S&L6B	1926	2015	90	3	0	.728	1.28	4.67	.811	.863	.313
1.93	.376	-.027	1									
34	S&L6C	1904	2014	111	4	0	.703	1.40	3.39	.752	.850	.288
1.76	.265	-.018	2									
35	S&L6D	1908	2015	108	4	1	.456	1.32	5.62	1.133	.780	.312
1.96	.305	-.057	1									
36	S5B	1913	2011	99	4	1	.397	.52	1.60	.284	.598	.400
1.85	.293	.001	1									
37	34Aab	1800	2014	215	6	1	.491	1.09	2.96	.656	.798	.349
2.01	.314	-.025	2									
38	4133Aab	1916	2012	97	4	0	.710	1.92	5.64	1.145	.697	.436
2.06	.444	.013	1									
39	4234B	1862	2014	153	6	0	.678	1.23	4.28	.950	.809	.411
2.05	.385	-.030	1									
40	4234A	1917	2014	98	4	0	.667	.55	1.99	.468	.864	.424
2.10	.434	-.014	1									
41	D135Aab	1866	2014	149	6	3	.382	1.19	11.82	1.353	.380	.410
2.14	.278	-.050	1									
42	41_33Bab	1916	2014	99	4	0	.747	1.78	21.65	2.523	.571	.510
1.97	.352	-.023	1									
---	-----	-----	---	-----	-----	-----	-----	-----	-----	-----	-----	---
---	-----	-----	---	-----	-----	-----	-----	-----	-----	-----	-----	---
Total or mean:				4187	156	7	.669	1.54	21.65	.898	.694	.374
2.20	.366	-.010										

$$- = [\text{COFECHA CORE8COF}] = -$$